LOCAL HEAT TRANSFER COEFFICIENT IN A BAFFLED SHELL AND TUBE HEAT EXCHANGER

A thesis submitted for the degree of

Doctor of Philosophy

by

John Norman Prowse

Department of Chemical Engineering

University of Aston in Birmingham

June 1977

LOCAL HEAT TRANSFER COEFFICIENT IN A BAFFLED SHELL AND TUBE HEAT EXCHANGER

JOHN NORMAN PROWSE

JUNE 1977

A thesis submitted for the degree of Doctor of Philosophy

SUMMARY

Local shell side coefficient measurements in the end compartments of a model shell and tube heat exchanger have been made using an electrochemical technique. Limited data are also reported for the second compartment.

The end compartment average coefficients have been found to be smaller than reported data for a corresponding internal compartment. The second compartment data have been shown to lie between those for the end compartments and the reported internal compartment data.

Experimental data are reported for two port types and two baffle orientations, with data for the case of an inlet compartment impingement baffle also being given.

Port type is shown to have a small effect on compartment coefficients, these being largely unaffected. Likewise, the outlet compartment average coefficients are slightly smaller than those for the inlet compartment, with the distribution of individual tube coefficients being similar.

Baffle orientation has been shown to have no effect on average coefficients, but the distribution of the data is substantially affected. The use of an impingement baffle in the inlet compartment lessens the effect of baffle orientation on distribution. Recommendations are made for future work.

KEY WORDS HEAT TRANSFER, HEAT EXCHANGER, SHELL SIDE, LOCAL COEFFICIENTS, ELECTROCHEMICAL TECHNIQUE.

ACKNOWLEDGEMENTS

The author wishes to express his gratitude to:-

The Department of Trade and Industry for sponsoring the work.

Dr. B. Gay and Dr. J. D. Jenkins for their supervision.

Professor G. V. Jeffreys for provision of research facilities in the Department of Chemical Engineering, University of Aston in Birmingham.

The technical staff of the department for their assistance in the construction of the experimental equipment.

CONTENTS

1. INTRODUCTION

Most of the work previously undertaken in the study of shell side heat transfer in shell and tube heat exchangers has been devoted to the effect of geometrical parameters on bundle average heat transfer coefficients.

In the past this has been adequate for the purpose of predicting shell side performance with the methods that were available at the time. However, the advent of precise design procedures for predicting shell side heat transfer performance has created a need for local shell side heat transfer data. One such method is being developed by the National Engineering Laboratory, the sponsors of this work.

As the local measurement of temperature differences in the side flow of shell and tube heat exchangers is difficult, if not impossible, to obtain with any accuracy, mass transfer modelling techniques have been developed by both Williams (2) and Mackley (1). Williams developed a mercury evaporation technique which did not prove entirely satisfactory, whereas Mackley developed an electrochemical technique which provided excellent data. It is this method which has been adopted in the present work. Heat transfer data can be predicted from the mass transfer data obtained by use of a suitable analogy, such as the Chilton - Colburn analogy (3).

Mackley performed a detailed study of the heat transfer performance of an internal baffle compartment of a shell and tube heat exchanger. This work is devoted to the study of the end compartments of a similar exchanger, where the differences in the flow pattern are thought to have a marked effect on heat exchanger performance.

2. SHELL SIDE HEAT TRANSFER - A REVIEW OF PREVIOUS WORK

2.1 INTRODUCTION

Probably the best means of heat transfer is by flow across tube banks, producing good fluid mixing and high heat transfer coefficients. In industry this is obtained by the use of shell and tube heat exchangers. These are essentially tube banks inserted longitudinally into cylindrical shells, fitted with baffles to guide the flow (Fig. (1)). However, the shell side flow is distorted from the ideal case, and the necessary clearances (Fig. (2)) reduce exchanger efficiency.

Heat transfer equipment design requires detailed knowledge of heat transfer coefficient data for 'clean' surfaces, fluid fouling characteristics, temperature driving force, and pressure drop data. The present work provides data for the first of these requirements, but is confined to single phase flow.

The analysis of tube side characteristics of shell and tube heat exchangers is reasonably straightforward, but shell side analysis is extremely difficult, due to the complex geometry. Full analysis needs consideration of tube outside diameter and arrangement, baffle cut, spacing and thickness, leakage clearances, and bundle by-pass characteristics.

There are a variety of types of shell and tube exchangers, and the design for the present work is based on a T.E.M.A. (34) 'E' type shell fitted with single segmental baffles as illustrated in Fig. (1).

2.2. HEAT TRANSFER ACROSS IDEAL TUBE BANKS

An ideal tube bank is defined as a laterally infinite geometrically regular tube arrangement. Half tubes used as side

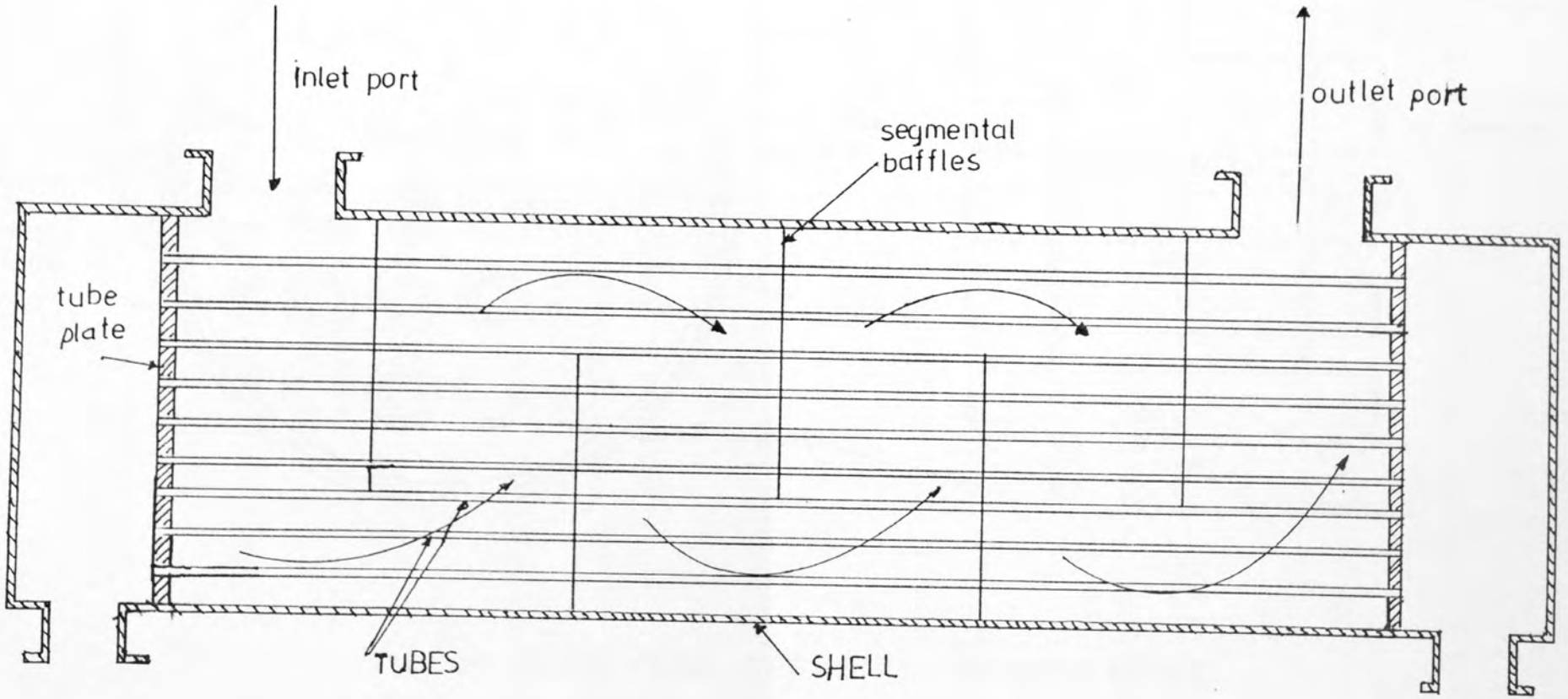

FIG. 1. SEGMENTALLY BAFFLED SHELL AND TUBE HEAT EXCHANGER WITH SINGLE PASS SHELL

(from Mackley)

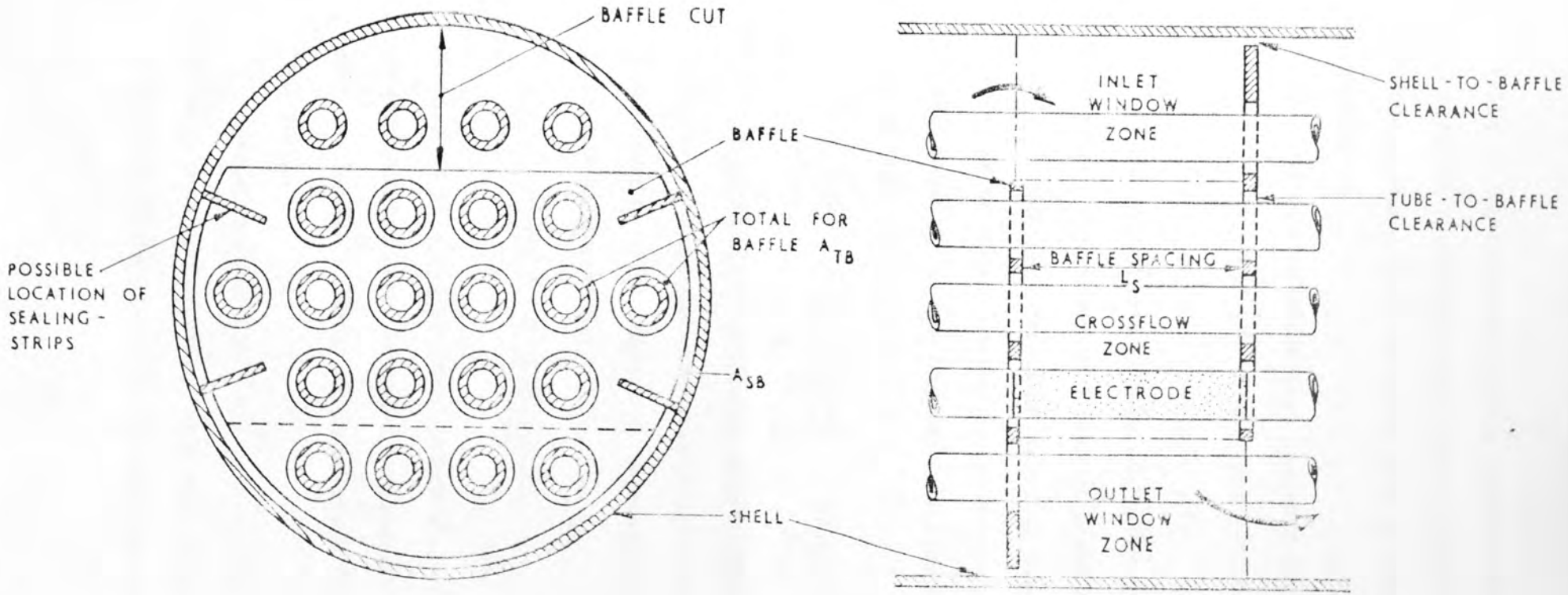

FIG. 2. SHELL-SIDE GEOMETRY NOMENCLATURE
(TUBE-ARRANGEMENT NOT TYPICAL OF THAT USED IN PRESENT WORK)
[TAKEN FROM MACKLEY]

walls in experimental studies approximate to lateral infinity. A study of rectangular tube banks in cross-flow gives a basis for investigations into the shell side of shell and tube heat exchangers.

Forced convection heat transfer for flow normal to tube banks can be described by an expression of the form:

$$Nu = c' \, Re^{m} \, Pr^{n} \qquad \text{.....2.1}$$

The constants have been evaluated by several investigations, and slight variations have been proposed by some workers.

Colburn (8) correlated existing data for staggered tube banks, using tube diameter as the characteristic dimension, basing velocity on the minimum free flow area for Re between 2000 and 32,000:

$$\frac{h\,d_t}{k_f} = .33 \left[\frac{C_p\,\mu}{k}\right]_f^{.33} \left[\frac{G_{max}\,d_t}{\mu_f}\right]^{.6} \qquad \text{.....2.2}$$

Grimison (35) correlated Huge's (36) and Pierson's (37) data for Reynolds numbers between 2000 and 40,000 for various tube arrangements. The constants, reproduced by McAdams (38), varied with tube arrangement:

$$\frac{h\,d_t}{k_f} = b' \left[\frac{G_{max}\,d_t}{\mu_f}\right]^{n} \qquad \text{.....2.3}$$

Sheehan et al. (39), however, showed that these correlations cannot be extrapolated above Reynolds numbers of 70,000, for they showed that the Reynolds number exponent rises from 0.6 to 0.8 above this range.

Bergelin et al. (41 - 43) investigated several tube arrangements in rectangular banks for a wide range of Reynolds number. In the work up to Re = 1000 the data was correlated in j-factor

form (8). A steeper slope was obtained than in the higher Reynolds number range of Colburn, but both workers concurred that for heat transfer, in-line arrangements were inferior to staggered tube banks. Their two sets of data did not correlate with a single function. Bergelin et al. (42, 43) later varied tube diameter and spacing, in a study which extended the Reynolds number range to 10,000. At the lower Reynolds numbers, staggered arrangements, regardless of tube size, showed smooth transition characteristics, with the in-line arrangements having considerable data spread and inferior heat transfer characteristics, with an abrupt transition at Re = 100. For Re = 4000, the square orientations gave coincident results, with the in-line data lying below these. However, there was some indication (41 → 43) that the data also converged at Reynolds numbers below 100. Significantly, Bergelin arbitrarally defined the laminar region as being below Re = 100, with turbulence existing for Re = 4000. The latter transition is supported by Bell (44).

Recently Zukauskas (45) surveyed heat transfer for flow across tube banks, recommending the following values of the Reynolds number exponent in expression 2.1.

Re. Range	Exponent Value	
	(a) Staggered	(b) In-line
$< 10^2$	0.4	0.4
* $10^2 \longrightarrow 10^3$	0.4 - 0.5	0.4 - 0.5
$10^3 \longrightarrow 2 \times 10^3$	0.6	0.63
$< 2 \times 10^5$	0.84	0.84

* transition zone - exponent value unreliable.

The minimum tube bank velocity was the basis of the preceding correlations, but by using a void fraction concept, Weisman (46) defined a Reynolds number based on the average tube

bank velocity, correlating the data of Pierson (37), Bergelin (41 - 43), Sheehan (39) and Kays (47) in the form:

$$j_h \varepsilon^{\phi b} = \text{Function}\left[\frac{d_t G}{\mu \varepsilon}\right] \qquad \ldots\ldots\ldots 2.4$$

where the coefficients ϕ and b were respectively dependent on the tube arrangement and the Reynolds number, with ε being the void fraction. Below Re = 30,000, the staggered arrangements (correlating to within 10 %) were superior to the in-line arrangements (correlating to within 15 %). At higher Reynolds numbers the data converged.

Recently, Whitaker (48) proposed a new correlation for the data of Bergelin (49, 50), Kays (47), Pierson (37), Fairchild (51), and Edwards (52) as:

$$Nu = (0.5\ Re^{0.5} + 0.2\ Re^{0.67})\ Pr^{0.33}\ \left(\frac{\mu}{\mu_w}\right)^{0.14} \ldots\ldots\ldots 2.5$$

This correlation was restricted to Re $>$ 100, for lower values of Re he recommended:

$$Nu = 2\ Re^{0.33}\ Pr^{0.33}\ \left(\frac{\mu}{\mu_w}\right)^{0.14} \qquad \ldots\ldots\ldots 2.6$$

Both correlations were restricted to void fractions of less than 0.65. While the data for staggered tube arrangements correlated well, in-line data produced a wide scatter, and Whitaker suggested that the effect of tube pitch be taken into account for these arrangements.

The use of the $\frac{1}{3}$ Prandtl number exponent in heat transfer correlations in tube banks was confirmed by Zukauskas et al. (53) in their investigations into 27 tube banks of different arrangements, using fluids with Prandtl numbers between 0.7 and 500. Also, the use of the $\frac{2}{3}$ property number exponent in the Chilton - Colburn

analogy (discussed in Section 3) was confirmed by Jenkins et al.(54) using the data of Mackley (1), Williams (2), Tompkins (44), Brown (44, 29), and Lucas (55, 9).

2.3. SHELL SIDE PREDICTION METHODS

The prediction of shell side characteristics of shell and tube heat exchangers can be classified into four types, as given below.

2.31 INTEGRAL METHODS

These are termed 'integral' because they consider the total shell side flow as being effective, and are extremely unreliable due to this assumption. The two main methods, due to Donahue (56) and Kern (57), are given below.

2.311 DONAHUE METHOD

By correlating the data of Short (58), Heinrich (59), Bowman (61), Gardener (60), and Tinker (62) for Re between 100 and 40,000, Donahue obtained the following expression:

$$\frac{h\,d_t}{k} = c'\left[\frac{G_Z\,d_t}{\mu}\right]^{.6}\left[\frac{C_p\,\mu}{k}\right]^{.33} \qquad \text{.....2.7}$$

where $$G_Z = (G_C\,G_W)^{.5} \qquad \text{.....2.8}$$

It is obvious that this expression is similar to that prepared by Colburn (8), where the constant 'c' depends upon leakage clearances and tube arrangement.

An improvement on the Donahue method was given by the British Ship-building Research Association (63), by correlating previous data (58, 62, 60) for Re $<$ 44,000:

$$\frac{h\,d_t}{k} = c'\left[\frac{P-d_t}{P}\right]^{.4}\left[\frac{A_W}{A_W+A_{SB}}\right]^{2}\left[\frac{G_{AV}\,d_t}{\mu}\right]^{.6}\left[\frac{C_p\,\mu}{k}\right]^{3}\left[\frac{\mu}{\mu_w}\right]^{.13} F_E \qquad \text{.....2.9}$$

where F_E, recommended by Tinker (62), accounted for the end baffle compartment characteristics. The data correlated to within 18 %.

2.312 KERN METHOD

A correlation of 'industrial data' for baffled shell and tube heat exchangers, for a variety of shells with 'typical' leakage clearances and a baffle cut of 25%, was given by Kern (57) below. No account was taken of variations in baffle cut, spacing or leakage. The correlation was quoted for Re in the range 2000 to 40,000, and was said to be accurate within 0 and 20%,

$$\frac{h D_h}{k} = \cdot 36 \left[\frac{G_k D_h}{\mu}\right]^{\cdot 55} \left[\frac{C_p \mu}{k}\right]^{\cdot 33} \left[\frac{\mu}{\mu_w}\right]^{\cdot 14} \qquad \ldots\ldots\ldots 2.10$$

Where D_h, the hydraulic mean shell diameter, is the characteristic dimension, and G_k characterises the maximum mass velocity between the tubes at the centre of the bundle.

In the past, the methods of Kern and Donahue were used in design offices, usually to the exclusion of all other means of predicting shell side heat transfer coefficients.

2.32 SEMI-ANALYTICAL METHODS

These methods were designed to give an improvement over the 'integral' methods, as they took some account of the flow distributions in baffled heat exchangers. The first approach to this method was given by Bell (64) following recommendations from the Delaware University Research Programme (29, 30, 41, 42, 43, 44, 49, 50, 65, 66, 67). The prediction correlation was a modified form of the 'integral' type equation, thus:

$$\frac{Nu}{RePr} = St = j_I \phi' \varsigma \gamma \lambda Pr^{2/3} \left[\frac{\mu}{\mu_w}\right]^{\cdot 14} \qquad \ldots\ldots\ldots 2.11$$

where j_I = ideal tube bank j-factor for any given tube arrangement.

ϕ' = baffle window correction factor.

ς = shell to bundle by-pass stream correction factor.

γ = leakage streams correction factor.

λ = tube-row number correction factor.

The individual factors are independent of each other, and are derived theoretically by Bell (64), as reproduced by Mackley (1). By using graphical simplifications, the method is simple to use.

2.33 STREAM ANALYSIS METHODS

The stream analysis methods are based on the work of Tinker (62), who recognised that the shell side flow problem can be solved by dividing the flow into a number of streams, giving each an effectiveness factor. The different streams are shown in Fig. (3). By defining an overall 'effective' mass velocity, the bundle heat transfer coefficient can be predicted from existing correlations for ideal tube banks.

Palen and Taborek (68) defined the following individual streams, (Fig. (3)), in decreasing order of effectiveness.

(1) B-stream, the true cross-flow stream, fully effective for heat transfer and pressure drop.

(2) A-stream, the stream passing through the baffle-tube clearance holes, fully effective for heat transfer, reducing pressure drop.

(3) C-stream, the bundle by-pass stream, only partially effective for heat transfer, passing around the outer halves of the outside ring of holes.

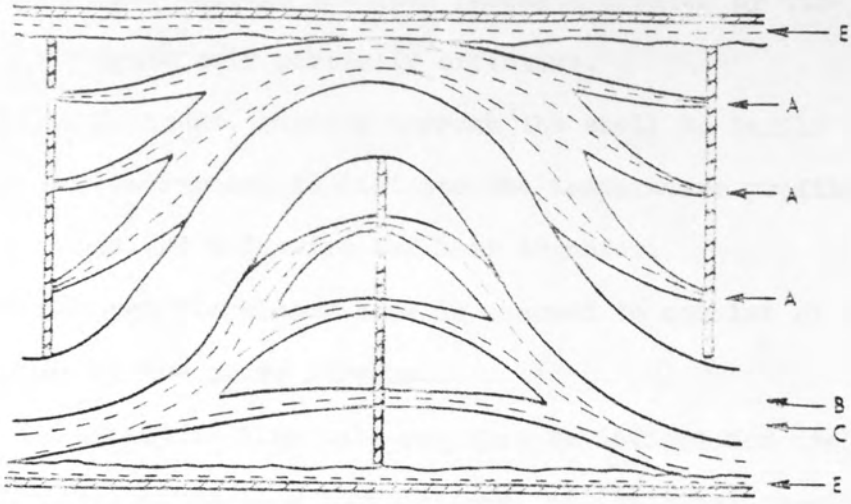

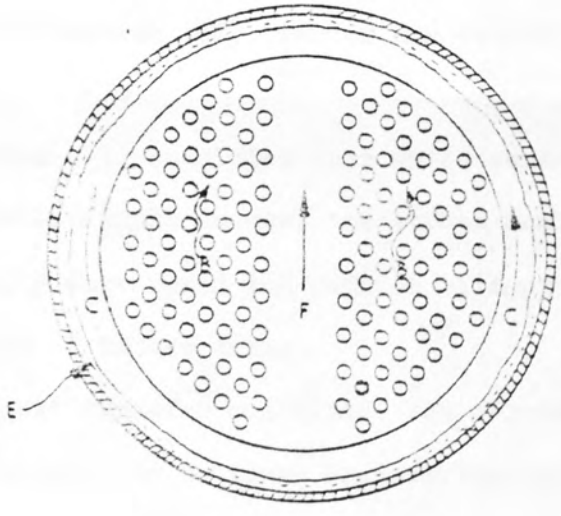

FIG 3 SHELL-SIDE FLUID STREAMS

(4) F-stream, in multitube pass systems, these streams pass through the open passages created by tube layouts, again only partially effective.

(5) E-stream, passing through the shell to baffle clearances, it distorts the temperature profile, and is not effective for heat transfer.

The flow through the window zone is assumed to consist of varying proportions of the above streams.

A net effective flow rate can then be defined for use in existing ideal cross-flow correlations, as described previously.

$$Q_{eff.} = \alpha_1 Q_B + \alpha_2 Q_A + \alpha_3 Q_C + \alpha_4 Q_F \qquad \ldots\ldots\ldots 2{\cdot}12$$

The effectiveness factors for each stream can be found from data fits, and the flow rate values can be found analytically, as in Palen and Taborek (68), Parker and Mok (69), Devore (70), and Grant (73).

Emerson (71) concludes that while semi-analytical methods are relatively simple to use, the stream analysis methods are fundamentally more sound and capable of improvement with the availability of better data.

The Heat Transfer and Fluid-flow Service (H.T.F.S.), in conjunction with the National Engineering Laboratory, are developing a stream analysis method (73), which requires knowledge of local heat transfer coefficients and pressure drops. Mackley (1) provided such data for internal baffle compartments. This work is an investigation into the end compartments.

2.34 NUMERICAL METHODS

Numerical methods are being developed by Spalding et al.(72)

as a new approach to the solution of shell side heat transfer problems. The equations which describe the flow of fluid in heat exchangers can be solved by numerical techniques. No comparisons are given with experimental data in (72). There, Spalding stresses the method's flexibility, but the accuracy of the analysis depends upon the accuracy of existing data for the flow resistance characteristics in the leakage and by-pass channels. Hence, currently stream analysis techniques are thought to be the most reliable for the prediction of shell side heat transfer.

2.4 PREVIOUS LOCAL SHELL SIDE HEAT TRANSFER STUDIES

The work on stream analysis methods led to a need for more detailed data for the shell side of shell and tube heat exchangers. Studies of heat transfer over sections of individual tubes in the bundle could provide such data. These are termed local shell side heat transfer studies.

The characteristic flow patterns in baffled heat exchangers have been identified by the flow visualisation studies of Gunter et al.(74) and Gupta and Katz (75). The main observations were that eddy currents, created behind baffles, were reduced by increasing the number of baffles (74), and the identification of three characteristic flow zones, longitudinal, true cross-flow, and eddy zones (75).

By using a heated sensing probe, Ambrose and Knudsen (76) studied local shell side heat transfer in a 152mm diameter shell with 25.4mm diameter tubes, with two bundles of four and fourteen tubes respectively. Tube increments at different positions of the bundle and variations of tube pitch and baffle spacing were investigated. More detailed studies of a single baffle

compartment were reported by Gurushankariah and Knudsen (77). Lee and Knudsen (79) extended the work to cover variations in tube baffle clearances at two baffle spacings.

The investigations showed that the baffle-tube clearance areas gave high heat transfer coefficients, as did the baffle window areas. However, increasing the tube-baffle clearance decreased the heat transfer coefficients. Also, heat transfer coefficients were reduced by increasing the baffle spacing. Confirmation of the three flow characteristics given by (77) was obtained, with the highest heat transfer coefficients being in the eddy zones. Mackley (1), suggested that this was due to high velocity jets through the tube-baffle clearances, Stachiewicz and Short (78) having shown that the reverse was true for the no-leakage case.

The fourteen tube bundle showed lower heat transfer rates than the four tube bundle, Ambrose and Knudsen attributing the reason to turbulent effects. Mackley (1), however, suggested that the increased effect of bundle by-passing was the cause, for although tube separation differed by a factor of five between the tube bundles, the clearance between the outer tubes and the shell was almost constant. Narayanan (79), using 19mm diameter tubes in the same shell, with bundles of 18 and 19 tubes found that the heat transfer coefficients were lower than was found by previous workers with similar baffle geometry, and he reasoned that this was due to a more compact bundle, but Mackley (1) suggested that it was probably due to increased bundle by-passing.

Williams (2, 80) applied a mercury evaporation mass transfer technique, predicting corresponding heat transfer data through the Chilton - Colburn heat-mass transfer analogy (3). The model

exchanger used was similar to the Model 9 exchanger of the Delaware programme (29). As with the Delaware model, internal leakage was eliminated by the use of rubber seals, with bundle by-passing reduced by careful arrangement of tubes and tie bars. Coefficients were measured for individual tubes in a central baffle compartment for a single spacing, with a variation in baffle cut (18.4%, 31.0% and 43.7%).

Baffle compartment average coefficients showed good agreement with the overall bundle data of Bergelin et al.(29), for similar bundle geometry. By calculating average coefficients for the window and cross-flow zones, the effects of baffle cut were correlated, using a suitably defined Reynolds number. Cross-flow data were correlated using a simple velocity based on the minimum flow area at the central row of tubes, whereas window zone data were correlated by use of a geometric mean velocity for cross-flow area and window area.

An analysis of individual data coefficients revealed that the distribution of heat transfer for segmentally baffled units was affected by the shell side flow rate as well as bundle geometry. For the lowest flow rates (Re = 54) the highest heat transfer occurred around the bundle perimeter, but at the highest flow rates studied (Re = 1625) the high heat transfer rates occurred in the cross-flow zone. Mackley (1) suggested that the flow resistance in the by-pass channel was lower that the bundle cross-flow region at low flow rates, but with increasing flow, the resistances became more comparable.

Williams also agreed with the flow visualisation studies that the flow distribution was distorted with increasing baffle cut, producing decreasing heat transfer characteristics, especially at

the window zone extremities where stagnant regions can exist.

The data obtained by Williams was used by Roberts (81, 82) for the determination of the distribution of local shell side velocities in the bundle. In his analysis he assumed that heat transfer variations were due to changes in local velocities around a particular tube. The velocity distribution patterns resulting from the analysis show that bundle by-passing was the major factor in flow distribution. The flow distribution was more uniform for the intermediate baffle cut (31%), and the lowest velocities, hence lowest heat transfer coefficients, existed in the outlet window zone, particularly for the largest baffle cut (43.7%).

It was noted that although Williams' studies modelled typical commercial exchangers, they were restricted to the case of no internal leakage, and the Reynolds number range covered (54 to 1625) only represented the lower end of the range used in industrial heat exchangers. However, Williams proved the viability of mass transfer modelling techniques for local shell side heat transfer studies.

Unfortunately, the mercury evaporation modelling techniques have certain disadvantages. They are very laborious, and totally unsuitable for rapid data acquisition. Also, they have certain inherent inaccuracies associated with fluid sampling and mercury deposition, discussed in detail by Mackley (1).

As a result of an extensive literature survey, a diffusion controlled electrochemical mass transfer technique was shown to have neither of these disadvantages, and such a technique was developed by Mackley for the modelling of shell side heat transfer. Sections (3) and (4) below respectively discuss the analogy between heat and mass transfer and the electrochemical technique, both aspects being fully discussed by Mackley (1).

2.5 LOCAL SHELL-SIDE HEAT TRANSFER USING AN ELECTROCHEMICAL TECHNIQUE

The electrochemical technique described below in section (4) was used by Mackley in his local shell side heat transfer investigations in shell and tube heat exchangers. His work was divided into two parts, the development of the technique, carried out at Aston, and the local mass transfer studies on the shell side of segmentally baffled shell and tube heat exchangers, using the purpose built rig at Winfrith.

The Aston work was carried out using a model shell and tube heat exchanger similar to that used by Williams (2) and Bergelin et al.(29). The bundle consisted of four 99mm long baffle compartments with 1.69mm thick baffles, using eighty 9.5mm diameter tubes arranged on a staggered square pattern with a 1.25 pitch to diameter ratio, with two baffle cuts being studied. Although most investigations were confined to the no-leakage situation, a limited investigation was carried out into shell-to-baffle leakage for the 31% baffle cut. Also investigated were variations of heat transfer along a tube length in a baffle spacing. The work covered the range $24 < Re < 1500$. Some pressure drop measurements were also made.

The Winfrith work again investigated the 133mm diameter shell, and covered leakage and non-leakage cases, together with pressure differential measurements for single segmental baffles for the range $300 < Re < 24,000$. The investigations cover two baffle spacings (48.5mm, 97mm) for three baffle cuts (18.4%, 25%, 37.5%). The non-leakage tests were carried out with 1.59mm thick baffles, the leakage tests including 3.18mm thick baffles. The leakage clearances used were based on the commercial 'Z' factors of 2.5 and

8 for shell-baffle and tube-baffle clearances respectively. The 'Z' factor is defined as:

$$Z = \frac{2 \times \text{Baffle thickness}}{\text{Diametrical clearance}} \quad \ldots\ldots\ldots 2.13$$

A limited amount of work was carried out on double segmental baffles for the leakage case using 3.18mm thick baffles for the 48.5mm baffle spacing and an 18.4% baffle cut.

2.51 ASTON DEVELOPMENT WORK

Mackley compared his compartmental average data with the similar data of Williams (2) and the bundle average data obtained by the direct heat transfer method of Bergelin et al.(29). The data for the 43.7% baffle cut were in good general agreement with that of Bergelin, and although there was a slight discrepancy at the lower Reynolds number, it was well within experimental error, as shown by Gay et al.(83). Williams' data, however, fell below Mackley's for both baffle cuts, the discrepancies being about 15% for the 31% baffle cut, and between 5% (Re = 1000) and 25% (Re = 50) for the 43.7% baffle cut. Unfortunately, no comparison was possible with Bergelin et al.(29) at the 31% baffle cut.

The explanation was thought to be that while Mackley used tight fitting plastic baffles to prevent internal leakage, Williams used metal baffles with rubber seals. During the many bundle rebuilds that were necessary in the mercury evaporation technique, the rubber seals were thought to have gradually worn giving rise to shell-baffle leakage. Photographs of Williams bundle gave evidence of such wear and tear. This resulting leakage would yield lower j-factors than a true non-leakage system. Another factor was also the inherent inaccuracies in the mercury evaporation method described previously.

Mackley also analysed his data by dividing the flow area into

zones as defined by Bergelin et al.(29). A window zone and a cross-flow zone were defined with their boundaries determined by baffle cut and baffle spacing, as in Fig. (2). The window zone was then sub-divided into an inlet and an outlet window zone depending on the direction of the shell side fluid flow.

The zonal averages were defined as the arithmetic mean of the j-factors of all the tubes contained in the particular zone. As the baffle tip coincided with the centre of a row of tubes, Mackley regarded the tubes on the baffle edges as having half their transfer surfaces in each of the zones concerned. For the zonal average coefficient calculations the coefficients of the divided surfaces were assumed to be equal.

For the 43.7% baffle cut, Mackley's data for the two window zones almost coincided, with the cross-flow zone data being considerably higher, which was predictable as visual studies (section 2.4) showed that the window areas produced stagnant zones, and also it could be expected that cross-flow would have a better transfer performance than longitudinal flow. However, at the 31% baffle cut the inlet window zone data coincided with that of the cross-flow zone, the outlet window zone data still being inferior. Although Mackley gave no explanation for this phenomenon, it was thought that the increased fluid velocity in the window area for the smaller baffle cut gave higher turbulence and hence higher inlet window zone heat transfer characteristics.

An analysis of the individual tube j-factors revealed that the j-factor variation through the bundle was less pronounced for the 31% baffle cut than for the 43.7% baffle cut. This indicated that the 31% baffle cut represented a more efficient geometry.

Mackley's limited Aston leakage investigations revealed that shell to baffle leakage had a considerable detrimental effect on the overall heat exchanger performance. It was noticeable that

Williams' data lay between Mackley's leakage and non-leakage data, providing some further indication of leakage in Williams' investigations, albeit on a lower scale than for Mackley's deliberate investigations.

Mackley's investigations into the distribution of heat transfer coefficients along tube lengths showed that the coefficients increased from the upstream to the downstream end of the tubes. Stochiewicz and Short (78) had similar findings, giving additional experimental evidence of eddy zones existing in the lee of the baffle. Measurements made in the presence of internal leakage gave indications of flow re-distribution, with a generally more even heat transfer distribution along a tube length.

Mackley performed pressure drop measurements to provide information on internal leakage, identification of flow regimes, and general bundle flow characteristics. The static pressure differentials between two adjacent points in the exchanger were reported. On comparison with the Bergelin work, it seemed that the Mackley exchanger had higher pressure drop characteristics than for the Bergelin model. Mackley thought that trapped gas in the Bergelin model could explain this, although the method of measuring pressure drop might lead to errors. These can be present, because consistent results between the Mackley and Bergelin data could only exist if the flow characteristics of the two exchangers were identical, which seemed unlikely. However, the data for the 31% baffle cut showed that pressure drop was inversely proportional to baffle cut, which was expected because of the higher flow resistances at the smaller baffle cuts.

Mackley's development work showed that the electrochemical mass transfer analogy method provided a suitable means of obtaining local heat transfer data. The second part of his work provided a

detailed study of shell side heat transfer for an internal baffle compartment.

2.52 LOCAL SHELL SIDE HEAT TRANSFER STUDIES AT WINFRITH

Mackley's investigations at Winfrith can be sub-divided into three sections, single segmental baffles without internal leakage, single segmental baffles with internal leakage, and double segmental baffles with internal leakage.

2.521 SINGLE SEGMENTAL, NO LEAKAGE CASE

The non-leakage investigations were carried out using 1.59mm thick baffles at two spacings and for three baffle cuts. The results were compared with those of Bergelin et al.(29) and Williams (2). The 18.4% baffle cut, 48.5mm spacing data on comparison with Bergelin gave almost complete agreement, and the 18.4% cut, 97mm spacing data were in good agreement with the corresponding data from Williams. This showed up inconsistencies in the work of Williams, as the Aston data (for different bundle geometries) was in complete disagreement with Williams. A pressure drop comparison with Bergelin also gave agreement, to within 10%.

Mackley compared the 'third' and 'fifth' compartments of his bundle for the short spacing, and found there to be a 10% discrepancy, with the data of the 'third' compartment being lower. As a statistical error analysis (84) on Mackley's data gave an accuracy of $\pm$ 3% for 95% confidence limits, this could be considered significant. The discrepancy was thought to be due to the flow into the 'third' compartment still possessing some entrance effects from the inlet port.

Mackley assumed in his development work at Aston that a line of symmetry existed in the bundle, hence he investigated only 44 of the 80 tube positions. The Winfrith data confirmed that, for all

six no-leakage baffle configurations, the mass transfer coefficients of symetrically positioned tubes were within 5% of each other. Furthermore, the mean coefficients for each half of the bundle were within 2%, hence, Mackley's assumption was justified.

Mackley analysed the compartment average data in three ways in an attempt to correlate for variation in baffle geometry as well as Reynolds number. The first used the characteristic velocity using the minimum cross-flow area at the centre row of tubes, but no overall correlation was obtained. By using a geometric mean of the cross-flow area velocity and the window area velocity the effect of baffle cut could be correlated within 10%, but the effect of baffle spacing was not so correlated. A similar result was obtained by using the arithmetic mean of the maximum and minimum cross-flow velocities and the window velocity. Jenkins et al.(85) presented a technique for the comparison of possible correlations by using a small digital computer giving a V.D.U. output. It could be concluded, therefore, that no simple characteristic velocity would correlate heat transfer data for all variations in geometry as well as Reynolds number. No improvement was found when the zonal average j-factors were studied, although confirmation of the Aston results was obtained showing that the highest j-factors were found in the cross-flow region of the bundle.

2.522 SINGLE SEGMENTAL BAFFLES WITH LEAKAGE

In this series of experiments, Mackley incorporated shell-baffle and tube-baffle leakage clearances into his model. The clearances are those recommended by TEMA (34), using the orifice shape factor, Z, that Bergelin et al.(30) define as:

$$Z = \frac{2 \times \text{BAFFLE PLATE THICKNESS}}{\text{DIAMETRICAL CLEARANCE}} \quad \ldots \cdot 2.13$$

Values of Z of 8 and 2.5 were used for tube-baffle and

shell-baffle clearances respectively, which appeared to be normal industrial practice. Investigations were reported with the inlet window to the test compartment in the top, bottom, and side position, for 3.18mm and 1.59mm baffle thicknesses at the short baffle spacing over three baffle cuts.

The compartment average j-factors for both baffle thicknesses at the 18.4% baffle cut were compared with the corresponding no leakage case. The results showed that the presence of internal leakage substantially reduced the compartment average j-factor. Further, the thinner baffles, with the corresponding smaller leakage areas showed better average j-factor characteristics than for the thicker baffles. Data were obtained for top and bottom inlets, and showed that the compartment average j-factor was independent of the orientation of the baffle inlet. It was suggested, that because of the significant difference between the two baffle thicknesses, and because the orifice shape factors were the same in both cases, the controlling influence was the leakage area available rather than the orifice shape factor.

An investigation of the zonal averages for the 18.4% baffle cut and the thicker baffles showed that the data for all zones for both top and bottom inlet positions agreed to within 10%. A study of the individual tube j-factors revealed that, in general, they lay within 10% of the compartment average j-factors. This showed that the j-factor distribution for the leakage case was very uniform. It was thought that this was caused by the introduction of longitudinal flow throughout the bundle (due to leakage) which suppressed turbulent eddies behind the baffle windows, leading to the more uniform j-factor.distribution.

A comparison for the data from the 1.59mm thick baffles at the 18.4% baffle cut with data from Bergelin et al.(30), with the

same characteristic velocity being used by both workers (minimum cross-flow area), showed no agreement. This can be explained by the differing leakage clearances, although the differences in slope of the two sets of data suggested that leakage had different effects on bundle average and compartment average data. Also, little was known about the effects of the inlet and exit ports of these two different types of exchanger.

Mackley also compared the pressure drop characteristics with Bergelin's data. Although the Mackley data fell above that of Bergelin, the data point scatter of both workers and the suspected inaccuracy in the pressure drop measurements, previously discussed, led one to believe that the differences were insignificant, and that the pressure drop characteristics were in agreement.

In commercial heat exchangers, the baffles are often arranged so that the flow weaves from side to side, that is, side inlets to the internal baffle compartments are used. This gives the advantage of a liquid drainage channel in the exchanger, and also allows full support of the tubes in the bundle.

Mackley gave comparisons of top, bottom, and side inlet data for both leakage and non-leakage situations which showed that baffle orientation had no effect on the compartment average j-factor.

Investigations into the effect of baffle cut for the 3.18mm thick baffles on compartment average j-factors for the leakage case were also reported for side to side flow. The compartment average j-factors for the three baffle cuts were compared, and the corresponding non-leakage data were also shown. Mackley's results demonstrated that although leakage produced lower overall j-factors, the effect of baffle cut was not as noticeable. The 18.4% and 25.0% baffle cuts fell on the same curve, with the 37.5% baffle cut

data falling on a curve no more than 20% lower. This could be expected because a smaller proportion of the flow actually passes through the window area, and the reduction in window area with decreasing baffle cut was offset by the increase in leakage areas. As could be expected it was seen that leakage had an increasing effect on the compartment average j-factors with Reynolds number.

A study of the individual tube data revealed that the j-factor distribution was more uniform across the bundle than for the no leakage case. The uniformity increased with decreasing baffle cut, which was expected because of the longitudinal flow presented by leakage, previously stated. This is smaller at larger baffle cuts, hence the uniformity was not so marked in these cases.

A comparison of the leakage and non-leakage pressure drop data revealed that, as expected, leakage produced a marked decrease in the pressure drop of the compartment. The reduction of pressure drop was about 600%, compared with the 60% reduction in the compartment average j-factor. Bergelin et al.(30) drew the same conclusions.

It may be concluded from Mackley's leakage investigations that baffle leakage had a far greater effect on pressure drop than it did on the compartment average j-factors, and also the distribution of individual tube j-factors were more uniform for the leakage case. It was known that shell-baffle leakage produced no desirable effects, and therefore effort should be made in industrial exchangers to reduce this to a minimum. It might be economically more efficient, however, to deliberately increase the tube to baffle leakage to reduce pressure drop and therefore reduce pumping costs, and also produce a more uniform distribution of heat transfer characteristics.

Another conclusion was that as the compartment average j-factors

were independent of baffle orientation, this consideration could be ignored in shell and tube heat exchanger design.

2.523 DOUBLE SEGMENTAL BAFFLES WITH LEAKAGE

In the last part of this work Mackley reported some experimental work using double segmental baffle designs. Unfortunately, no previous data were available, hence no direct comparisons with previous work were possible. Due to the less tortuous nature of the flow path, it was thought that the pressure drop would be considerably less than for the corresponding single segmental case. However, the shell side heat transfer coefficients were also thought to be smaller due to the further deviation from ideal cross-flow.

With double segmental baffles, geometric symmetry existed about a plane through a diameter parallel to the baffle cut, and the shell side flow was assumed to be equally distributed between these two halves of the bundle, with the flow in each half similar to flow in a single segmental heat exchanger. It was therefore thought that a double segmental baffle unit could be analysed as two equal single segmental baffled units fitted in parallel, although there was a liquid/liquid interface present between the two halves of the bundle.

Single shell inlet and outlet ports produced mal-distribuutions of the flow in the end baffle compartments, with the result that true symmetrical flow might only exist in a few central compartments.

Mackley's experiments on double segmental baffled heat exchangers demonstrated the general performance characteristics of these baffle arrangements. His reported results were limited to the short baffle spacing with an 18.4% double segmental baffle cut configuration, and pressure drop measurements were also given. The baffles used were the 3.18mm thick leakage baffles cut down to a

double segmental design. Hence, no non-leakage cases were investigated. The velocity used for the Reynolds number was based on a hypothetical non-leakage cross-flow velocity, based on the minimum area for cross-flow in the middle row of tubes in one half of the bundle, i.e. in the middle of the cross-flow zone.

A comparison of data from the two half bundles was given in order to test symmetry. It was shown that for the compartment tested (fifth of nine), that there was no significant difference between the compartment average coefficients for the two halves of the bundle, i.e. the assumption of symmetry was justified for the test compartment.

In adjacent baffle compartments, the shell side flow converges and diverges respectively, hence a comparison was required. Mackley's comparison showed that the two sets of data were in complete agreement. The comparison was also made for the zonal averages, with no significant difference being noticeable between the zonal average j-factors. This showed that in double segmental baffled exchangers the shell side j-factor distribution is extremely uniform.

As it was thought that double segmental exchangers were equivalent to two equal parallel single segmental exchangers, some test of this was obviously needed. Unfortunately, Mackley was unable to provide an exact comparison between the double segmental data and 'data' for two equal single segmental exchangers in parallel of total cross-sectional area equal to that of the double segmental exchanger. However, Mackley assumed that the flows in the two halves of the double segmental exchangers were equal, as symmetry for the test compartment had been confirmed. Data from this 'half' bundle were then compared with data from the corresponding single segmental work at flow rates equal to those in the 'half' bundle

of the double segmental exchanger. The double segmental data fell significantly above those from the single segmental exchanger, and Mackley reasoned that this was due to differing amounts of leakage in the two arrangements. He attempted to correct for this using the leakage/non-leakage comparisons of his single segmental work, although the difference in the two data sets was reduced, it was still significant. It should be noted that a comparison between the half compartment double segmental data and the single segmental compartment average data, based on the same flow rate in the single and the 'half' double segmental exchangers was not entirely valid for the following reasons.

(1) The 'half bundle' of the double segmental exchanger had approximately only half the cross-sectional area of the single segmental exchanger and was also geometrically different.

(2) The two sets of data were based on two different characteristic flow areas. In the single segmental work, the velocity was based on the minimum flow area of the centre row of tubes in the cross-flow area, a row of eight tubes. In the double segmental half bundle, the velocity was based on the same criteria, but here, the middle row of tubes in the cross-flow zone contained only seven tubes in a narrower segment of the exchanger. Hence, the two areas on which the velocities were based are different for equal flow rates. This means that, although the volumetric flow rates were the same in Mackley's comparison, the velocities, and hence the Reynolds numbers, were different. Therefore, Mackley's attempts at comparing the j-factors were for two different baffle arrangements for Reynolds numbers defined differently. Hence, no true comparison could be made since no common basis for comparison existed.

A comparison of the mass transfer performance, on a total shell side flow basis, of the 18.4% baffle cut double segmental exchanger with the 37.5% baffle cut single segmental exchanger showed some agreement. However, it was not clear what basis Mackley used to derive the velocities for the double segmental case, hence the previous comments might also apply here. A comparison of the pressure drop characteristics of the two exchangers gave good agreement, hence it was thought that the overall performance of a double segmental heat exchanger could be matched by that of a single segmental exchanger with twice the baffle cut. However, double segmental arrangements showed more uniform j-factor distributions than the single segmental exchangers with larger baffle cuts.

Mackley's data showed that there could be similarities in the performance of heat exchangers with differing baffle design. A plot of the mass transfer and pressure drop data for all the baffle configurations examined, at a single flow rate, showed that the data fell near to a single curve. Hence, a required heat exchanger performance could be obtained from more than one baffle design and arrangement. It was also shown that any increase in heat transfer characteristics would be matched by a corresponding increase in pressure drop characteristics, so design optimisation must take both into account.

3. THE ANALOGY BETWEEN HEAT AND MASS TRANSFER

3.1 INTRODUCTION

The similarities that exist between the differential equations that describe heat, mass and momentum transfer enable analogies to be made, from which expressions can be derived to predict heat and mass transfer data from corresponding fluid friction data. Hence, heat transfer data can be predicted from experimental mass transfer data and vice-versa.

The differential equations describing the convection of heat and mass in steady flow simplify to (in their vector form):

$$C_p \rho \, u.\nabla T = k \nabla^2 T \qquad \text{.....3.1}$$

(heat transfer)

$$u.\nabla C = D_v \nabla^2 C \qquad \text{.....3.2}$$

(mass transfer)

Many heat and mass transfer analogies have been proposed from the solution of these differential equations for dynamically similar conditions.

As the complete analytical solution of these equations is generally impossible, the analogies so formed are of semi-empirical form. One such analogy, which Mackley (1) has chosen for his work, and is retained for the present work, has been proposed by Chilton and Colburn (3).

3.2 THE CHILTON - COLBURN ANALOGY

Reynolds (4) first suggested an analogy between heat and momentum transfer. By assuming that the fluid was turbulent right up to the solid surface he showed that

$$\frac{\tau}{\rho u^2} = \frac{h}{\rho u C_p} \qquad \text{.....3.3}$$

However, this expression is only valid when the Prandtl number of the fluid is close to unity.

By assuming the existence of a laminar sub-layer where heat and momentum transfer takes place solely by molecular diffusion, Taylor (5) and Prandtl (6) modified the Reynolds analogy. However, it assumes that the Reynolds analogy is applicable right up to the edge of the laminar sub-layer from the bulk stream of the fluid. By making these assumptions Taylor and Prandtl derived the expression:

$$St = \frac{h}{\rho u C_p} = \frac{\tau}{\rho u^2} \cdot \frac{1}{1 + \sqrt{(Pr - 1)}} \qquad \ldots\ldots\ldots 3.4$$

It can be seen that when the Prandtl number is close to unity, the expression reduces to the Reynolds analogy.

Sherwood (7) developed a corresponding expression for the analogy between mass and momentum transfer, as given below:

$$\frac{K_c}{u} = \frac{\tau}{\rho u^2} \cdot \frac{1}{1 + \sqrt{(Sc - 1)}} \qquad \ldots\ldots\ldots 3.5$$

These expressions are derived by making the assumption that there is an abrupt transition from turbulent to laminar flow at the boundary of the laminar sub-layer.

By correlating in terms of j-factors, Colburn (8) showed for turbulent flow in pipes, that heat transfer data showed the same characteristics as a friction factor correlation. He represented the heat-momentum relationship by the expression :

$$j_h = \frac{h}{\rho u C_p} Pr^{2/3} = \frac{\tau}{\rho u^2} = .023\, Re^{-.2}$$

$\ldots\ldots\ldots 3.6$

where j_h is defined as the heat transfer j-factor. It can

be seen that the term $Pr^{2/3}$ replaces the term $[1 + v(Pr - 1)]^{-1}$ as the correction factor to the Reynolds analogy.

By defining a mass transfer j factor, j_M, Chilton and Colburn (3) applied the Colburn analogy to the analogy between heat and mass transfer:

$$\frac{K_c}{u} Sc^{2/3} = j_M = j_h = \frac{h}{\rho u C_p} Pr^{2/3} \qquad \text{.....3.7}$$

This empirical analogy has been shown to be applicable to the flow across tubes and over plane surfaces, as well as to flow in tubes.

Dynamic similarity and similarity of boundary conditions are required by the analogy. The use of the Reynolds number fulfils the first condition. The second condition implies that the type of boundary condition is the same in both cases. However, Lucas (9), in his studies of rapid heating furnaces, showed that the analogy still held for the case of a constant heat flux system being modelled by an electrochemical mass transfer method.

3.3 RANGE OF APPLICATION

The analogies between momentum, mass and heat transfer have all been derived for turbulent flow, and Colburn originally defined the analogy to be true only for Reynolds numbers in excess of 10,000. This is because in laminar flow the distortion of the velocity gradient by thermal gradients in heat transfer is far greater than by the corresponding concentration gradients in mass transfer.

However, the Chilton - Colburn analogy can be applied to shell side flow for much lower Reynolds numbers, because laminar flow is thought only to exist in this case at very low Reynolds numbers, because of the distortion of shell side flow due to the

presence of the exchanger tube bundle. Mackley, in his studies of internal baffle compartments, has shown this to be true, for satisfactory data has been obtained using the Chilton - Colburn analogy for Reynolds numbers as low as 24.

4. THE ELECTROCHEMICAL TECHNIQUE

4.1 INTRODUCTION

With this technique the transfer surface, in this case the relevant sections of the heat exchanger tubes, is replaced by a suitable electrode. A suitable electrolyte is used as the flow medium and an electrical potential is applied between this and another electrode elsewhere in the system. By operating under diffusion-controlled conditions, the mass transfer coefficient for the electrode is obtained from electric current measurements.

The technique has several advantages over other mass transfer modelling techniques and methods of direct heat transfer measurement, as it allows not only the measurement of space averaged values, but also local values of transfer rates as well. The simplicity of the method enables a minimum of instrumentation to be used, and it also leads to high accuracy as electric current and velocity are effectively the only measured variables.

However, this technique has the limitation of being only directly applicable to the study of transport phenomena associated with liquids. Also, the choice of liquids is restricted to those that exhibit diffusion controlled electrochemical reaction characteristics.

4.2 THE DEVELOPMENT OF THE TECHNIQUE

The usefulness of diffusion controlled electrochemical processes in transport phenomena studies was discovered in the early work of Levich (10) and Agar (11), and since then the diffusion controlled electrochemical technique has been used in a variety of convective heat and mass transfer studies. Mizushina (12) gave an appraisal of the technique in transport phenomena. The technique was applied to the study of flow in pipes (13, 14, 15), pipe flow at abrupt expansions (16), flow in

annuli (17, 18, 19), flow over cylinders (14, 20, 21, 22), and flow through packed and fluidised beds (23, 24, 25). Recently the use of the electrochemical technique has been reviewed by Wragg (40).

Mackley (1) developed the technique for the study of heat transfer on the shell side and tube heat exchangers.

4.3 THEORY OF THE ELECTROCHEMICAL TECHNIQUE

The electrochemical process can be seen as a heterogeneous chemical reaction in that ions move from the bulk of the electrolyte to the surface of the electrode where chemical and physical changes occur. The operating conditions are chosen so that the transfer rate of the ions to the electrode surface is made the controlling step, hence the effect of the electrochemical reaction rate at the electrode surface is assumed to be zero. This is convenient because when the current becomes independent of the applied potential (the limiting current), the surface concentration of the reacting ions can be taken as zero, and hence only the bulk concentration, effectively a constant, need be taken.

The rate of the electrochemical reaction is controlled by the movement of the reacting ions to the electrode surface. This movement is brought about by migration due to the potential field, diffusion due to the concentration gradient, and forced convection by fluid flow.

If a large excess of an indifferent electrolyte is added to the solution, then the effect of migration due to the potential field can be neglected, (Butey and Knudsen (26)). Hence, the transfer rate of the reacting ions can be expressed as:

$$N = Kc.\ S.\ (C_b - C_s) \qquad \ldots\ldots\ldots 4.1$$

Now, the current density at the electrodes is given by:

$$I = N.\ n_e.\ F. \qquad \ldots\ldots\ldots 4.2$$

Hence:

$$K_c = \frac{I.(n_e.F.)^{-1}}{(C_b - C_s)\ s} \qquad \ldots\ldots\ldots 4.3$$

where I is termed the 'diffusion current', as it is associated with pure diffusion mass transfer.

The surface concentration is zero when the current density is at the limiting value (Mackley (1)), i.e. when no further increase in the current can be made by increasing the electrode potential. This is given by a plateau on the current-potential plot. However, if the potential is increased too much, the occurrence of secondary electrode reactions can increase the current density. This can be easily avoided as the plateau is quite clearly marked in the system used. Hence, by operating at the limiting current density, the surface concentration is effectively zero, and the mass transfer coefficient is given by:

$$K_c = \frac{I_L.(n_e.F.)^{-1}}{C_b.\ s} \qquad \ldots\ldots\ldots 4.4$$

In practice, the theoretical limiting current density cannot be fully reached because of chemical polarisation in the region of the electrode. However, Wilke et al.(27) has found that a value of 10^{-3} for the ratio C_s to C_b is obtainable, hence for practical purposes the assumption of C_s being zero is justified.

However, for every electrochemical system a critical fluid velocity exists. If this is exceeded the plateau on the current-potential plot cannot be achieved. This is due to chemical polarisation becoming significant, as the reacting ions cannot be removed from the electrode surface at the higher diffusion rates. Hence, the surface concentration is no longer zero and equation (4.4) is no longer valid. However, this difficulty need not arise if the velocity is kept from reaching the critical value.

The diffusion controlled phenomenon, however, requires that

the other electrode in the system is non-controlling, i.e. the current density at the other electrode is negligible in comparison to that of the test electrode. This is achieved by making the other electrode large in comparison with the test electrode.

4.4 THE POTASSIUM FERRI-FERROCYANIDE SYSTEM

The potassium ferri-ferrocyanide system is the one chosen by Mackley (1) as the electrolyte medium for his work, and the same system is retained for the present studies.

The system chosen is the cathodic reduction of potassium ferricyanide on nickel electrodes. It consists of equimolar concentrations of potassium ferricyanide and potassium ferrocyanide, with sodium hydroxide as the indifferent electrolyte.

The principal electrochemical reactions of this REDOX system are:

$$Fe\ (CN)_6^{3-} \longrightarrow Fe\ (CN)_6^{4-} \qquad \text{(Cathode)}$$

$$Fe\ (CN)_6^{4-} \longrightarrow Fe\ (CN)_6^{3-} \qquad \text{(Anode)}$$

A detailed discussion of the theory of this system is given by Mackley (1).

The choice of this system over other electrochemical systems has been made because:

(1) The electrodes are unchanged by the process.

(2) Chemical polarisation is usually negligible, even at high mass transfer rates because of the rapidness of the electrochemical reactions. This leads to the system having a high critical velocity. (4.26 m/s - Eisenberg et al.(28)).

(3) Steady state electrode potentials are achieved rapidly.

(4) As this is a REDOX system, where the reactions at the electrodes are complementary, the bulk concentrations of the reacting ions remain constant. Competing electrochemical reactions

can be avoided if the discharge potential range for the limiting current is not exceeded.

(5) The concentration of the chemicals in the system can be determined easily and accurately by volumetric titrations.

Certain precautions are necessary when using the ferri-ferrocyanide system, due to the relative instability of the ferri-and ferrocyanide ions when in solution. Dissolved oxygen and sunlight can considerably affect the solution, oxidising the ferrocyanide to ferricyanide, and also oxidising the ferricyanide to ferric oxide, which is then deposited. Mackley (1) gives the precautions which should be taken to overcome these unwanted reactions, and these are discussed in a later section.

5. EXPERIMENTAL EQUIPMENT

5.1 INTRODUCTION

The experimental technique for the electrochemical method has been developed in detail by Mackley (1), but new apparatus has been designed and built at Aston for the present work. This has been found necessary because of certain modifications that are needed to the design of the previous apparatus.

The experimental rig has been designed to be as compact as possible so that the quantity of electrolyte that is needed for the experimental work is reduced from approximately 500L to 100L. The reasons for this course of action are mainly economic, although from the safety aspect it is wise to have as small as possible quantity of caustic soda up at any one time. Other modifications to the apparatus design are described below.

5.2 ESSENTIAL FEATURES

The electrolyte, that is the shell side fluid, is circulated through the model heat exchanger. Measurements of mass transfer coefficients on the shell side of the tubes are made using the electrochemical technique previously described. A tube side fluid is not necessary because of the nature of the technique.

The materials of construction are based upon recommendations given by Mackley. Perspex is used in the construction of the model heat exchanger, whereas QVF glassware is used in the construction of the flow circuits.

Due to the size of the available pump, the equipment is limited to a maximum flow rate of approximately 130 L/min corresponding to a shell side Reynolds number of approximately 11,000.

5.3 ELECTROLYTE FLOW CIRCUIT

The electrolyte flow circuit is designed to be as compact

as possible. A flow diagram of the circuit is given in Fig. (4). The pipework, storage vessels, and the pump are constructed from standard QVF glassware, the model heat exchanger being constructed from perspex. Standard QVF P.T.F.E. bellows protect the flow circuit from pump vibrations and also from movement of the model heat exchanger on tube bundle removal. Gaskets are constructed from either P.T.F.E. sheathed compressed asbestos or from neoprene rubber. Except for the flow measurement section, which is sized to fit the flowmeters, the pipework is of 1½ in. (38mm) nominal bore.

The electrolyte storage vessel is of 18 in. (457mm) diameter QVF glassware with a capacity of 200L. A stainless steel sparge pipe feeds nitrogen into the vessel for the removal of dissolved oxygen from the electrolyte (Mackley (1)). Also a nitrogen bleed pipe is attached to prevent oxygen entering the storage tank. The electrolyte return line from the model exchanger, the by-pass line, and the nitrogen lines all enter the storage vessel through a 5/8 in. (16mm) thick perspex lid, attached to the vessel by standard QVF compression fittings with a standard QVF gasket. The nitrogen pressure is kept constant by a nitrogen outlet in the perspex lid passing through a water lute relief valve, set to 5 in. water gauge. The activation electrolyte storage vessel is similar, except that there is no nitrogen sparge pipe, and that it is built from 12 in. (305mm) diameter QVF glassware with a 50L capacity. A combined drainage-filling point is attached to the connecting pipe between the two vessels. Each vessel can be isolated from the flow circuit, so that the same circuit is used for both the activation process (preparation of the electrodes before commencement of experimental work) and the main electrochemical process. This modification has been made to

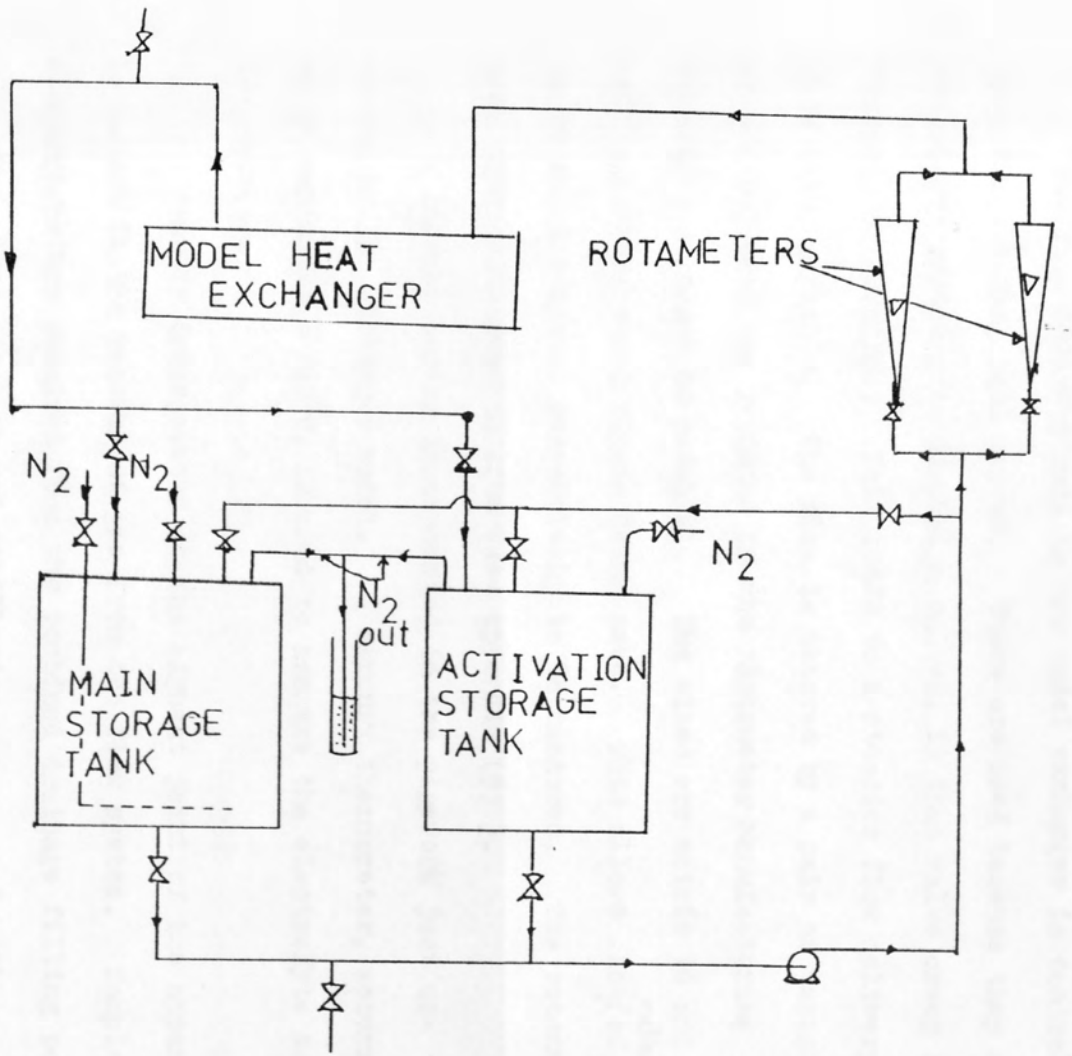

FIG. 4.

ELECTROLYTE FLOW CIRCUIT

reduce the capital cost of the rig.

A G.P.R. 9 QVF centrifugal glass pump is used. The impeller as well as the body is constructed of glassware, with the gland being P.T.F.E. with a ceramic facing. A by-pass line is incorporated into the delivery line to prevent overloading at low flow rates.

The flow delivery rate to the model exchanger is controlled by 1 in. (25.4mm) ball valves. These are used because they are considered superior to diaphragm valves, in that valve creep is reduced to a minimum. This leads to a steadier flow delivery rate being possible. The flow is metered by a pair of variable area flowmeters (as produced by the 'Rotameter Manufacturing Company') arranged in parallel. The sizes are metric 18 and 65, with stainless steel floats being used. This allows flow rates of up to 10 and 200 L/min. respectively to be measured. The rotameters have been calibrated in situ (see appendix (5)).

A thermometer is incorporated in the pipework just upstream of the exchanger model. A mercury thermometer, accurate to an estimated $\pm$ 0.2°C, is used to measure the electrolyte solution temperature.

A vent is incorporated at the highest point of the apparatus to assist in the removal of gas from the flow system. Samples of electrolyte are obtained from the combined drainage filling point.

The glass pipework and ancillaries are covered with aluminium foil to protect the electrolyte from the effects of sunlight (Mackley (1)).

5.4 THE MODEL HEAT EXCHANGER

The heat exchanger model employed in the present work is based upon the models previously in use by Williams (2) and Mackley (1). It is also geometrically similar to the heat exchanger of Bergelin

et al.(29, 30) in their overall shell side heat transfer work.

5.41 TUBE BUNDLE CONSTRUCTION

The tube bundle is comprised of eighty 9.8mm O.D. perspex tubes approximately 455mm long arranged on a staggered square pattern with a 1.25 pitch to diameter ratio. Fifteen of the tubes have 9.8mm O.D. electrodes 48.1mm long attached to their ends, and are strategically placed in the bundle. The end plate at the non-electrode end of the bundle consists of two chrome-plated mild steel full face baffle plates sandwiching a sheet of neoprene rubber, cut to give a tight seal for both tube-baffle and shell-baffle edges. Both the neoprene rubber and the metal baffles are 1.6mm thick. The first five baffle plates from the non-electrode end are standard 1.65mm thick chrome-plated mild steel with leakage clearances and 18.4% baffle cut down. The next two baffle plates are of 3.3mm thick polypropylene sheet made to a tight fit to eliminate internal leakage. These also have an 18.4% baffle cut. The electrode end plate is also of 3.3mm thick polypropylene made to a tight fit for no leakage, this baffle being full face. As the end baffle compartments only are to be studied in detail, it is considered that this arrangement is adequate for non-leakage studies.

The baffle spacing is maintained by eight 3.3mm diameter stainless steel screwed rods. The separation of the tube plates is fixed at 16in (406mm). A constant baffle spacing of 47.6mm is used throughout, and the 18.4% baffle cut-down is used throughout the experimental work.

5.42 SHELL CONSTRUCTION

The shell design is based upon the model Mackley had used in his development work. A detailed design drawing of the shell is given in Fig. (5).

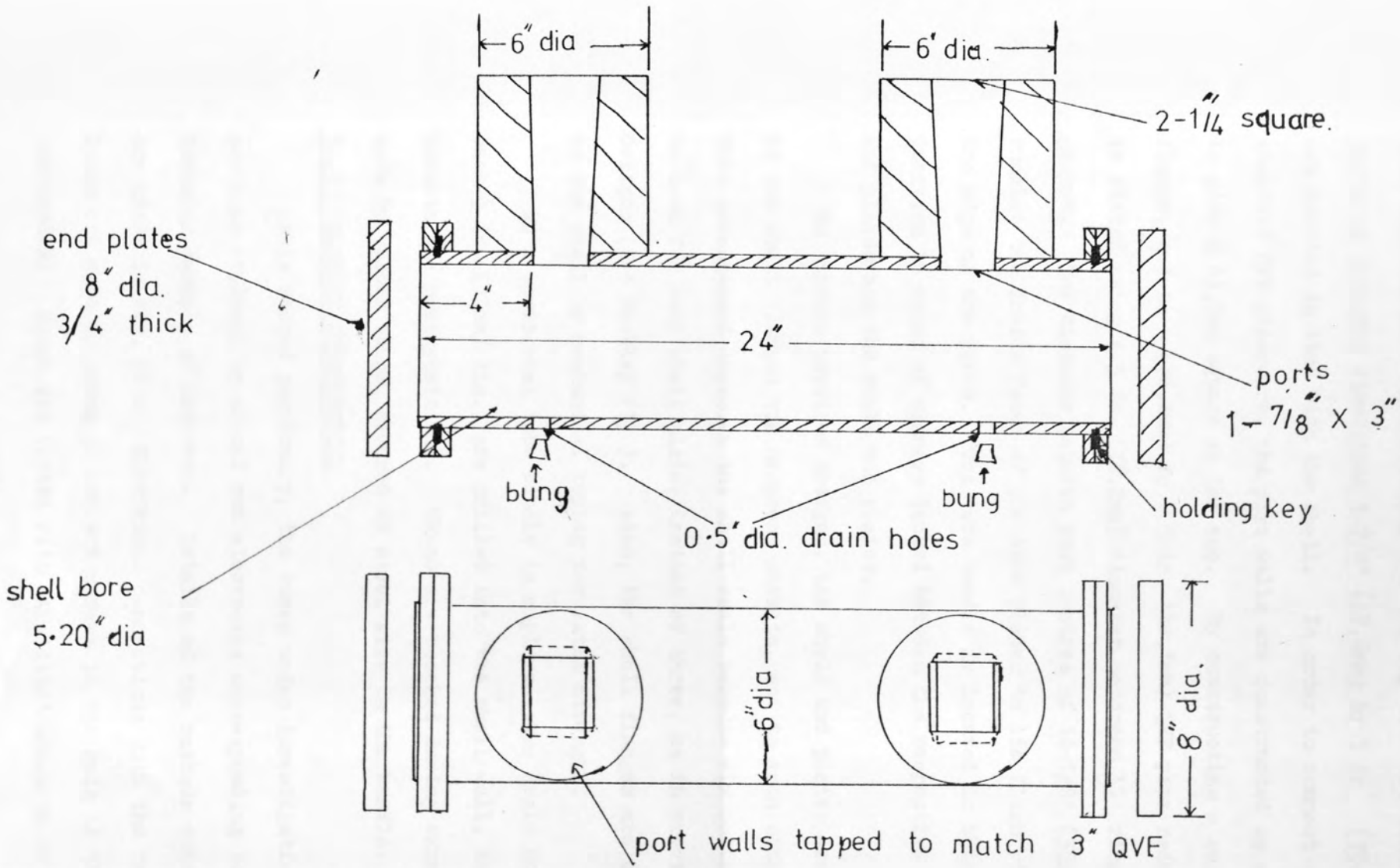

FIG 5 SHELL CONSTRUCTION

The shell is 24 in (610mm) long with a 5.2 in (132mm) I.D. constructed in 3/8" (9.5mm) thick perspex. Two rectangular ports of internal dimensions 1-7/8" (47.6mm) by 3 in (76.2mm) are mounted in line with the shell. In order to connect on to standard QVF glassware, the port walls are constructed so as to give a 63.5mm square at the top. By constructing a suitable flange, a 3 in (76.2mm) to 1.5 in, (38.1mm) QVF pipe reducer is fitted using a 3 in, (76.2mm) diameter neoprene 'O' ring as gasket. The distance between port centres of 14-1/8" (359mm) enables the inside faces of the tube plates to lie flush with the edge of the ports. The tube bundle is located in this position by means of spacers locked between the respective tube end plates and the shell end plates.

To improve previous designs, the shell end plates are bolted to the shell flanges via neoprene gaskets, not to each other. This arrangement improves the shell seals because six bolts can be used for each shell plate, instead of three, as in previous designs (see Mackley (1)). Also, the shell flanges are attached to the shell by mechanical keying for extra strength.

As a horizontal tube bundle is employed, two drain holes, each $\frac{1}{2}$ in, (13mm) dia., are drilled into the shell wall, immediately beneath the port positions. These are blocked during experimental work by rubber bungs, secured by steel wire to the bundle.

5.43 CATHODE CONSTRUCTION

As is stated previously, the tubes under investigation have sections replaced by nickel rod electrodes corresponding to the transfer surface of interest. Details of the cathode construction are given in Fig. (6). Electrical connections with the terminal leads are made by means of contact screws in the ends of the electrodes. These are coated with 'Araldite' adhesive to ensure

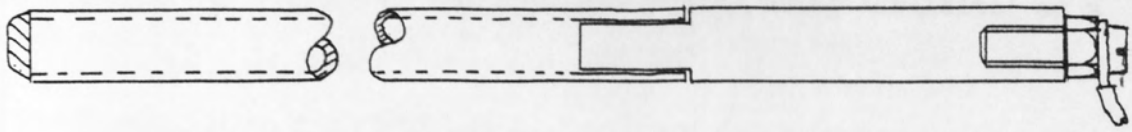

FIG. 6. CATHODE CONSTRUCTION
(actual size)

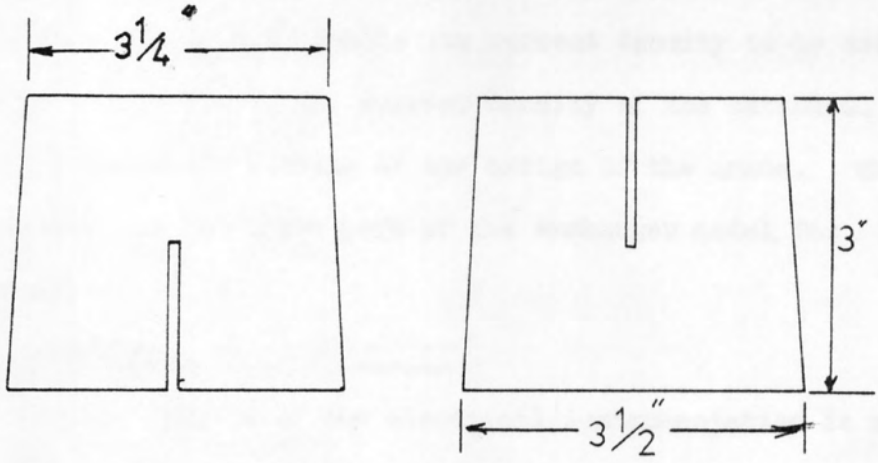

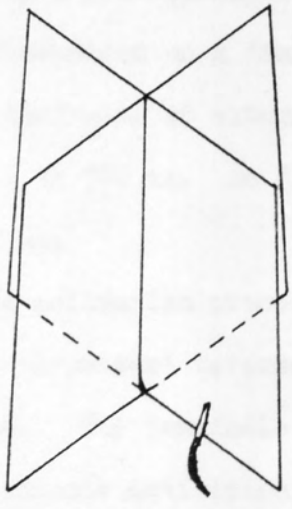

ASSEMBLED
ANODE

FIG. 7. ANODE CONSTRUCTION

electrical insulation. The leads come out of the exchanger shell through one of the shell end plates, using 'Araldite' as a sealing compound.

5.44 ANODE CONSTRUCTION

The anode is constructed from thin copper sheet, with the connection lead soldered to it. The completed anode is then electroplated to give a nickel coating. This has been done for reasons of availability of materials. The surface area of the anode is sufficient to enable its current density to be assumed zero in comparison to the current density of the cathodes. Fig. (7) shows the details of the design of the anode. The anode is situated in the inlet port of the exchanger model for convenience.

5.5 ELECTRICAL INSTRUMENTATION

A flow diagram of the electrical instrumentation is shown in Fig. (8). The DC voltage is supplied by a 12 volt lead-acid battery, controlled by a potentiometer.

The current is measured on a 'Sangamo Weston' 12in. (254mm) scale DC ammeter, fitted with an external shunt to give an instrument range of 0 to 100 mA. An 'Avometer' is used to measure the electrode potential.

For the cathode activation process, the ammeter is isolated, the terminals of the 'Avometer' reversed, and the terminals of the battery also reversed. The terminals of the cathodes are joined. For full details of cathode activition, see Appendix (2) and Section (6).

5.6 PORT INSERTS

The model heat exchanger has been fitted with parts identical in size to those used by Bergelin (29, 30). However, the experimental programme has dictated that measurements be taken

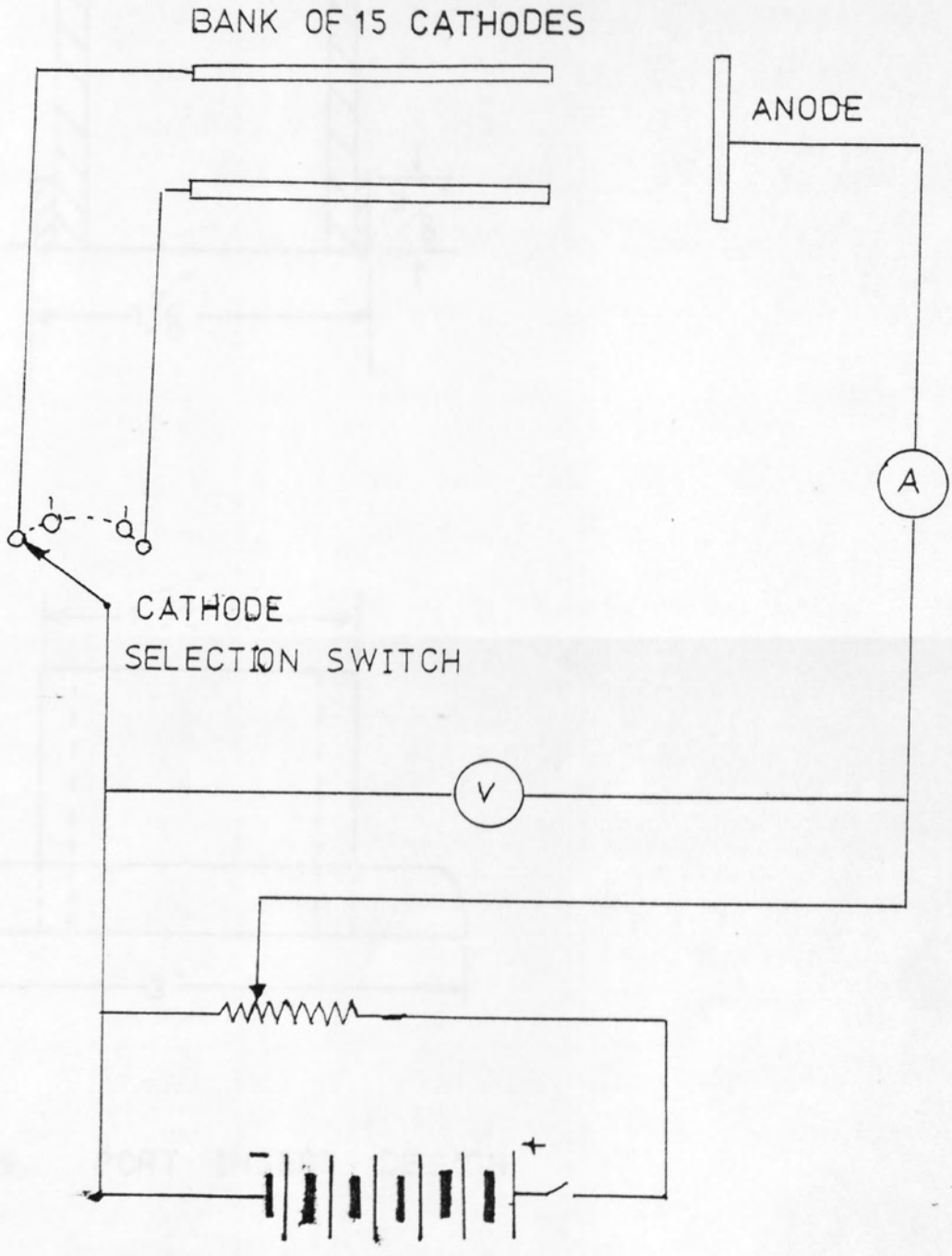

FIG 8 ELECTRICAL CIRCUIT

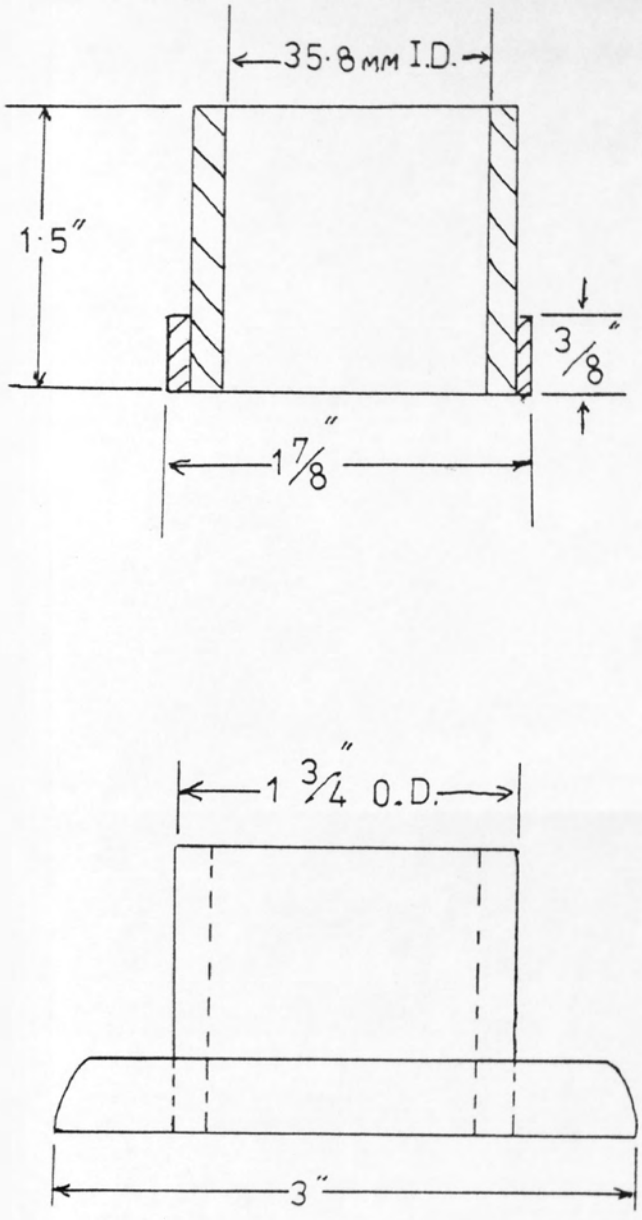

FIG. 9. PORT INSERT DESIGN

with a commercial type port.' This problem has been overcome by the use of port inserts (35.8mm dia) placed into the original ports, sealed with 'Araldite', to similate the commercial type situation. The design of these inserts is shown in Fig. (9).

6. EXPERIMENTAL PROCEDURE

6.1 ASSEMBLING THE TUBE BUNDLE

The baffles and the full face bundle end plates are assembled along the tie bars with a constant 2in. (50.8mm) baffle spacing. The nickel cathodes are then polished and rinsed in dilute sulphuric acid. Prior to fitting in the shell, the anode has also been rinsed in sulphuric acid. No polishing of the anode is carried out, as this can erode the nickel plating and expose the copper base.

The cathodes and the plain tubes are inserted into the appropriate positions in the bundle. Glycerol is used as a lubricant, for the baffles are tight fitting. Where tube insertion is particularly difficult, light tapping with a mallet overcomes the problem. Glycerol is used because of its good miscibility with water. The cathode tubes are located in the bundle with the nickel sections exactly spanning one of the end compartments. The tubes are held in place by the tight fitting baffles.

The tube bundle is inserted into the shell, again using glycerol as a lubricant. The cathodes are then located under the relevant port by sight, and the bundle is held in this position by end stops located between the shell backing plates and the bundle end plates. The shell backing plates are now secured to the exchanger shell.

6.2 MAKING UP THE ACTIVATION SOLUTION

The capacity of the activation storage tank is known, with the 50L level marked on the side of the tank.

All the valves are closed. The activation tank bottom valve is then opened together with the drain valve. Approximately 25L of water are now introduced to the tank, via plastic tubing

connecting the drain valve and the water mains. Both valves are now closed. The activation tank top valve on the by-pass line is opened.

The appropriate weight of sodium hydroxide is dissolved in water in a mixing bucket. The end of the plastic tubing, having been disconnected from the water mains is next inserted into the solution. After the pump is started, the by-pass line control valve is opened. The drain valve is opened to enable the solution to be drawn into the activation tank via the by-pass line. The drain valve is now closed and the pump switched off. The mixing bucket is filled with water and the above process is repeated, using only water, until the correct level in the tank is reached. After this the drain valve is closed, the activation tank bottom valve opened and the solution is circulated via the by-pass line to ensure a homogeneous solution. The nitrogen bleed is used to remove any air from the system. When this is completed the pump is switched off and the activation tank is isolated from the system. The excess solution is then drained from the system in preparation for the make up of the electrolyte solution.

6.3 MAKING UP THE ELECTROLYTE SOLUTION

The capacity of the electrolyte tank is known, and although the tank is graduated at the 100L, 150L, and the 200L levels, the 100L level only is required for the present work.

Initially, all the valves are closed, next the electrolyte tank bottom valve is opened together with the drain valve. Approximately 50L of tap water are introduced to the electrolyte tank, with the nitrogen purge in operation to remove dissolved oxygen from the water. The appropriate amount of sodium hydroxide is subsequently introduced as before, together with the

correct quantities of potassium ferricyanide and potassium ferrocyanide. The solution is made up to 90L, using the same procedure as in the activation solution make-up. After circulating the solution, to ensure homogenity, the ferricyanide ion concentration is determined (see appendix (1)), and the concentrations of the other two components are found by proportion. The concentrations are now corrected by adding the correct amount of water that is required. The solution is circulated as before while the nitrogen purge is continued for about 1 hour, reducing the oxygen content which extends the life of the electrolyte, and reducing chemical costs. If this procedure is not carried out the electrolyte is rendered useless in less than 24 hours because of the effect of dissolved oxygen (Mackley (1)). The life is extended to approximately ten days by using the nitrogen purge.

6.4 CATHODE ACTIVATION

The electrolyte storage tank is isolated from the rest of the system, and the nitrogen bleed to the activation tank begins. Any excess electrolyte is drained from the system, and the activation isolation valves are opened.

The circulation pump is started with both the flow control valves and the pump by-pass valve fully closed. The by-pass line is then fully opened. Water is now circulated through the system cooling coil. The flow valves are now carefully fully opened, and the by-pass line is closed. Circulation is continued in this way until all trapped gas has been driven to the activation tank. Excess air is removed from the system by the nitrogen bleed. The flow is reduced to about 50L/min., and each cathode is activated as described in appendix (2). At the end of the activation period the voltage supply is interrupted, and the

pump is stopped after closing the flow control and by-pass valves.

The activation tank bottom valve is closed, and the activation fluid is drained from the model heat exchanger. The fluid is then returned to the activation tank as described in Section 6.2. All the excess activation fluid is drained from the system, and the activation tank isolated.

6.5 EXPERIMENTAL RUN

The electrolyte tank isolation valves are fully opened. With the flow control and by-pass valves shut, the circulating pump is started, and the by-pass valve is opened, as are the flow control valves. The nitrogen purge is started at the same time to drive out air from the system. Also, the cooling water is fed to the cooling coil. The electrolyte is allowed to circulate for 30 min at the maximum flow rate to ensure that the electrolyte is homogeneous. The flow control valves and the by-pass valve are now adjusted to give a flow of about 50L/min, and the circulation is kept at this rate until all trapped gas is driven from the system.

When all gas has escaped from the system, the flow control valves are adjusted to give the required flow rate. It has been found that the by-pass valve need only be used for the lower flow rates that are studied. The D.C. potential is now connected across the anode and the cathode tube banks. The cathodes are investigated individually. For each cathode, the potential is incrementally increased, and the values of current and voltage recorded to find the limiting current plateau. It has been found with practise that this need only be done for one tube at each flow rate, as the plateaux for the individual tubes have been found to coincide.

Therefore, a voltage is selected in the middle of the plateau. The limiting currents at the other cathodes are then recorded, using the same potentiometer setting as for the original cathode. During the recording of the cathode limiting currents, the mean electrolyte temperature is determined for the flow rate under investigation. This procedure is repeated for other flow rates, allowing each new flow rate to reach steady state before commencing each set of measurements. Samples of electrolyte are taken periodically, for the determination of the ferricyanide ion concentration (see appendix (1)).

On completion of a series of experimental runs, the pump is stopped, and the nitrogen and cooling water supply are turned off. The electrolyte solution is returned to the main tank, which is then isolated. Any remaining electrolyte in the pipeline is then drained from the system, and all remaining valves are closed. Periodically the electrolyte solution is renewed.

7 SCOPE OF EXPERIMENTAL WORK

The experimental work is confined to a study of the end compartments of the model shell and tube heat exchanger. Investigations are carried out for a constant baffle spacing of 47.6mm. Single segmental baffles are used throughout the experimental work at a constant baffle cut down of 18.4%. The investigations are also confined to the case of no internal leakage.

Two types of port with two baffle orientations are studied, with the investigations also covering the use of an impingement baffle. The port types under investigation are the rectangular design of Bergelin et al.(29, 30), which is thought to give minimum disturbance to the flow, and a cylindrical port typical of that in use in industry. The two baffle orientations used are the horizonal orientation (Fig. (10)), and the vertical position (Fig. (11)), sometimes in use where extra tube support is required.

The investigations are carried out for electrolyte flow rates in the range 1 to 125 L/min, which correspond to Reynolds numbers of 100 to 10,000.

Investigations are carried out using the Bergelin-type ports fitted to the shell. As Mackley (1) has shown that the distribution of heat transfer coefficients in the baffle compartments is symmetrical about a vertical central axis, the tubes under investigation in the present work are confined to one half of the bundle. The electrode rod configuration is shown in Fig. (12).

Mass transfer studies are carried out for the horizontal baffle cut orientation in the inlet and outlet compartments of the model heat exchanger. The investigations are repeated for the baffle cuts orientated vertically. The same electrode rod configuration is used as before, but as symmetry cannot be assumed

in this case, the investigations are carried out in two sections, with the bundle being rotated through 180° for each port. Hence, for the vertical orientation, the electrode rod configuration is essentially as shown in Fig. (13). Repeatability tests are carried out for the horizontal baffle orientation in both end compartments.

The investigations are also carried out for the 35.8mm. diameter ports in both end compartments for the baffle orientations, described above. The same tube configurations are used as for the rectangular ports (Figs. (12, 13)).

Further investigations are carried out with an impingement baffle (35.8mm. by 30mm.) in conjunction with the 35.8mm. diameter ports in the inlet compartment for both baffle orientations. The impingement baffle is constructed from 1.65mm. thick polypropylene sheet, and is located centrally on the second row of tubes (the top tube having been removed), and held in place by wires attached to the tie rods. The baffle holes vacated by the top tube are sealed by pieces of 1.65mm. thick polypropylene sheet attached with 'Araldite' adhesive. Fig. (14) shows the positioning of the bundle in the shell, together with the impingement baffle positioning. The electrode rod configurations for the impingement baffle tests are shown in Figs. (15, 16).

A limited investigation into the heat transfer performance of the second compartment (next to the inlet compartment) is undertaken. Three electrodes are positioned in the cross-flow region of the second compartment in the positions shown in Fig. (17), and measurements of mass transfer taken over the range $100 < Re < 10,000$. This completes the experimental work.

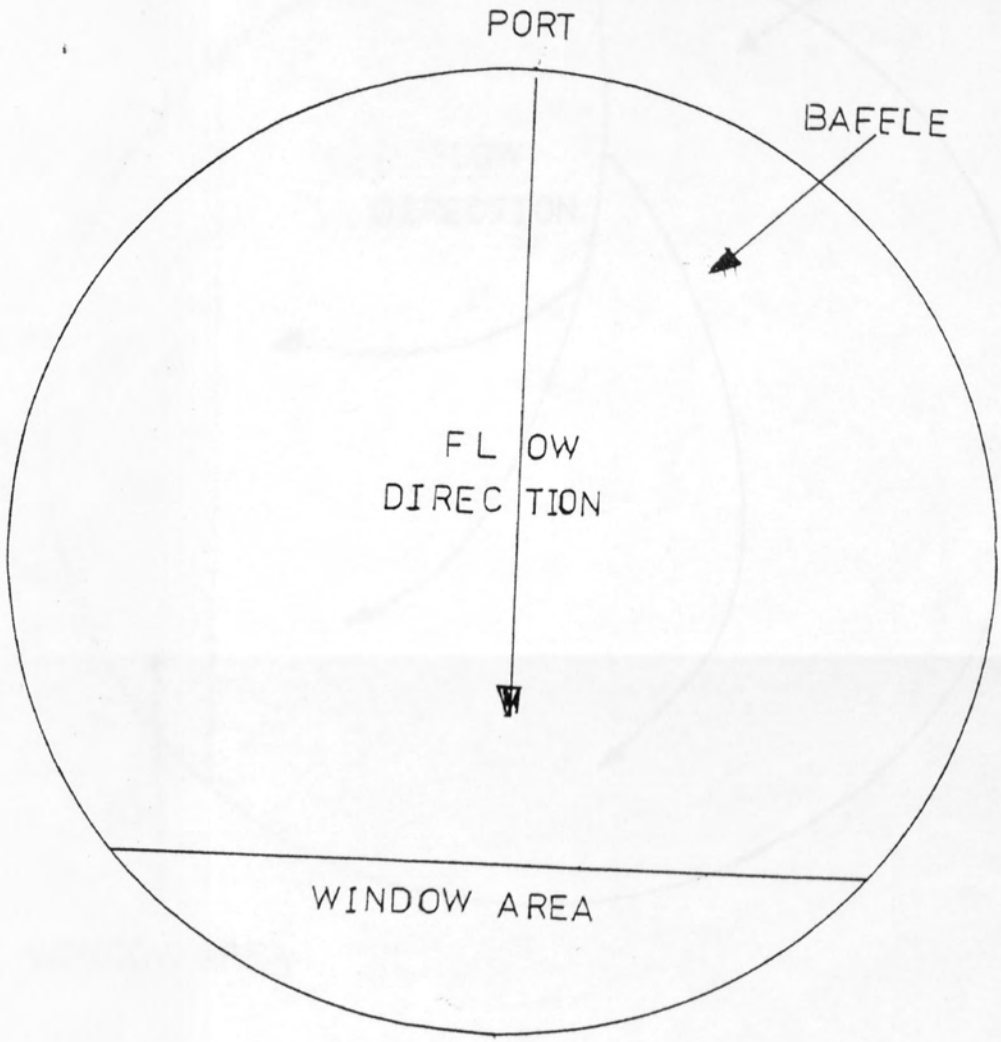

FIG. 10. HORIZONTAL BAFFLE CUT

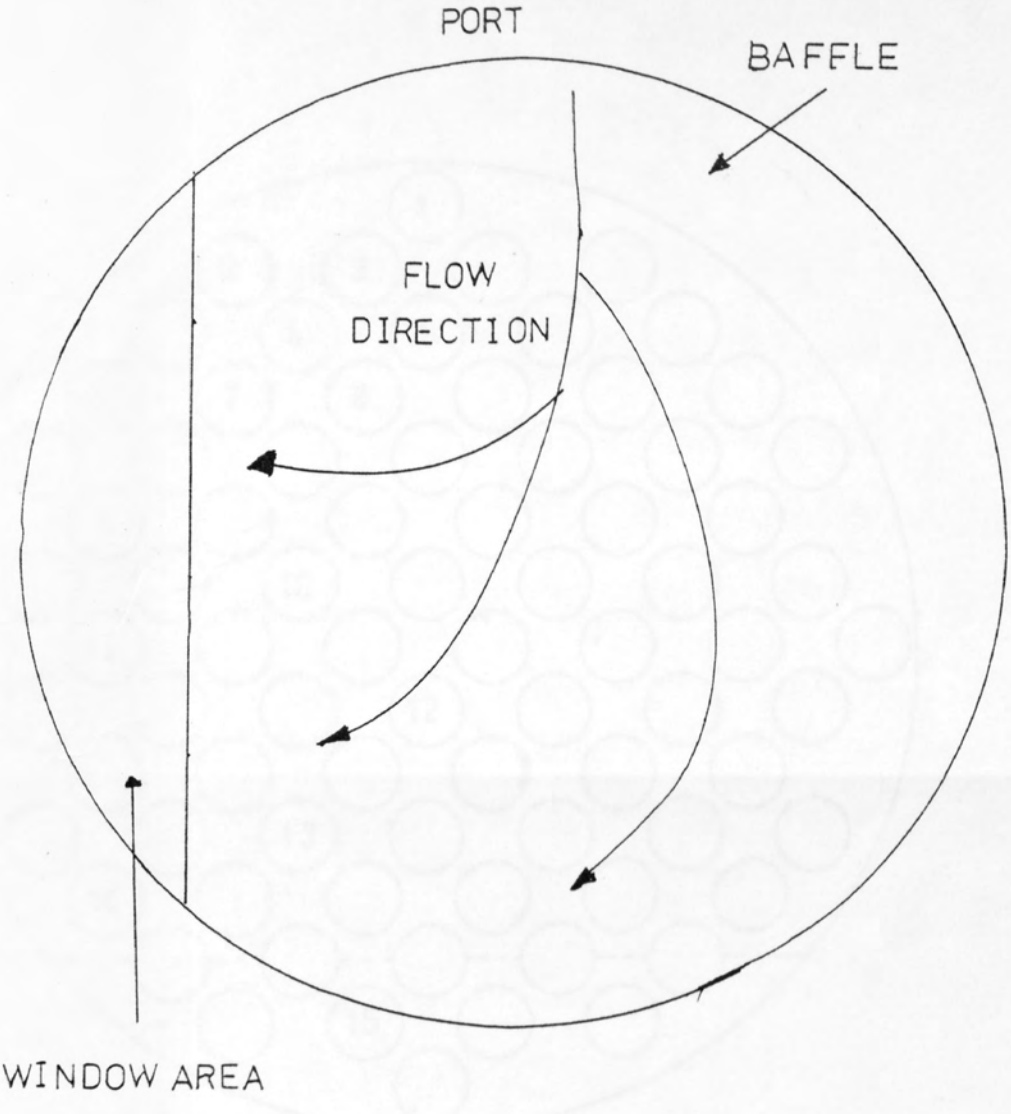

FIG. 11. VERTICAL BAFFLE CUT

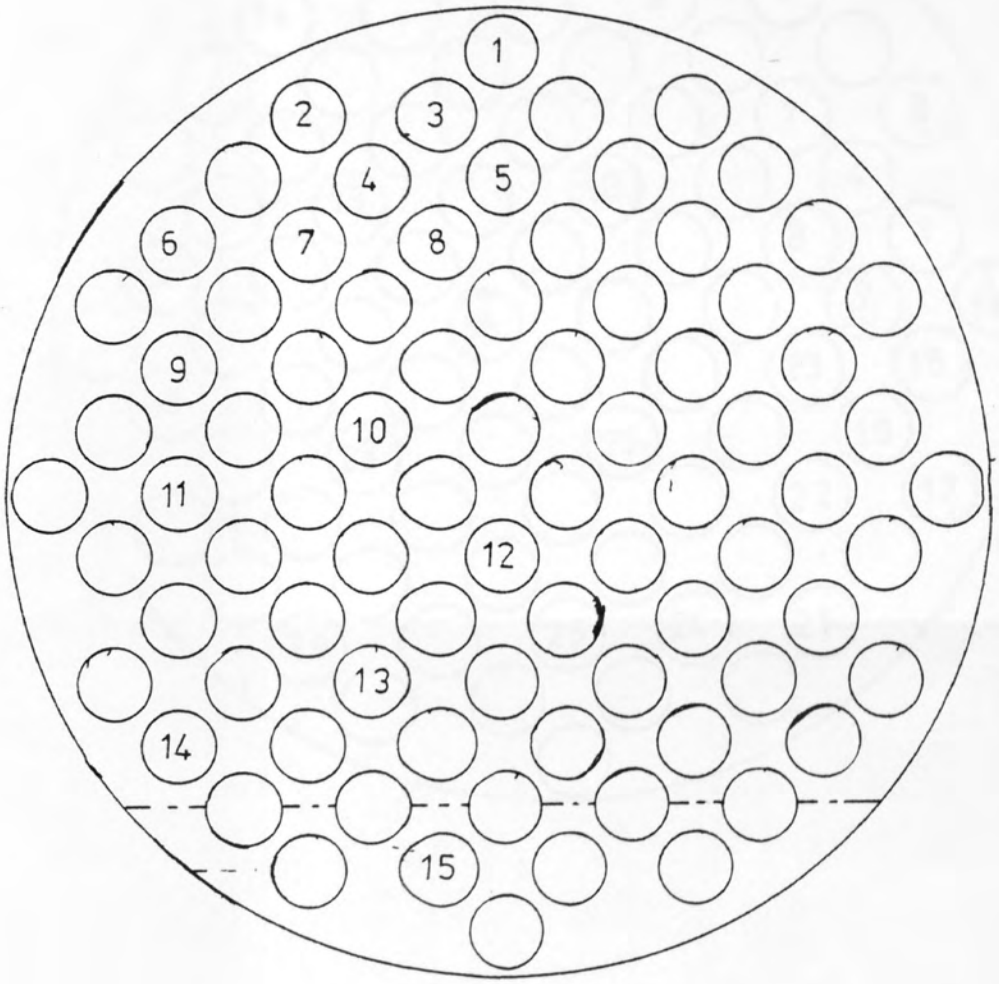

FIG. 12. ELECTRODE CONFIGURATION — HORIZONTAL BAFFLE CUT

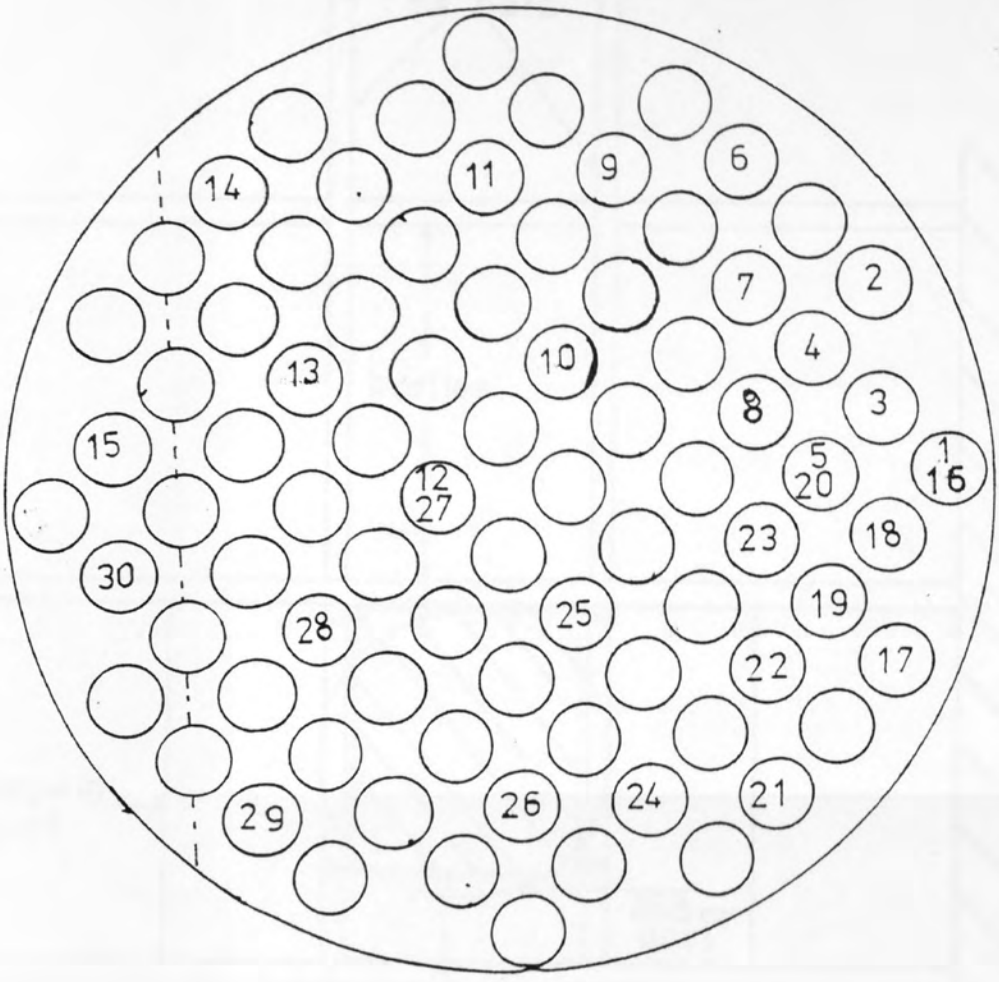

FIG 13 ELECTRODE CONFIGURATION — VERTICAL BAFFLE CUT

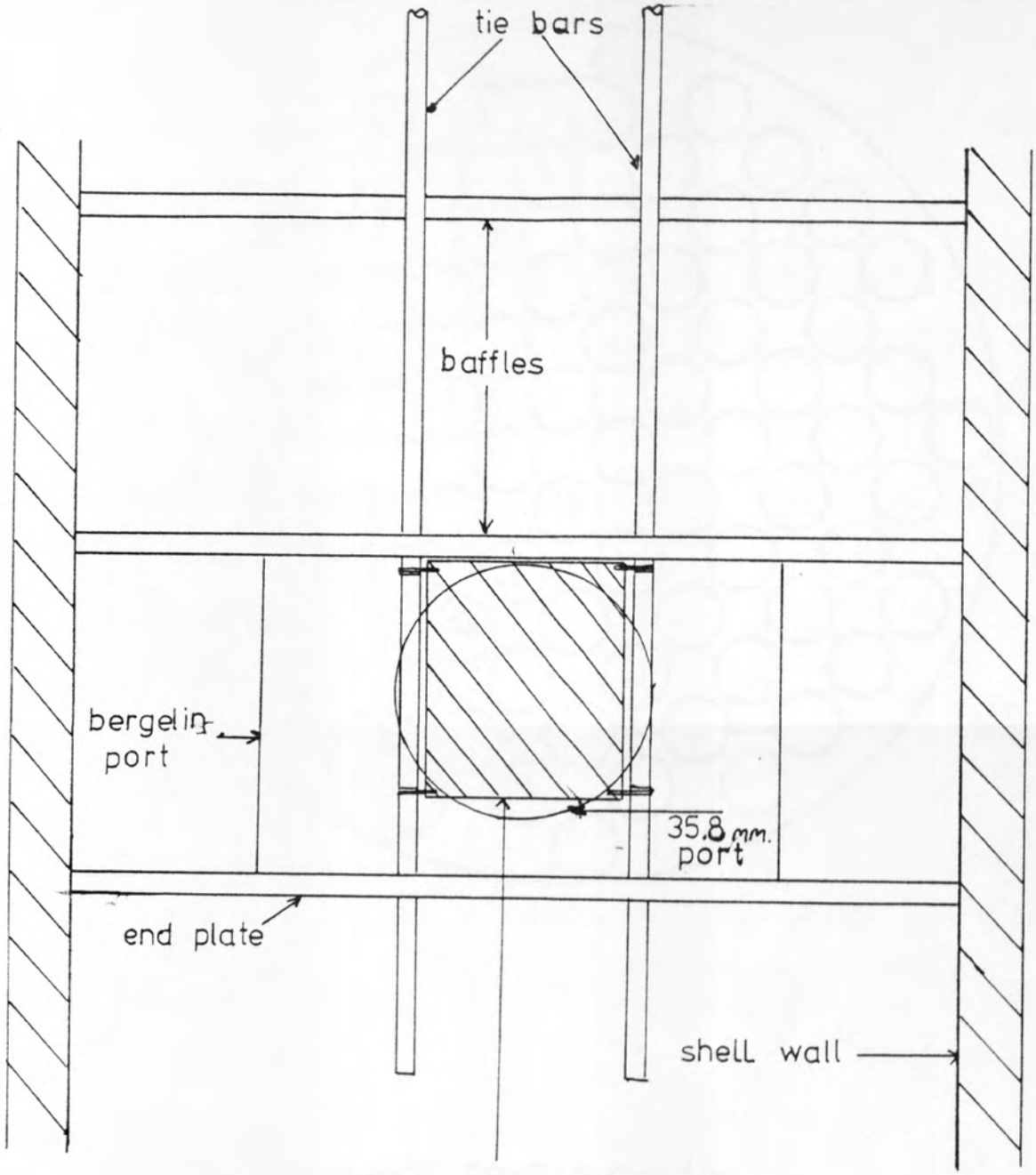

FIG. 14. BUNDLE POSITIONING

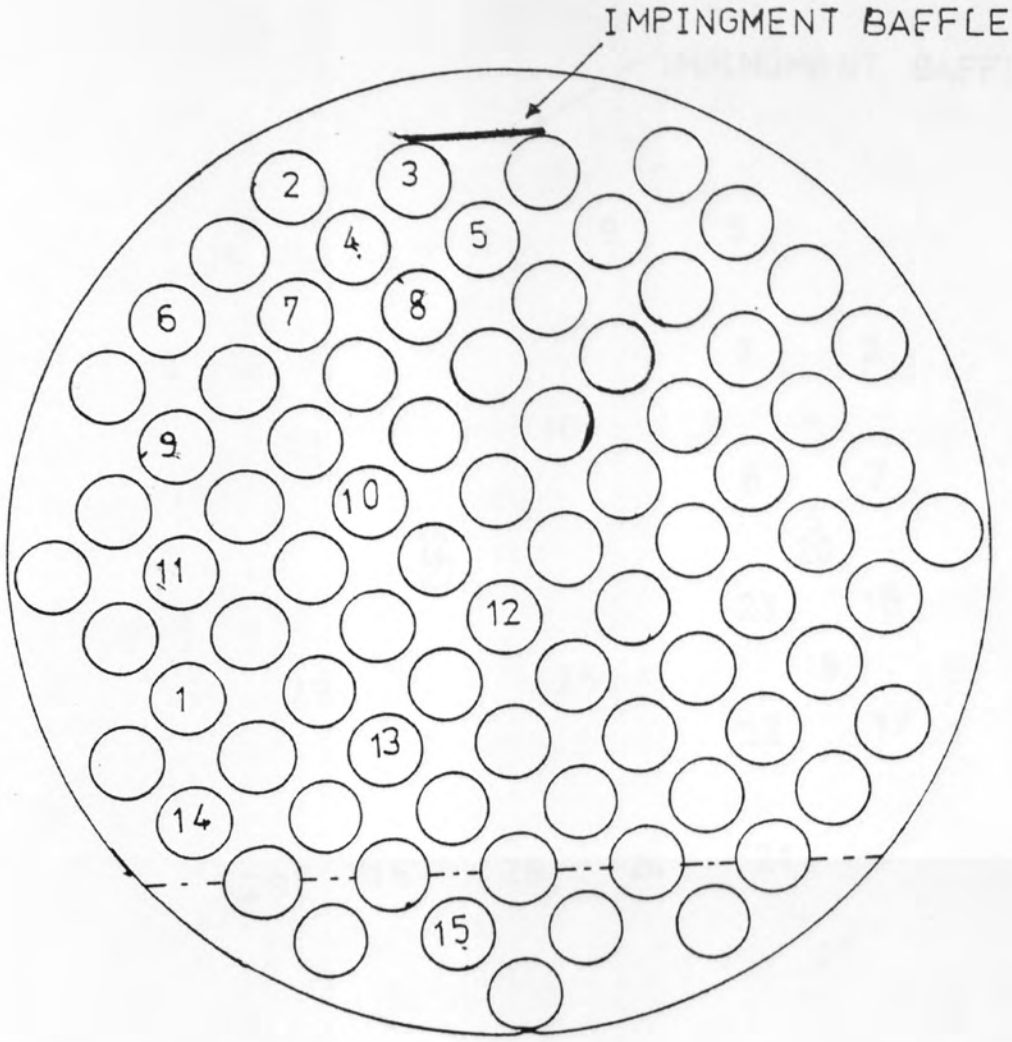

FIG 15 ELECTRODE CONFIGURATION ——
HORIZONTAL BAFFLE CUT

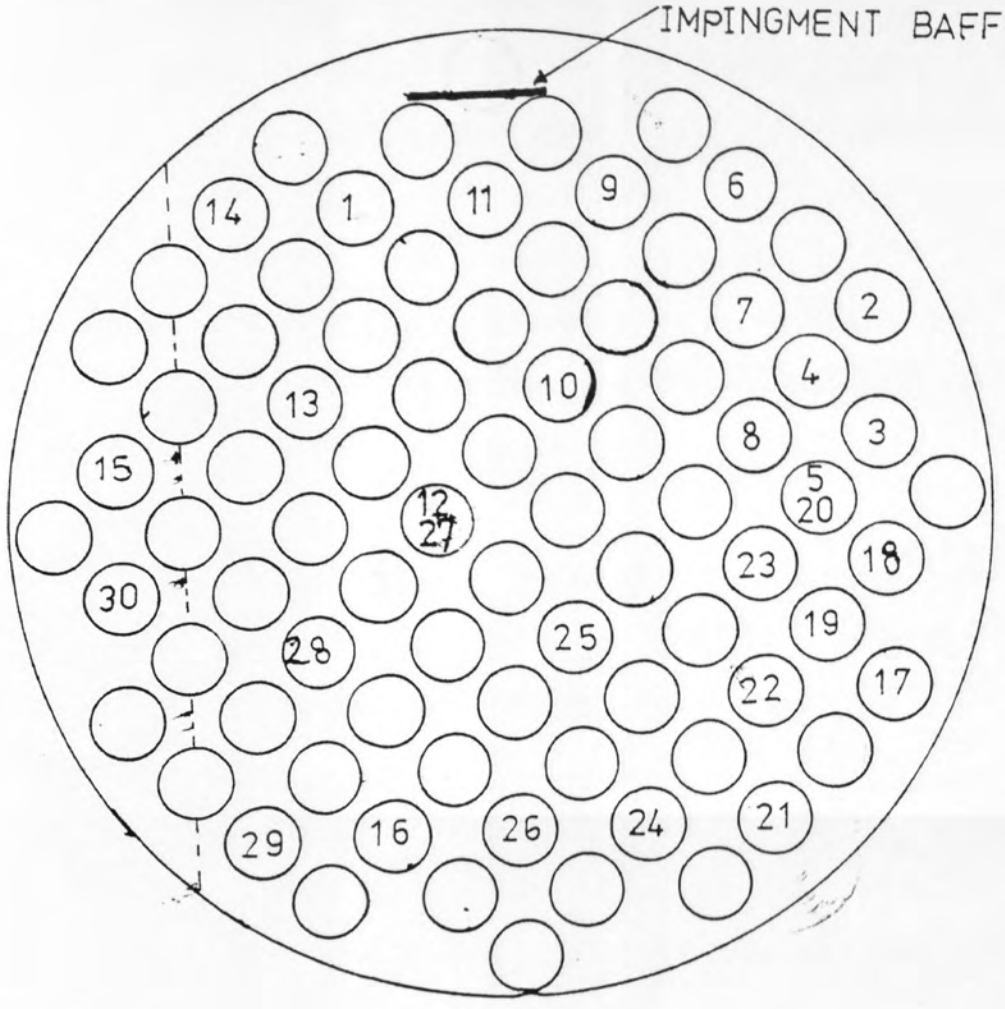

FIG 16 ELECTRODE CONFIGURATION ——
VERTICAL BAFFLE CUT

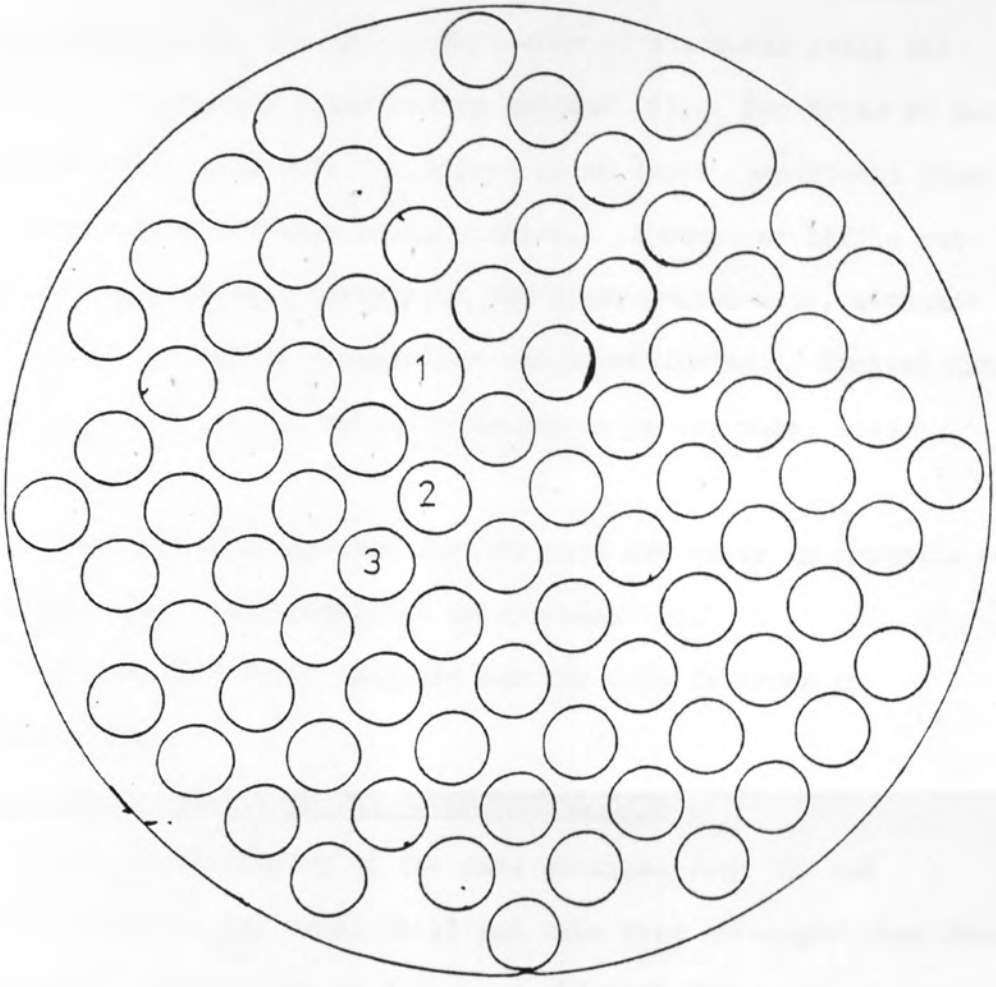

FIG. 17. SECOND COMPARTMENT CONFIGURATION

8. DISCUSSION OF RESULTS

8.1 INTRODUCTION

Mass transfer data for the case of no internal leakage were obtained for the end compartments of the model shell and tube heat exchanger described in section (6). Two types of port were investigated, with the effect of an inlet compartment flow impingement baffle also being studied. A constant baffle cut and spacing was used throughout the experimental work, although the effect of baffle orientation was investigated. Limited data were obtained for the second compartment of the model heat exchanger.

Specimen calculations for the data are given in appendix (6), with the data being tabulated in appendix (5).

A detailed error analysis for the data is given in appendix (4).

8.2 REPEATABILITY OF THE EXPERIMENTAL DATA

The repeatability of the data obtained from the end compartments of the model shell and tube heat exchanger has been examined. Three sets of data were obtained from each of the two end compartments using the Bergelin type ports with the horizontal baffle cut orientation. The tests were performed over a period of six weeks together with other experimental investigations.

The data from these investigations are plotted in Figs. (18, 19) for the inlet and outlet compartments respectively. Good agreement is shown for each end compartment, demonstrating the consistency of data obtained from the model heat exchanger using the electrochemical technique.

8.3 COMPARISON WITH THE INTERNAL COMPARTMENT DATA OF MACKLEY

The inlet compartment data for the horizontal baffle cut

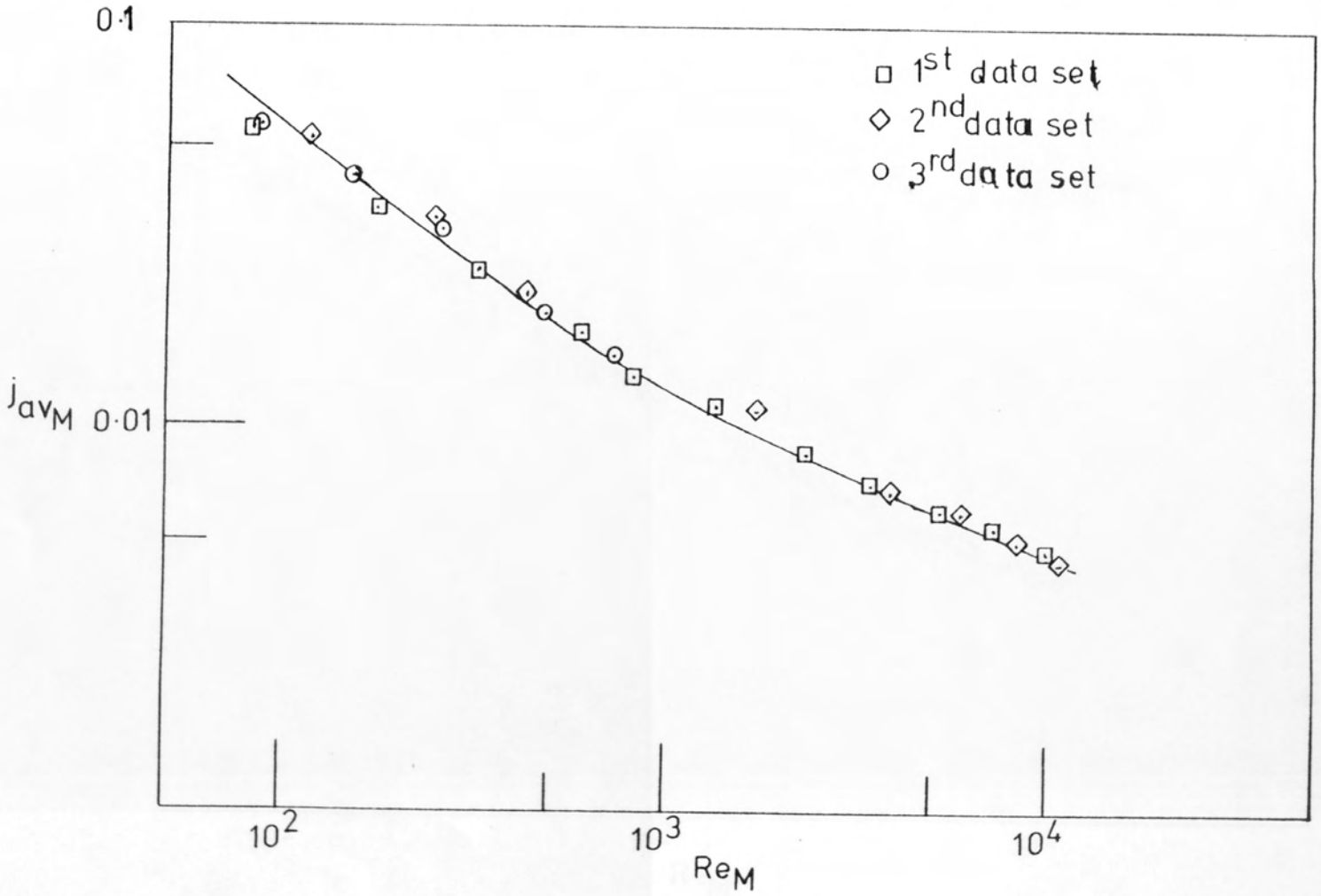

FIG 18 INLET COMPARTMENT — DATA REPEATABILITY

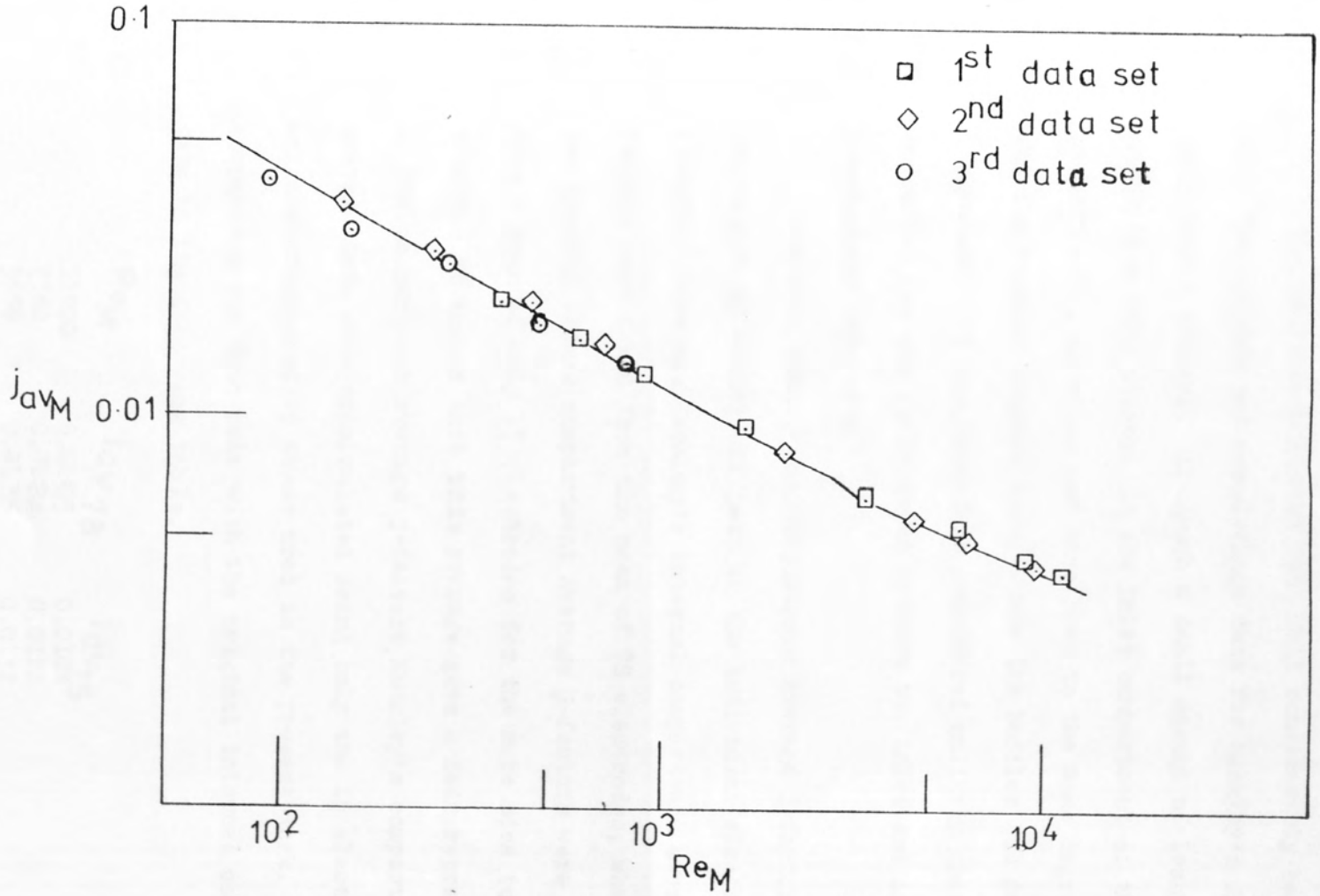

FIG 19 OUTLET COMPARTMENT — DATA REPEATABILITY

orientation with the Bergelin type rectangular ports were compared with the corresponding internal compartment leakage and non-leakage data of Mackley (1) in Fig.(20).

The inlet compartment data fell considerably below both the leakage and non-leakage data for Mackley's internal compartment studies. Although a small amount of leakage might have been present in the inlet compartment of the present work, it would not have been to the same degree as for the Mackley leakage case, where the baffles had deliberate clearances. It was therefore considered unlikely that leakage accounted for the differences between the inlet and internal non-leakage data sets.

For both works, the compartment average j-factors were calculated by taking the mean of the individual electrode j-factors. However, Mackley's internal compartment average j-factors were found from the mean of 78 electrodes, whereas the present work's compartment average j-factors were found from a mean of only 15 electrodes for the same size tube bundle. To ensure that this average gave a fair representation of the compartment average j-factors, Mackley's compartment average data were recalculated using only the 15 electrodes which corresponded to those used in the present work. A comparison was then made with the original internal compartment data in the following table.

Re_M	$j_{av_{78}}$	$j_{av_{15}}$
11900	0.0105	0.0104
7380	0.0124	0.0122
5550	0.0136	0.0132
3310	0.0167	0.0164
2350	0.0184	0.0181
972	0.0272	0.0269
524	0.0354	0.0349
310	0.0439	0.0431

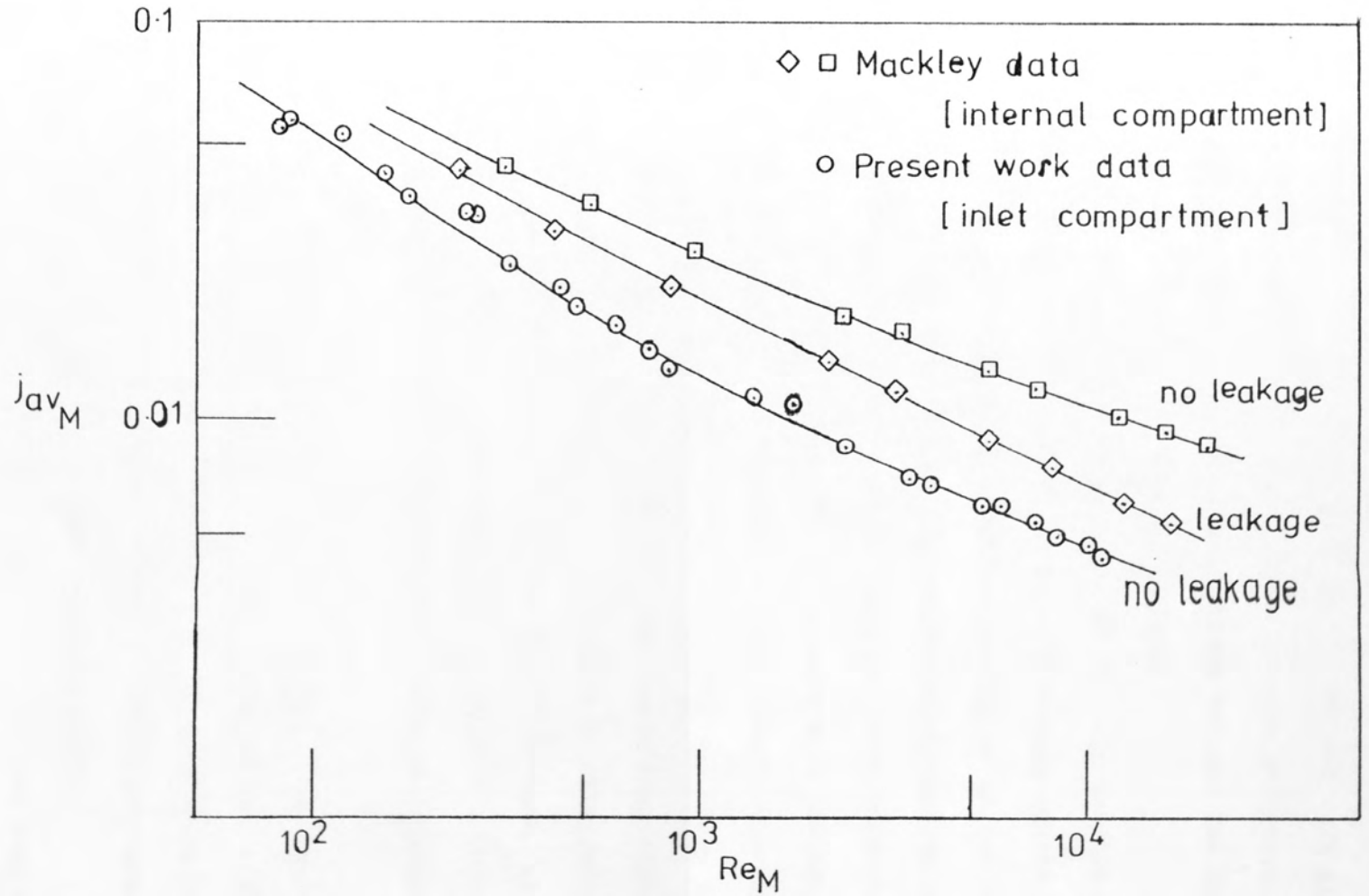

FIG 20 COMPARISON WITH PREVIOUS WORK

The discrepancies between the two sets of compartment average j-factors are less than 2%, which is within the experimental error. It can therefore be assumed that the electrode configurations used in the present work give a fair representation of the compartment average j-factors, and does not account for the large differences between the data of the present work and that of Mackley.

Mackley gave a comparison in his work between the fifth and third compartments of the heat exchanger bundle for a baffle cut of 37.5% and a baffle spacing of 48.1mm for the non-leakage case, showing the third compartment to have lower heat transfer characteristics than the fifth compartment.

To enable a comparison to be made with the second compartment data of the present work, crossflow averages for these compartments were calculated using the three tubes corresponding to those used for the second compartment investigations of the present work. The data so obtained were then plotted in Fig. (21). An estimation of the data for the third compartment of Mackley's bundle at the 18.4% baffle cut could now be made using Fig. (21) and the baffle cut correlation given in (85).

This estimation is given in Fig. (22), together with the corresponding three tube crossflow averages for Mackley's fifth compartment at the 18.4% baffle cut and the second compartment crossflow data of the present work. The inlet compartment average data from Fig (20) are also included.

The second compartment data lie between that of the inlet compartment and the curve estimated for the third compartment, with the data for the fifth compartment being above that for the third compartment.

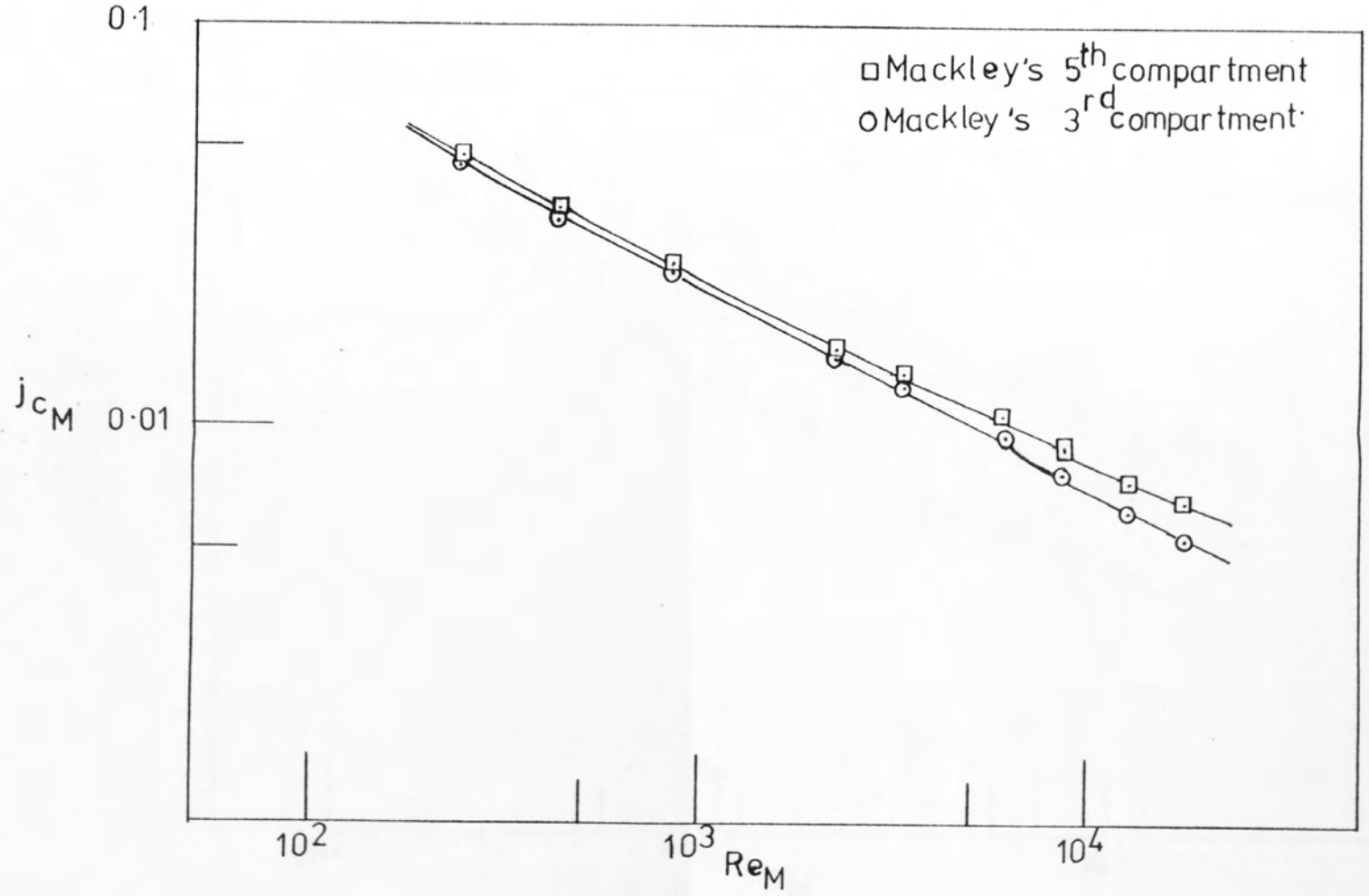

FIG 21 MACKLEY'S COMPARISON OF THE 5th AND 3rd COMPARTMENTS
[for 3-tube crossflow average]

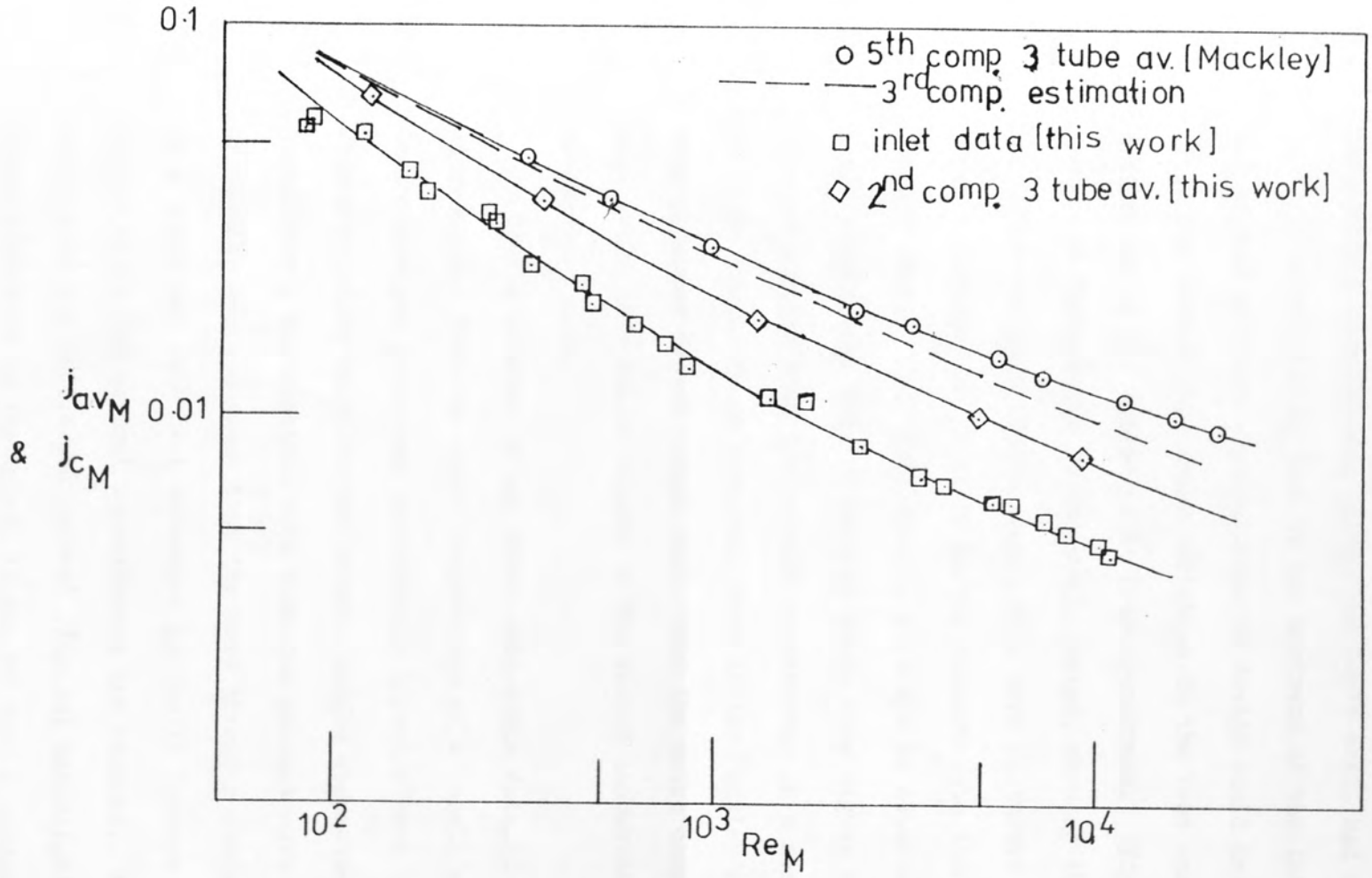

FIG 22 COMPARISON OF COMPARTMENT CROSSFLOW AVERAGES FOR DIFFERENT BAFFLE COMPARTMENTS

Mackley's third compartment data (37.5% baffle cut) were obtained by removing the first three baffles, leaving the electrodes in precisely the same position as for the fifth compartment experiments. Also, Mackley's shell had an unusual inlet compartment, in that it lay upstream of the inlet port. The effect of these abnormalities of design could have led to unusually smooth flow characteristics in the test compartment, regardless of the number of baffles downstream. Fig.(23) shows the differences in the shell design, showing that the shell for the present work would show more disturbed flow characteristics in the early baffle compartments than the Mackley shell. For this reason, it could be expected that the third compartment data of Mackley would show higher transfer characteristics than for a third compartment in a normal shell. It might therefore be expected, that if the Mackley data had been obtained from a normal shell that the third compartment data would have fallen closer to the second compartment data of the present work.

In the absence of any other comparable data, it can only be concluded that the inlet compartment of a shell and tube heat exchanger possesses considerably inferior heat transfer characteristics than for the central baffle compartments. Furthermore, the combined data from the present work and that of Mackley would suggest that the heat transfer characteristics of a shell and tube heat exchanger gradually improve along the bundle until the central compartments are reached. As it is shown that the outlet compartment (Fig.24) has slightly inferior characteristics to the inlet, it may be that a gradual decrease in the transfer properties exists between the central and the outlet compartments. It must be stressed, however, that the

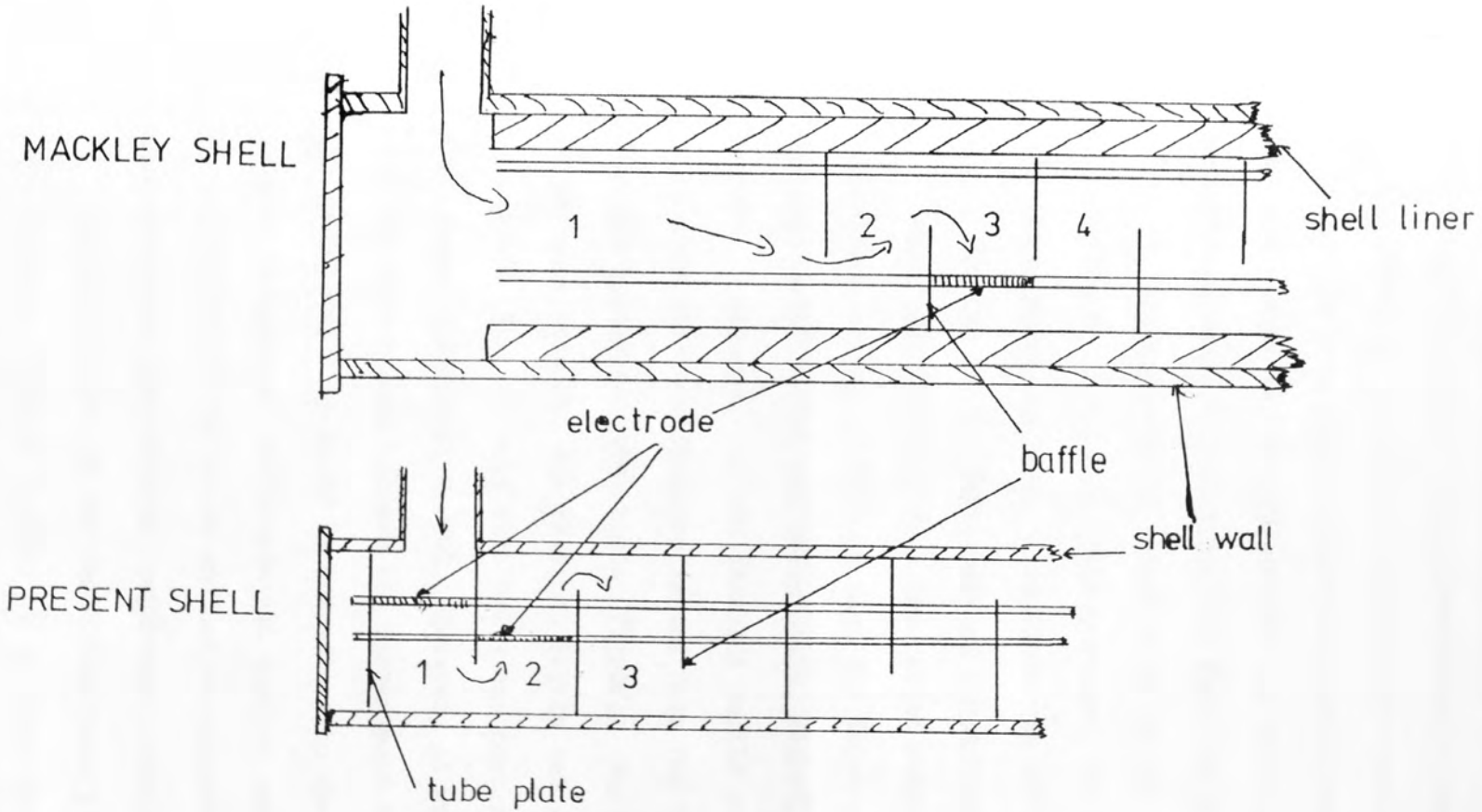

FIG 23 DIAGRAM TO SHOW DESIGN DIFFERENCES

present work is only a preliminary investigation into the end compartments of shell and tube heat exchangers and further work must be carried out before any final conclusions can be reached.

8.4 COMPARISON OF THE INLET AND OUTLET COMPARTMENTS

The heat transfer characteristics of the inlet and outlet compartments of the model shell and tube heat exchangers were compared for both types of port and baffle orientations. Figs. (24 to 27) show the comparisons of the inlet and outlet compartment average j-factors, and Figs.(28 to 35) give the relative distributions of j-factor in the end compartments in the middle of the Reynolds number range. For Figs.(28 to 35) the actual j-factors were 'normalised' by dividing the individual tube j-factors by the corresponding compartment average j-factors.

Figs.(24, 26) show that the outlet compartment has lower compartment average j-factors than the inlet compartment for the horizontal baffle cut orientation, regardless of the type of port. However, for the vertical baffle orientation, there is no appreciable difference in the data for the two compartments with the commercial type ports (Fig.27). Furthermore, the outlet compartment data for the vertical baffle cut with the Bergelin type ports (Fig.25) only fall below the corresponding inlet compartment data above Re=800. However, it must be appreciated that the differences between the compartment data in Figs. (24 to 26) are only small in comparison to the differences between the present work's data and that of Mackley, and it may be concluded that the inlet and outlet compartments of the model heat exchanger show similar compartment average j-factors.

On examination of the individual tube j-factor distributions (Figs.28 to 35), it is clear that for both types of port investigated, the inlet and outlet compartments have

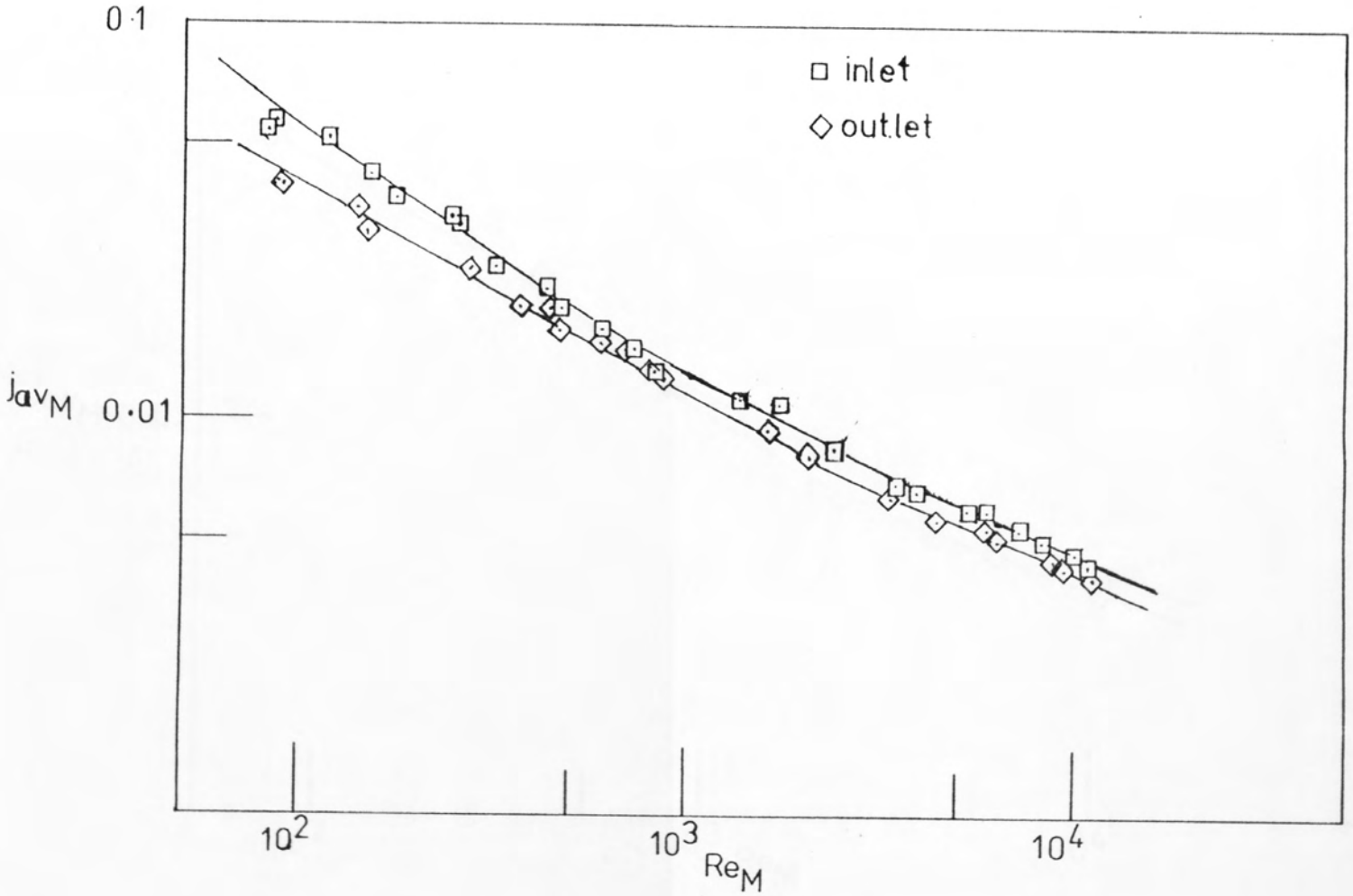

FIG 24 COMPARISON OF INLET & OUTLET COMPARTMENTS
[Bergelin type ports, horizontal baffle cut]

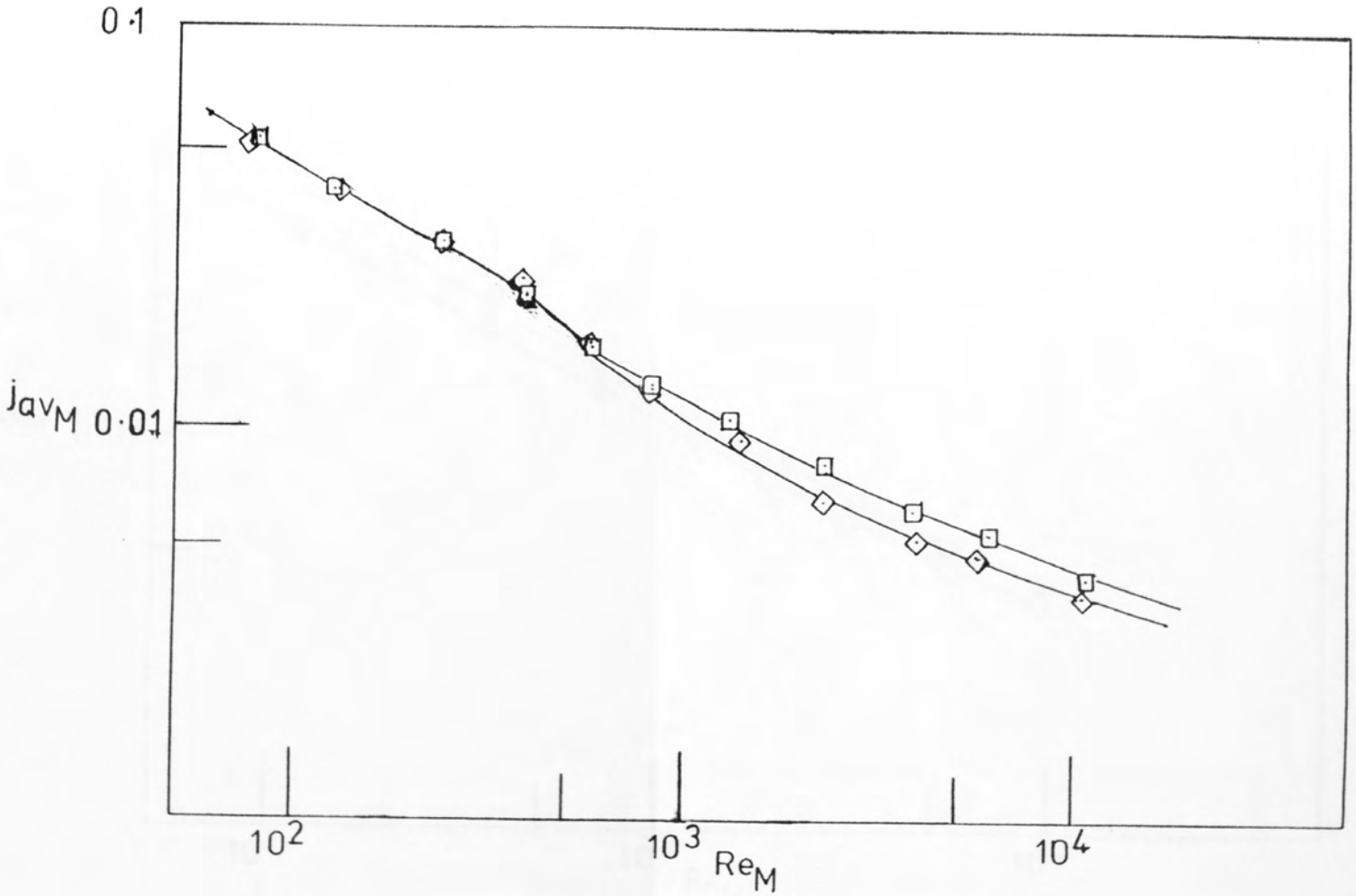

FIG 25 COMPARISON OF INLET & OUTLET COMPARTMENTS
[Bergelin type ports, vertical baffle cut]

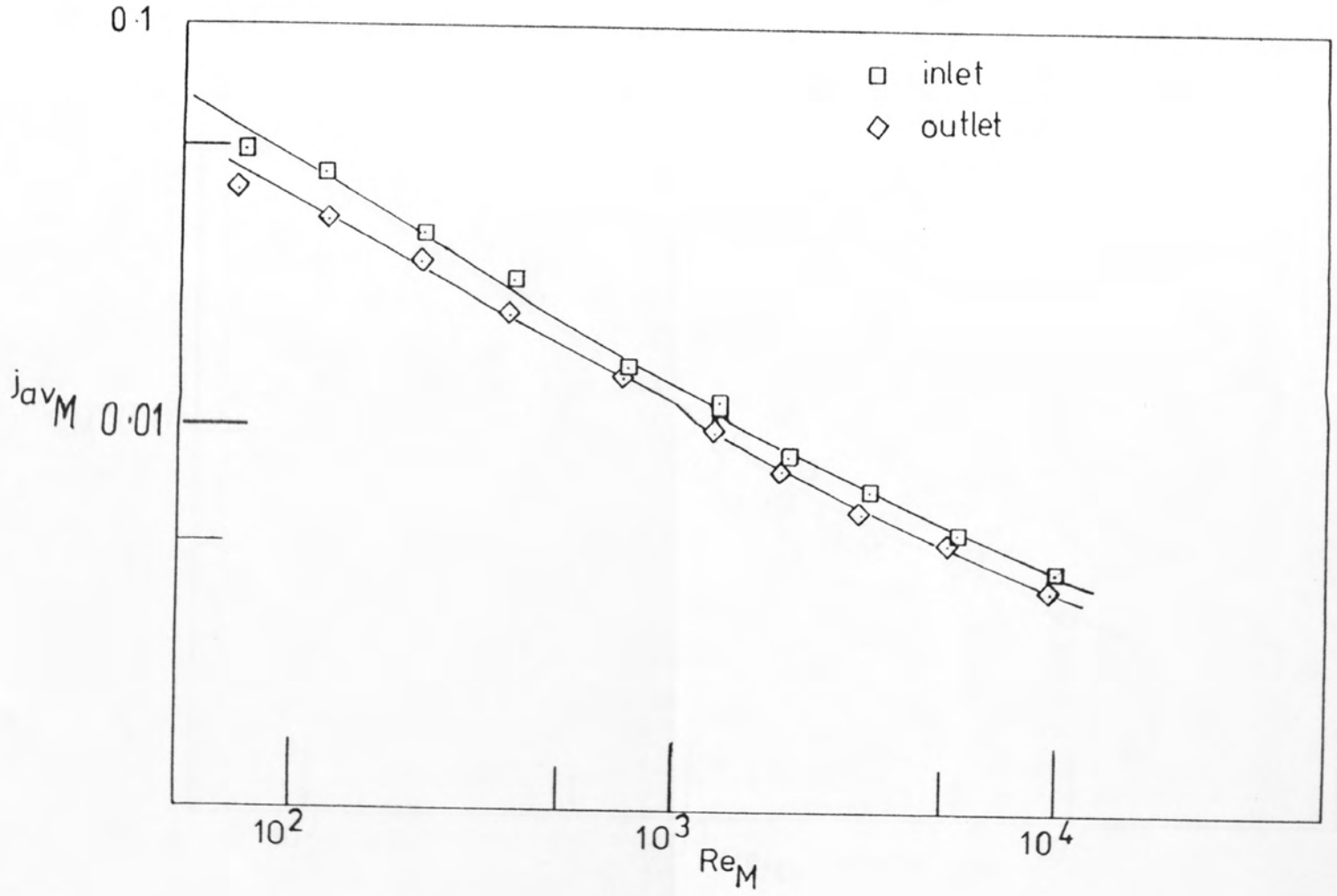

FIG 26 COMPARISON OF INLET & OUTLET COMPARTMENTS
[commercial type ports, horizontal baffle cut]

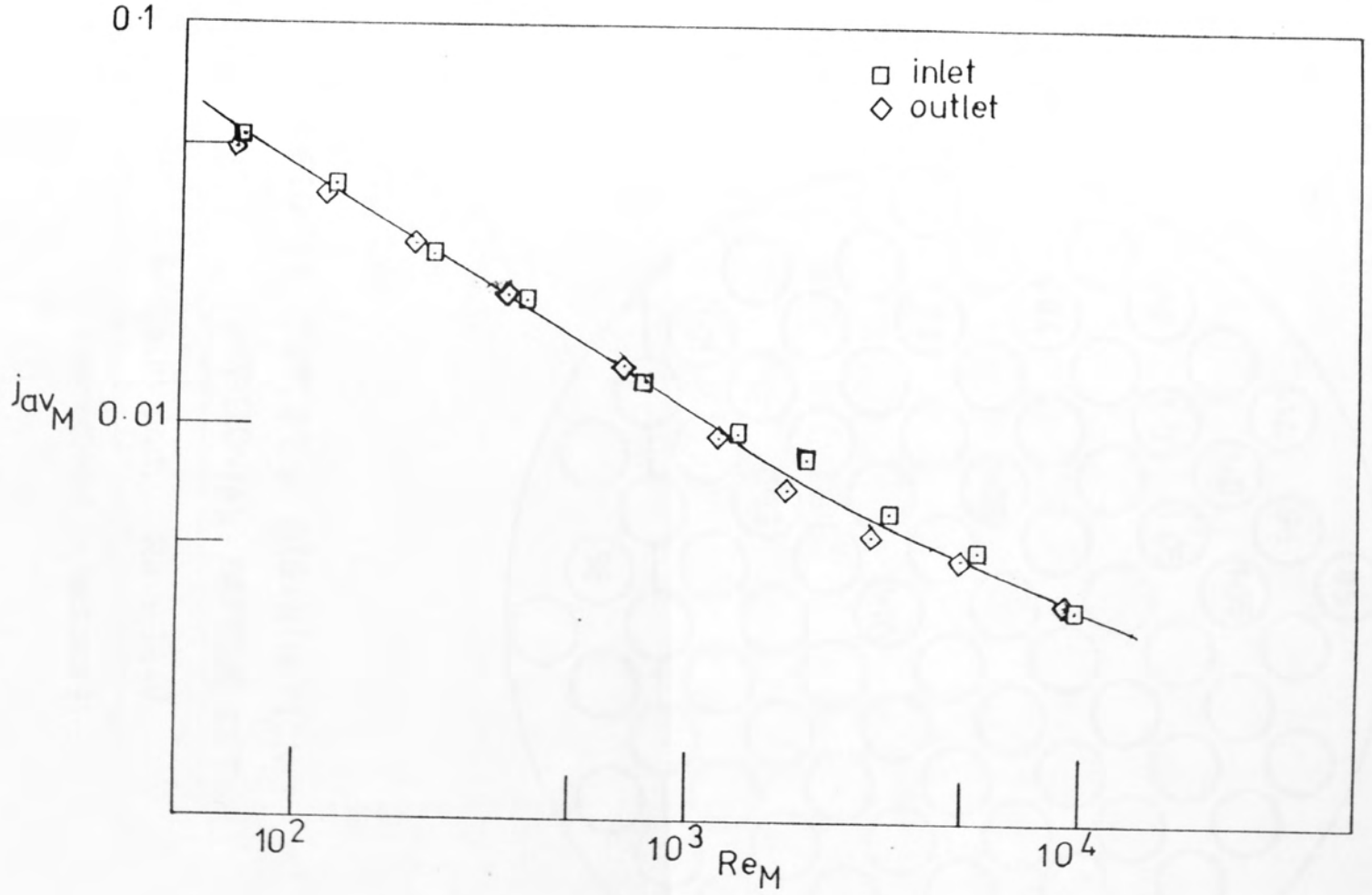

FIG 27 COMPARISON OF INLET & OUTLET COMPARTMENTS
[commercial type ports, vertical baffle cut]

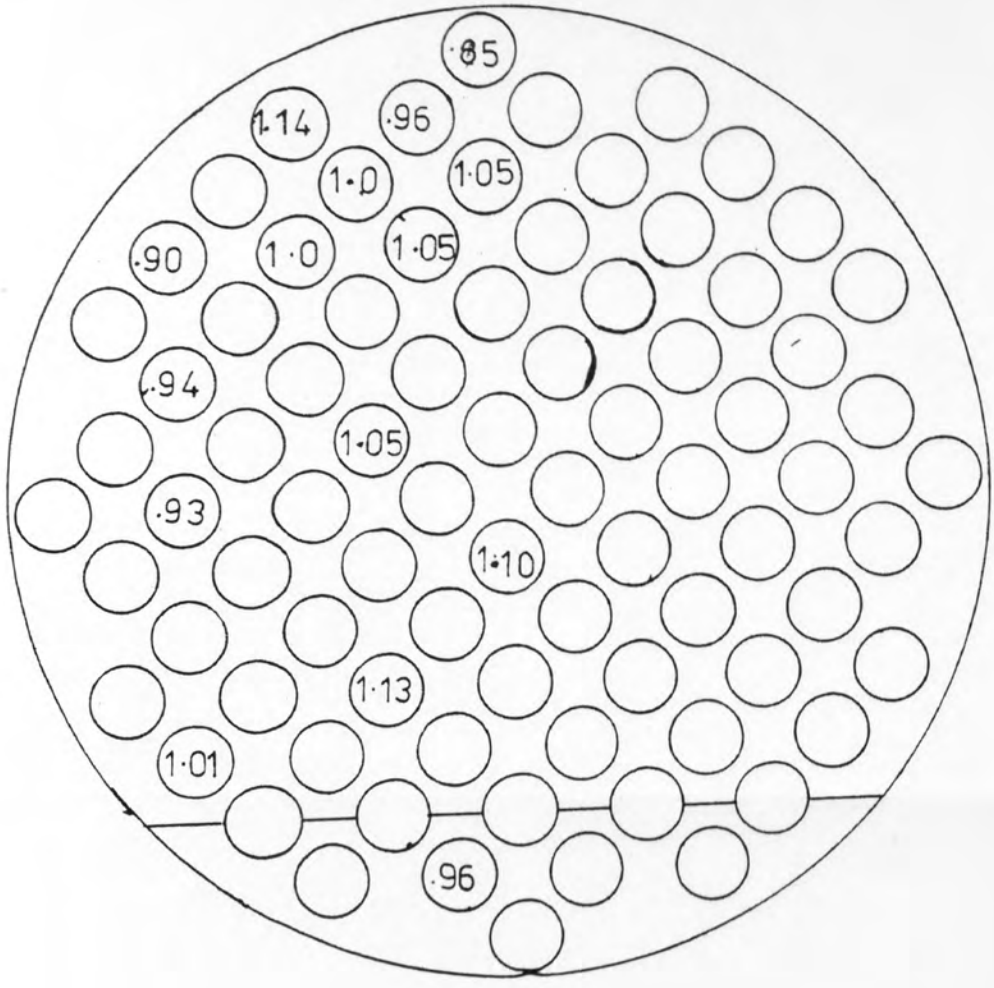

FIG 28 OUTLET j DISTRIBUTION
HORIZONTAL BAFFLE CUT

Bergelin port, $Re = 1640$

(normalised j-factors)

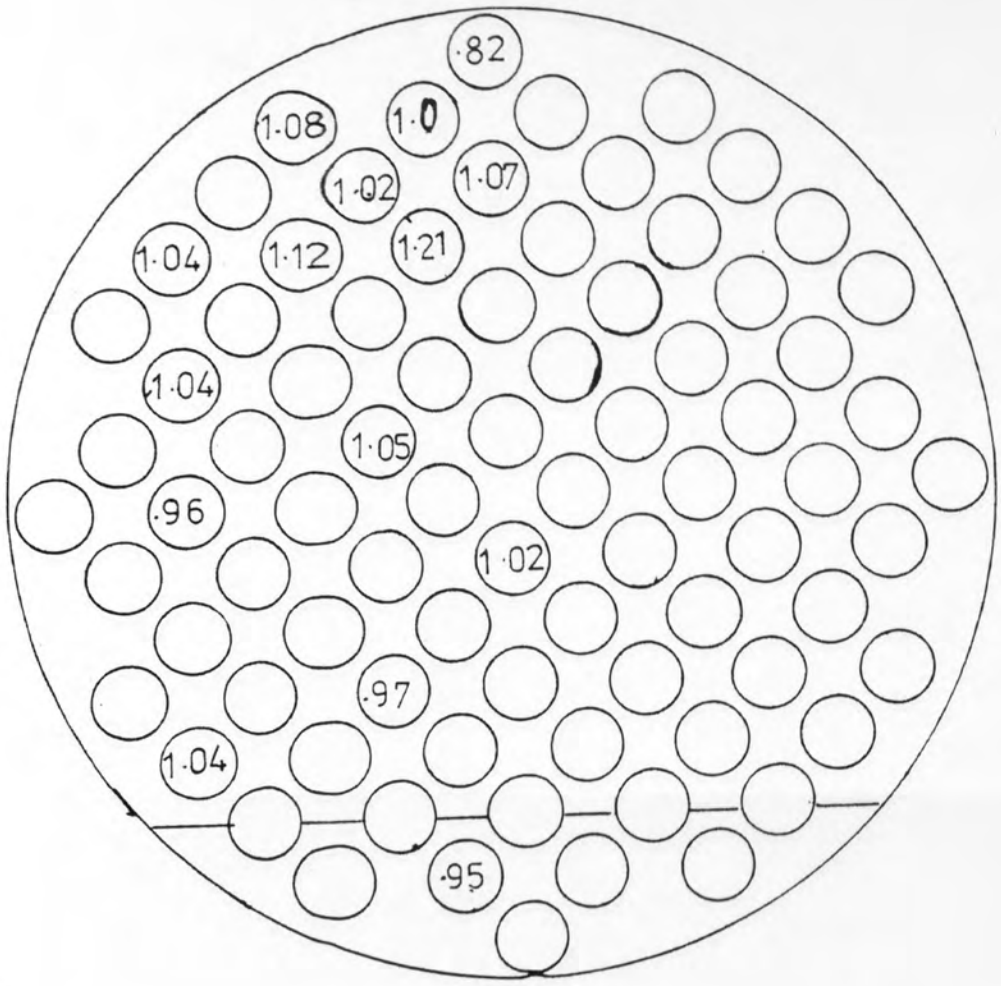

FIG 29 INLET j DISTRIBUTION

HORIZONTAL BAFFLE CUT

Bergelin port, Re = 1330

(normalised j - factors)

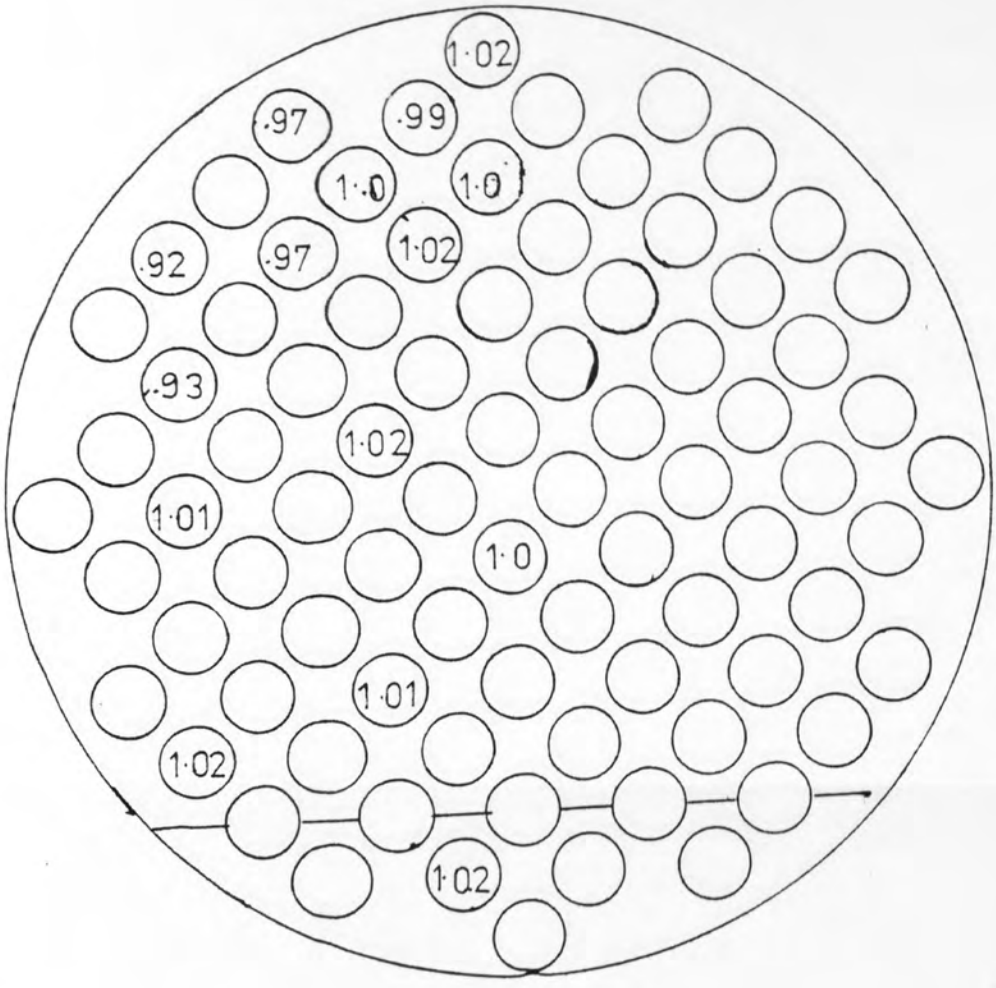

FIG 30 OUTLET j DISTRIBUTION
HORIZONTAL BAFFLE CUT

commercial port, Re =1250

(normalised j - factors)

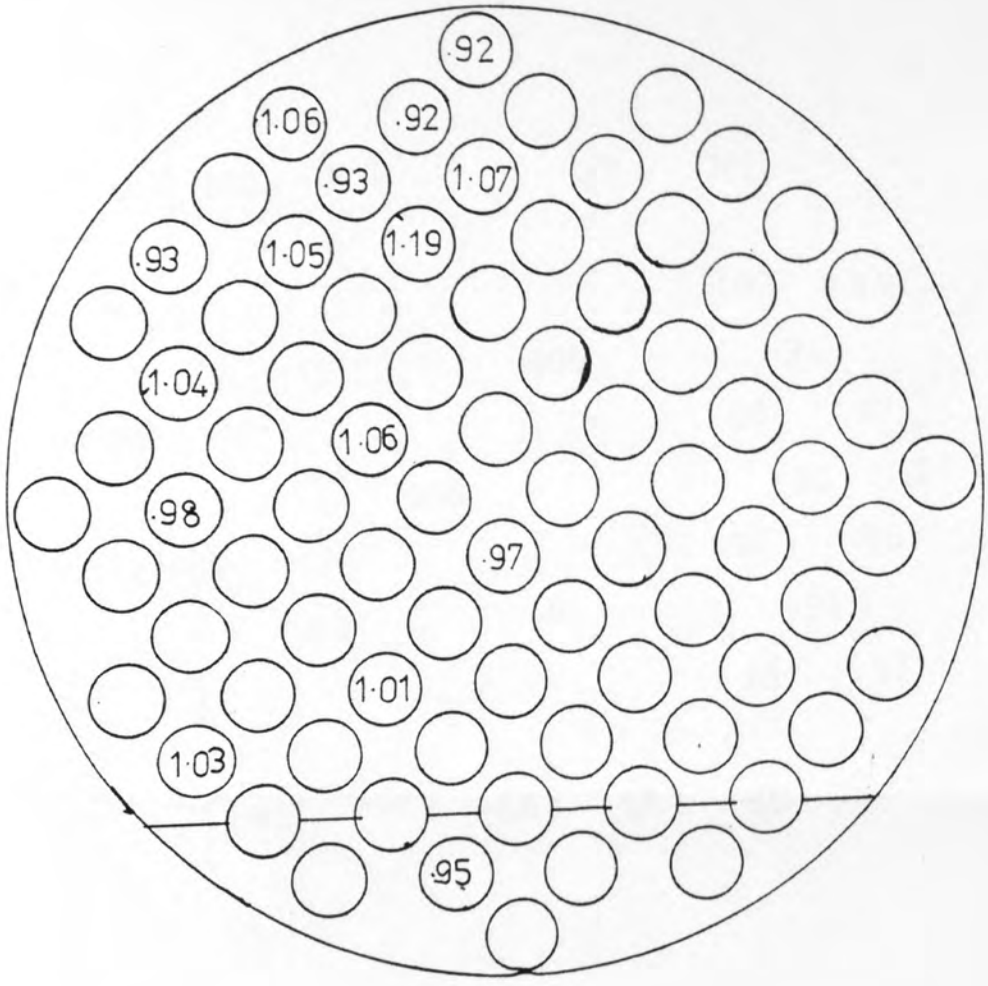

FIG 31 INLET j DISTRIBUTION

HORIZONTAL BAFFLE CUT

commercial port, Re = 1290

(normalised j-factors)

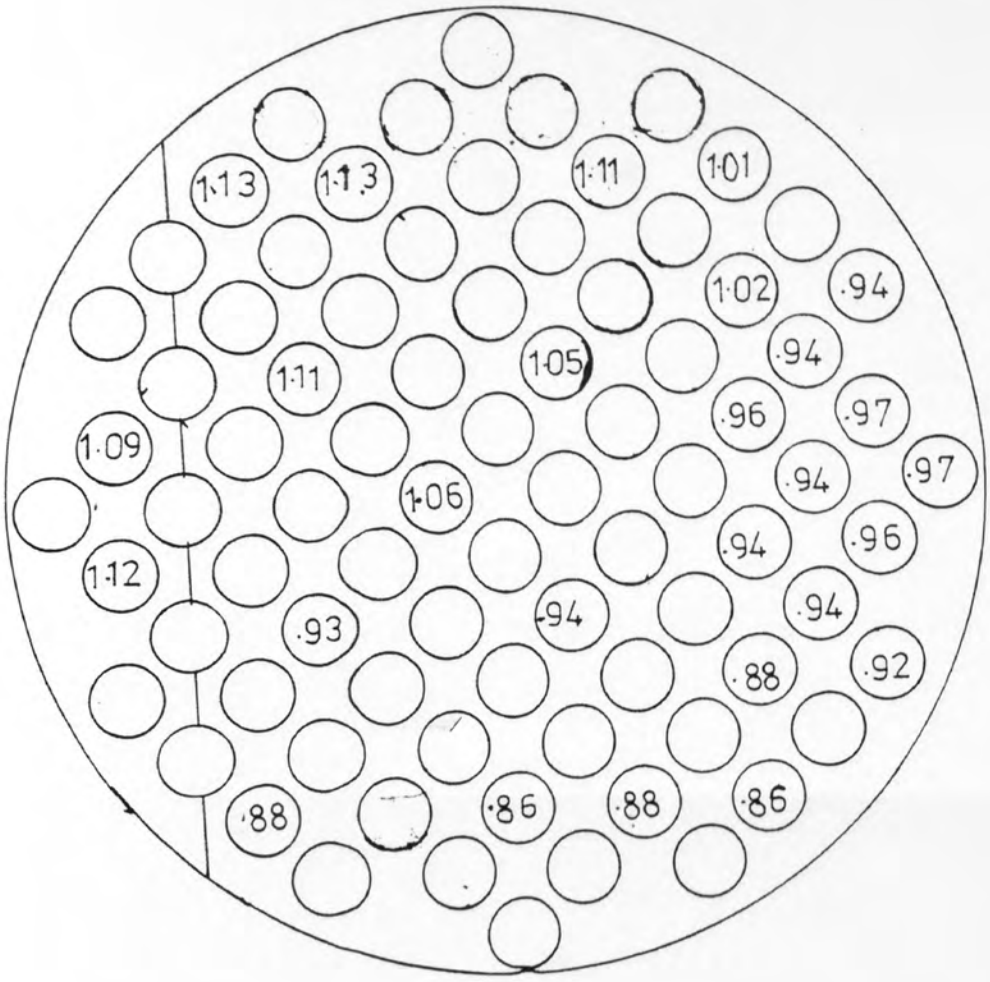

FIG 32 OUTLET j DISTRIBUTION

VERTICAL BAFFLE CUT

Bergelin port, Re = 1410

(normalised j-factors)

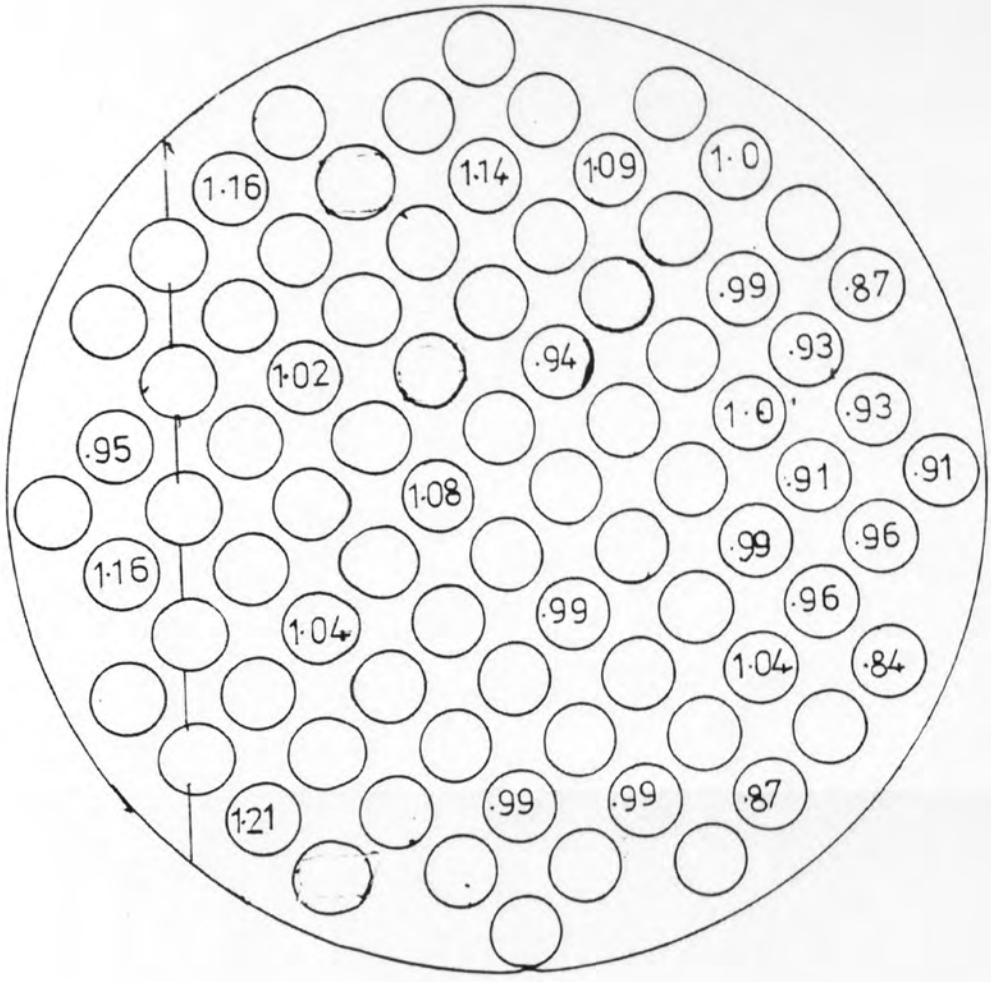

FIG 38 INLET j DISTRIBUTION
VERTICAL BAFFLE CUT

Bergelin port, Re = 1330

(normalised j-factors)

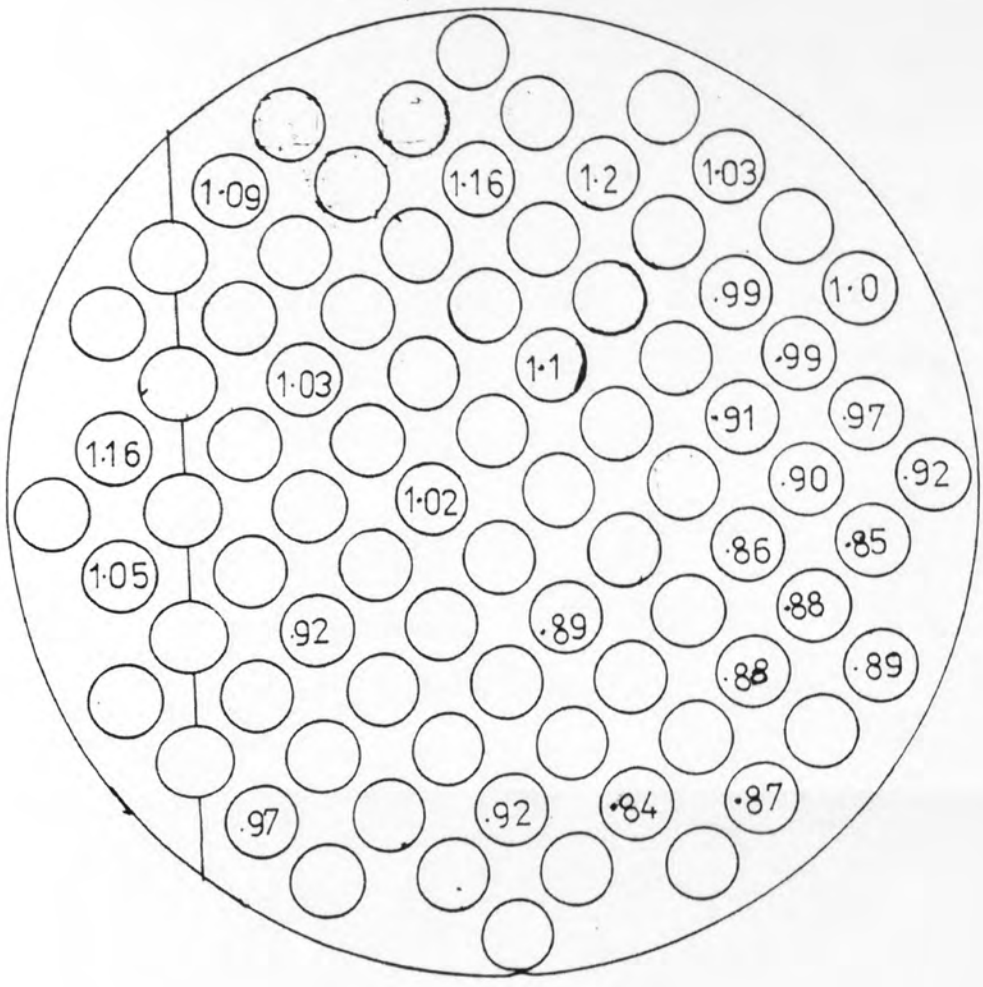

FIG 34 OUTLET j DISTRIBUTION

VERTICAL BAFFLE CUT

commercial port, Re = 1170

(normalised j- factors)

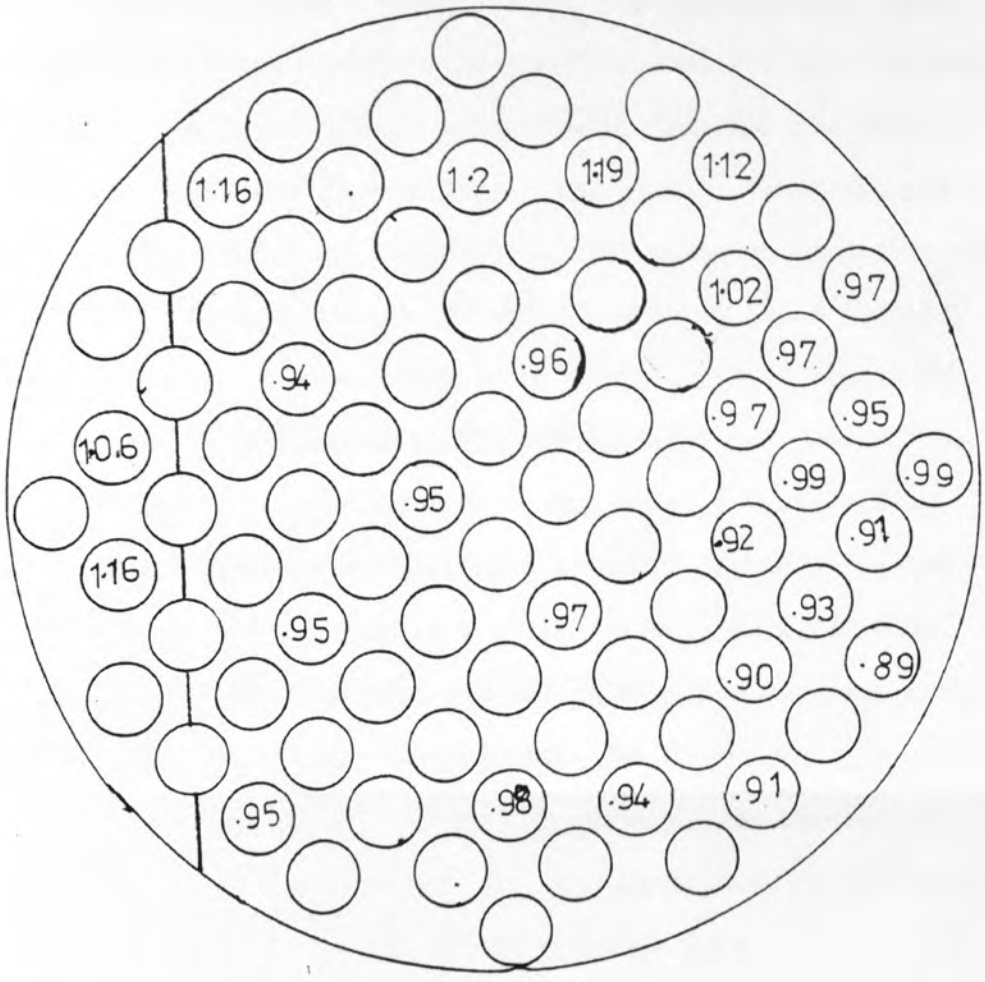

FIG 35 INLET j DISTRIBUTION

VERTICAL BAFFLE CUT

commercial port, Re = 1320

(normalised j-factors)

almost identical j-factor distributions when the baffle cuts are orientated vertically (Figs.32-35) with the bulk of the shell side flow seemingly avoiding a large part of the compartment. This is reasonable as the distribution suggests that the flow follows the shortest path through the compartment, i.e. for the inlet, from top to side, and vice-versa for the outlet. However, for the horizontal baffle cut orientation, the j-factor distributions are much more uniform across the whole bundle for both compartments (Figs.28 to 31), as there is no 'short cut' for the flow to take with the horizontal baffle cut orientation. Whilst the outlet compartment j-factors have a very uniform distribution, those for the inlet compartment give slightly higher j-factors in the middle of the bundle (the crossflow zone as defined by Mackley (1)) than elsewhere, but the differences are very small. It may be fair to assume, however, that the differences in the distribution of j-factors between the vertical and horizontal baffle cut orientations account for the differences in the inlet - outlet compartment average j-factor comparisons.

8.5 EFFECT OF BAFFLE ORIENTATION

In industrial shell and tube heat exchangers, the baffle cut is usually arranged so that the flow weaves from side to side. This provides a channel for liquid drainage along the whole length of the bundle, and also helps to prevent bundle sagging by providing extra support for the heat exchanger tubes. Normally, the positioning of the inlet and outlet ports for the shell side flow would allow for this consideration, to ensure that the baffle cuts in the end compartments are parallel to the plane of the flow ports. However, this design is not always possible, and hence a study of the effect of having the baffle cut perpendicular to the plane of the flow ports is needed. In the

present work, the vertical baffle cut orientation corresponds to this special case, and the horizontal baffle cut orientation corresponds to the design normally used.

The compartment average j-factors for the horizontal and vertical baffle cut orientations were compared in Figs. (36 to 39) for both the inlet and outlet compartments and for the two ports studied.

Both the inlet compartment comparisons (Fig.(36) Bergelin type ports and Fig.(38) commercial type ports) show that the vertical baffle cut data fall slightly below the horizontal baffle cut data, although both data sets can be well represented by the same curve. The outlet compartment averages, however, (Figs.(37,39)) show that, although the vertical baffle cut data fall below those for the horizontal baffle cut above Re=1000, below this figure the reverse is true, although it must again be stressed that the differences are small and that again, in each case, a single curve can represent both the horizontal and the vertical baffle cut data.

As the differences in overall compartment average j-factors between the horizontal and vertical baffle cut orientations are extremely small, it is fair to conclude that the compartment average j-factor is independent of baffle orientation.

A study of the relative j-factor distributions would reveal a better basis for comparison of baffle orientation than a study of compartment average j-factors. Figs.(40 to 55) give the normalised j-factor distributions for the low and high regions of the Reynolds number range. The corresponding distributions for the middle of the Reynolds number range have previously been given in Figs.(28 to 35). The following table

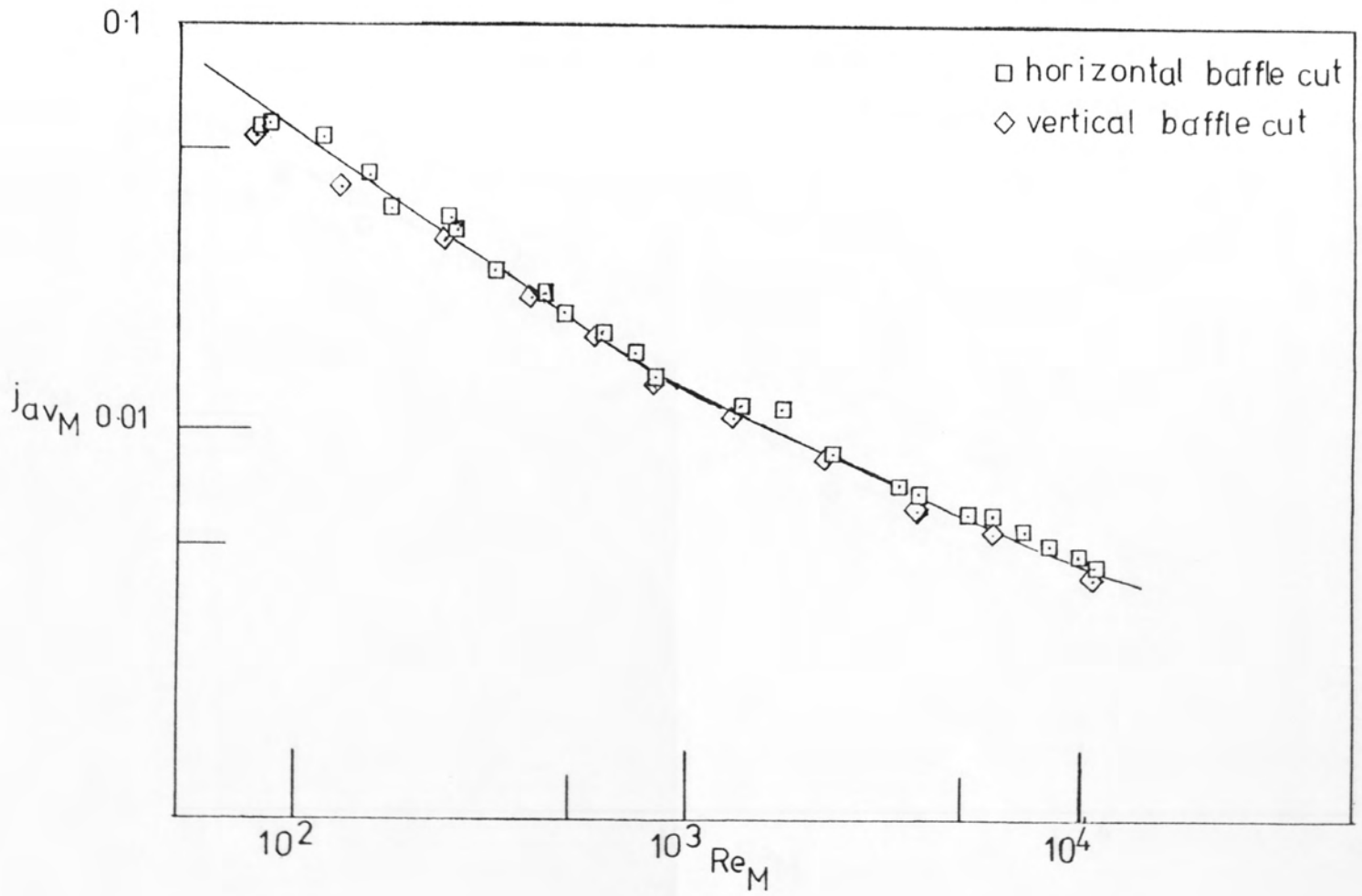

FIG 36 EFFECT OF BAFFLE ORIENTION

(Bergelin ports, inlet compartment)

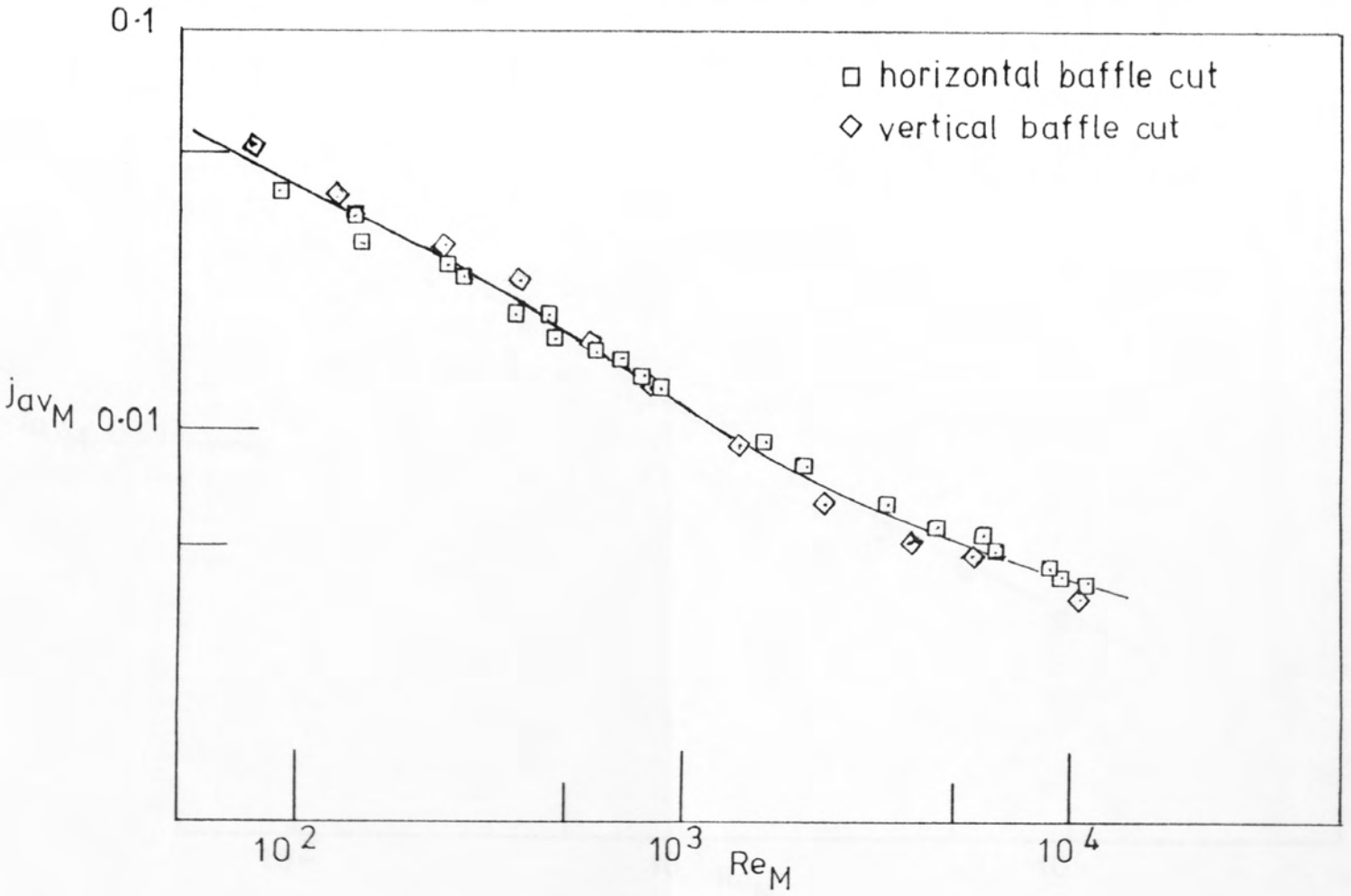

FIG 37 EFFECT OF BAFFLE ORIENTATION
(Bergelin ports outlet compartment)

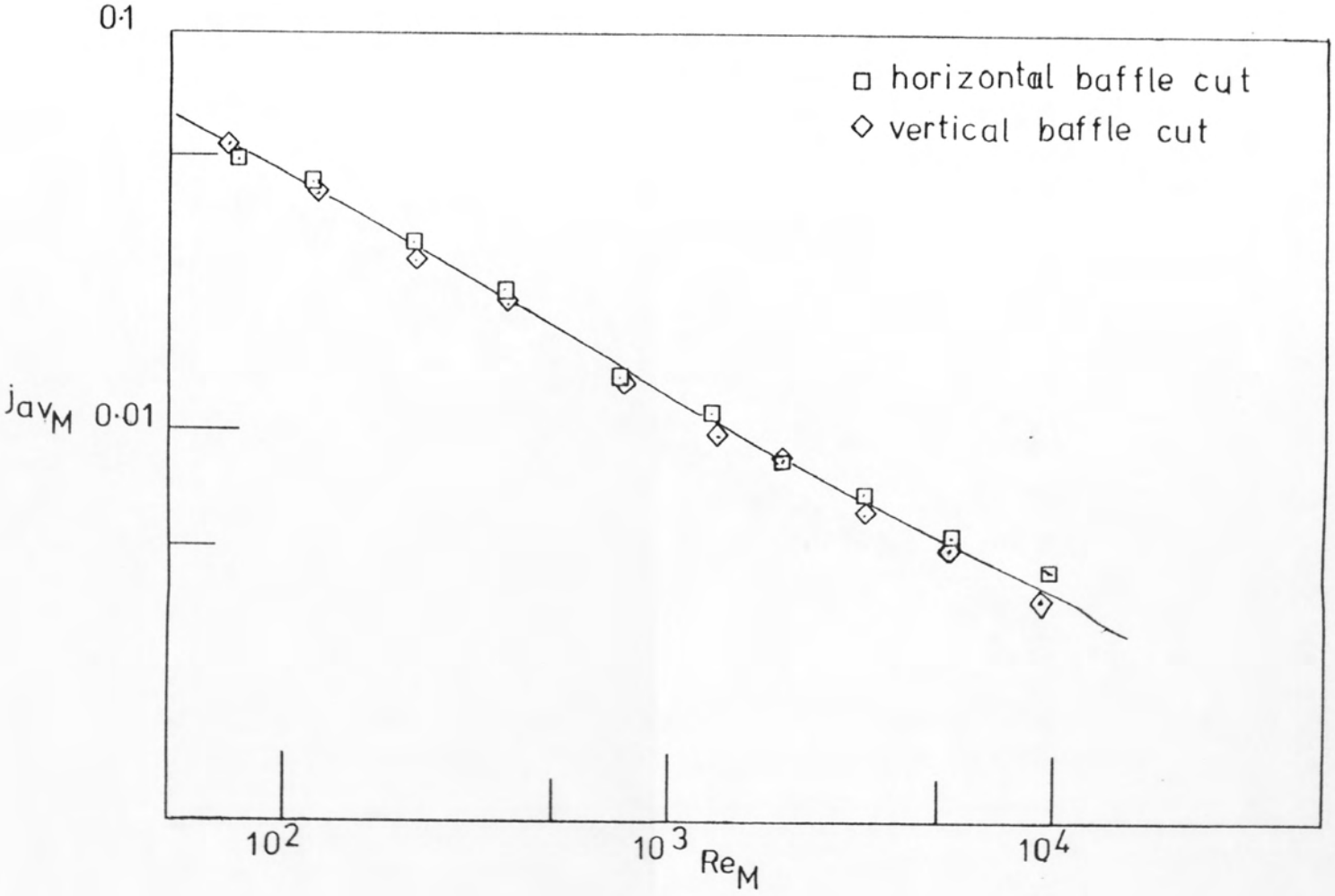

FIG 38 EFFECT OF BAFFLE ORIENTATION
(commercial ports, inlet compartment)

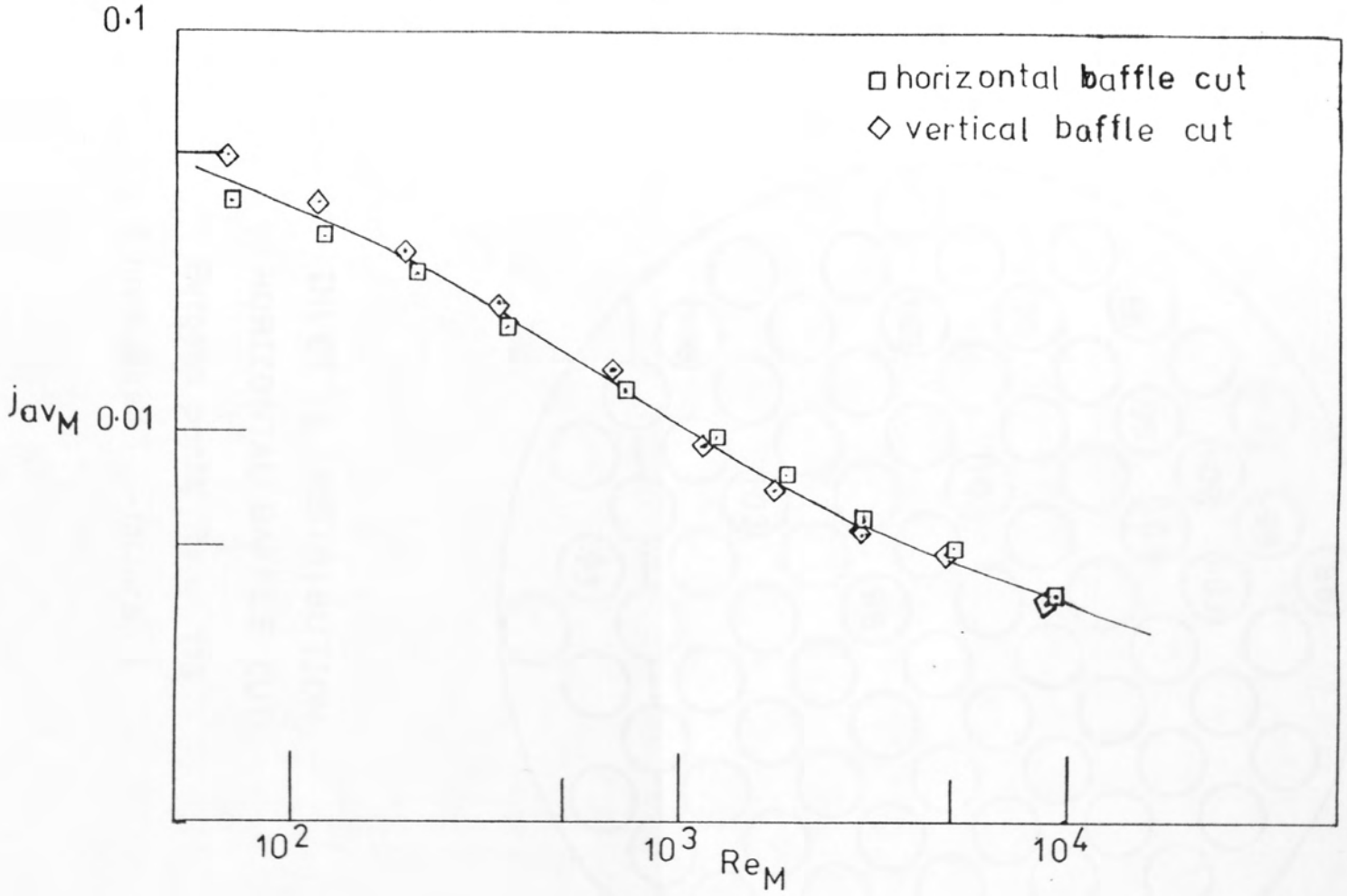

FIG 39 EFFECT OF BAFFLE ORIENTATION
(commercial ports, outlet compartment)

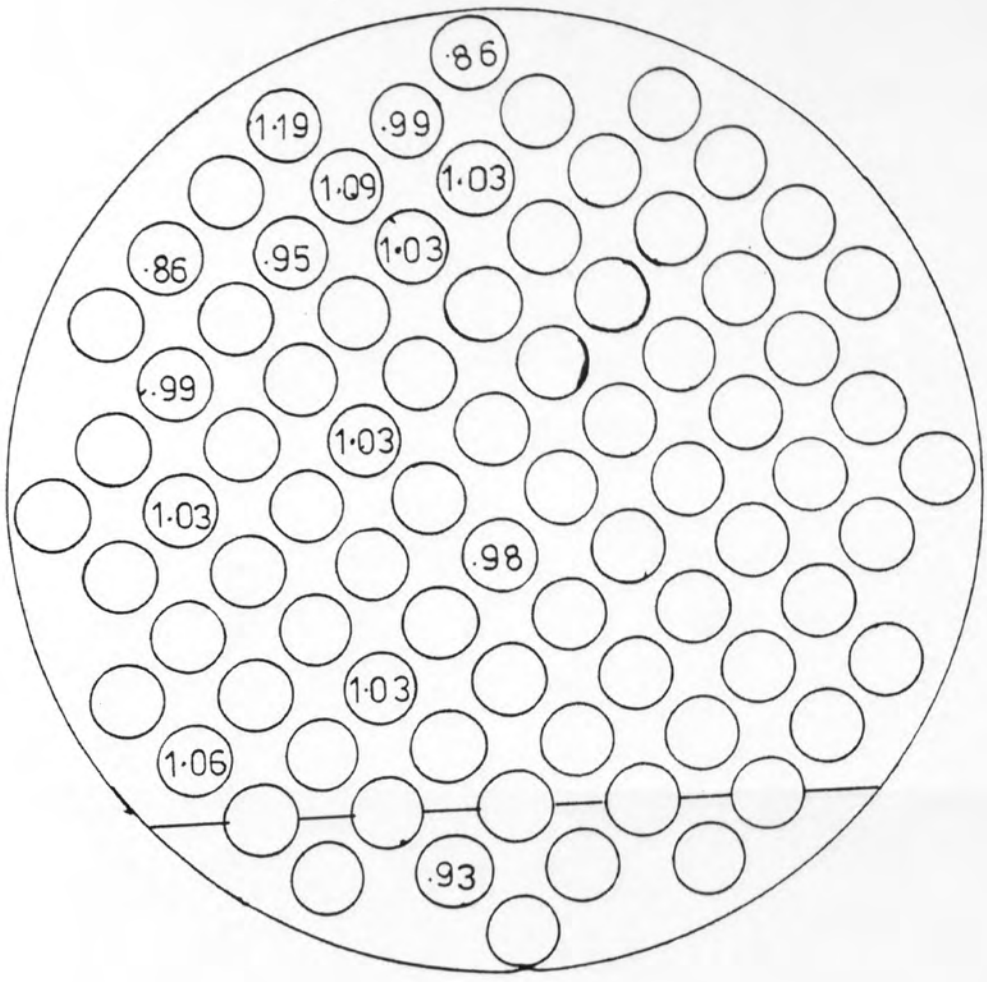

FIG 40 INLET j DISTRIBUTION
HORIZONTAL BAFFLE CUT
Bergelin ports, Re = 118
(normalised j-factors)

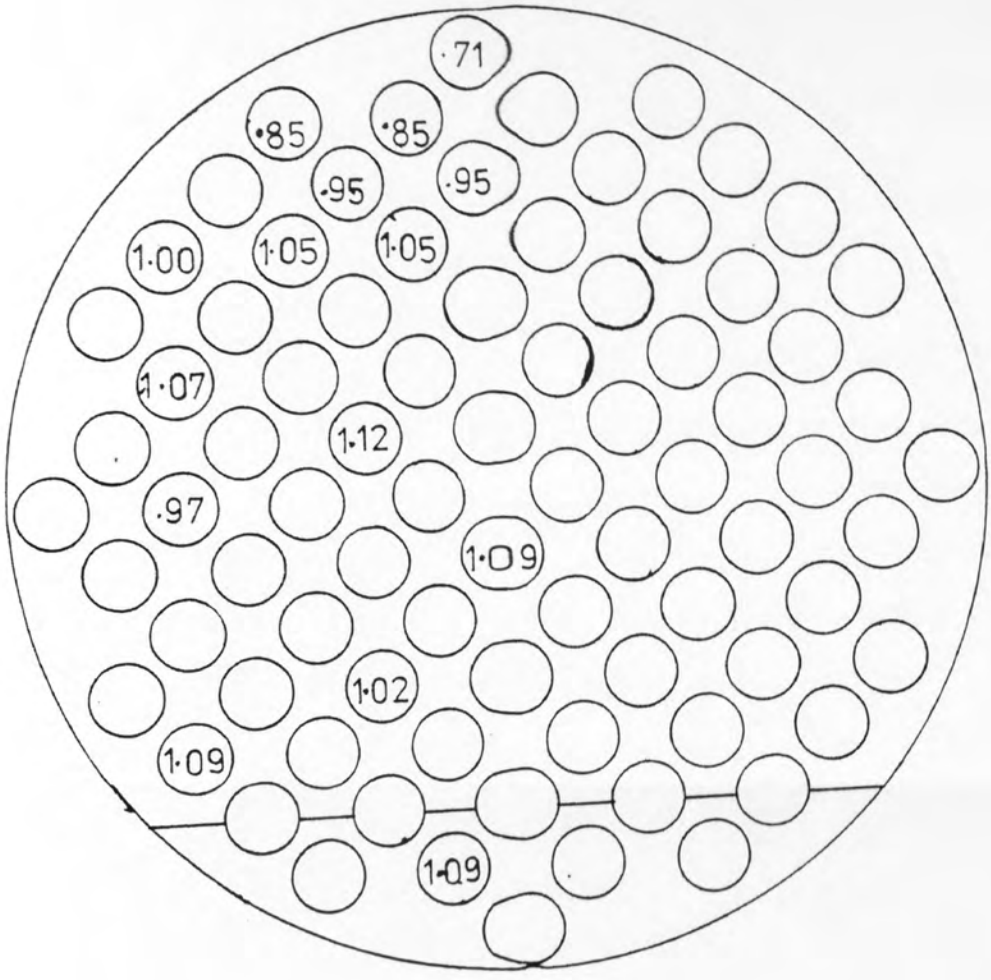

FIG 41 OUTLET j DISTRIBUTION

HORIZONTAL BAFFLE CUT

Bergelin ports, Re = 141

(normalised j-factors)

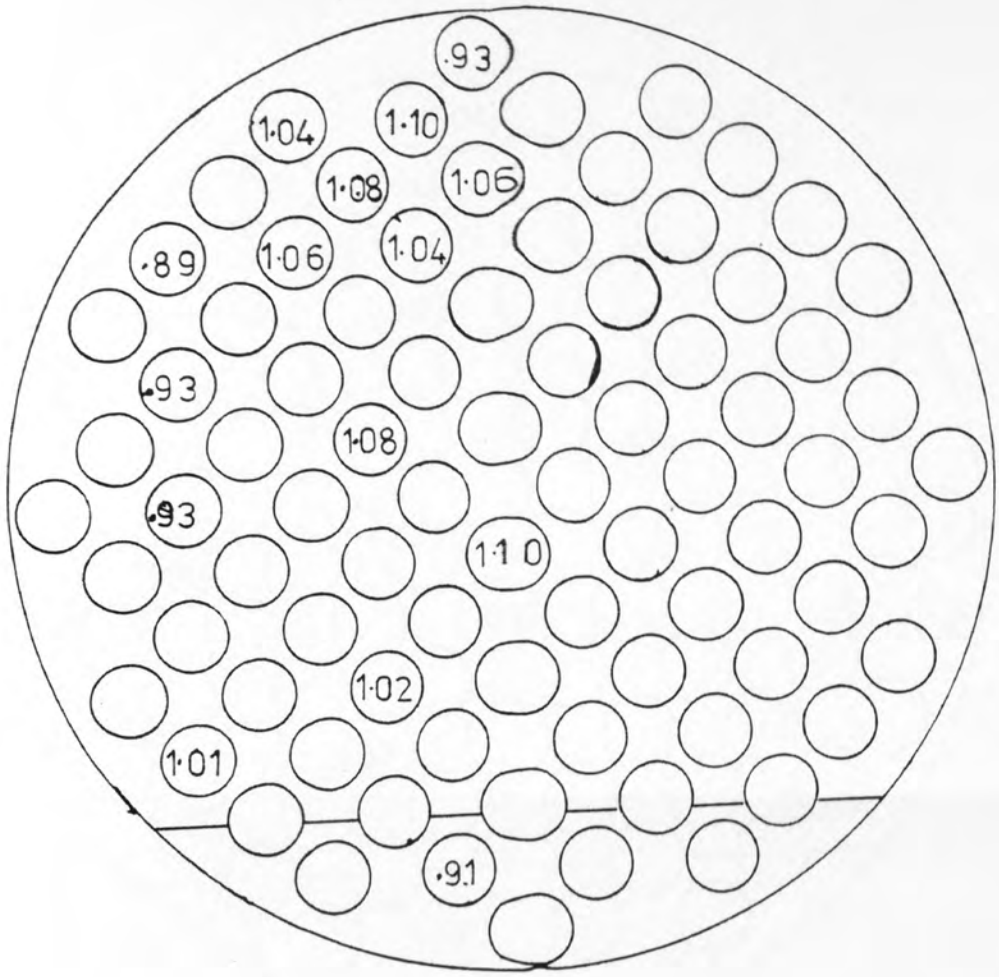

FIG 42 INLET j-DISTRIBUTION

HORIZONTAL BAFFLE CUT

commercial ports, Re = 117

(normalised j-factors)

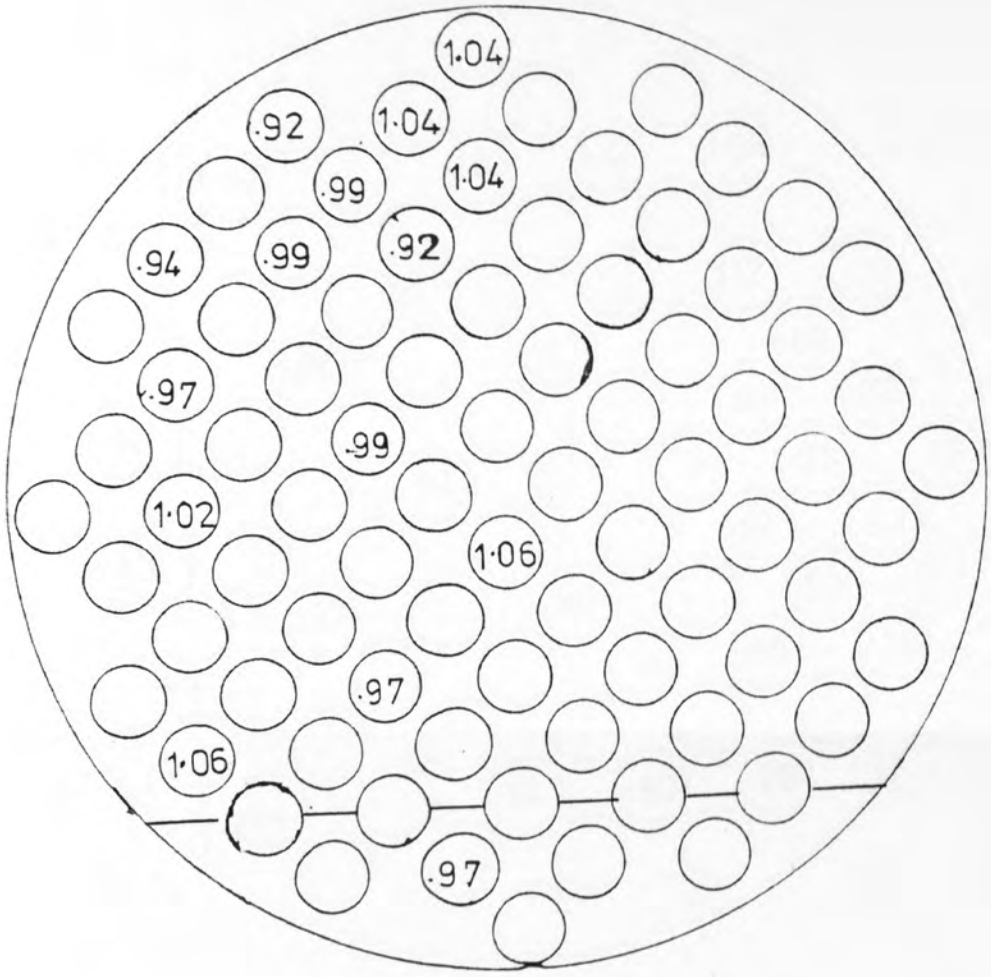

FIG 43 OUTLET j DISTRIBUTION
HORIZONTAL BAFFLE CUT
commercial ports, Re = 121
(normalised j - factors)

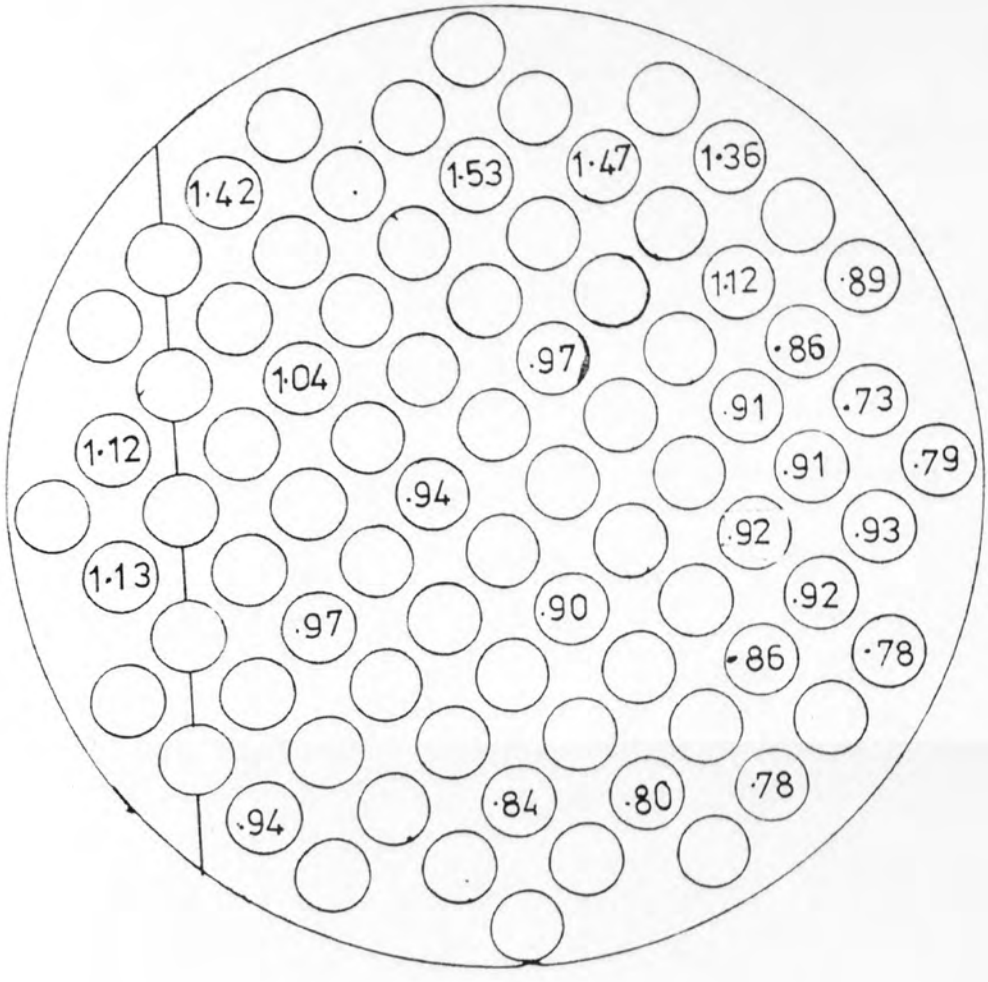

FIG 44 INLET j DISTRIBUTION

VERTICAL BAFFLE CUT

Bergelin ports, Re = 129

(normalised j - factors)

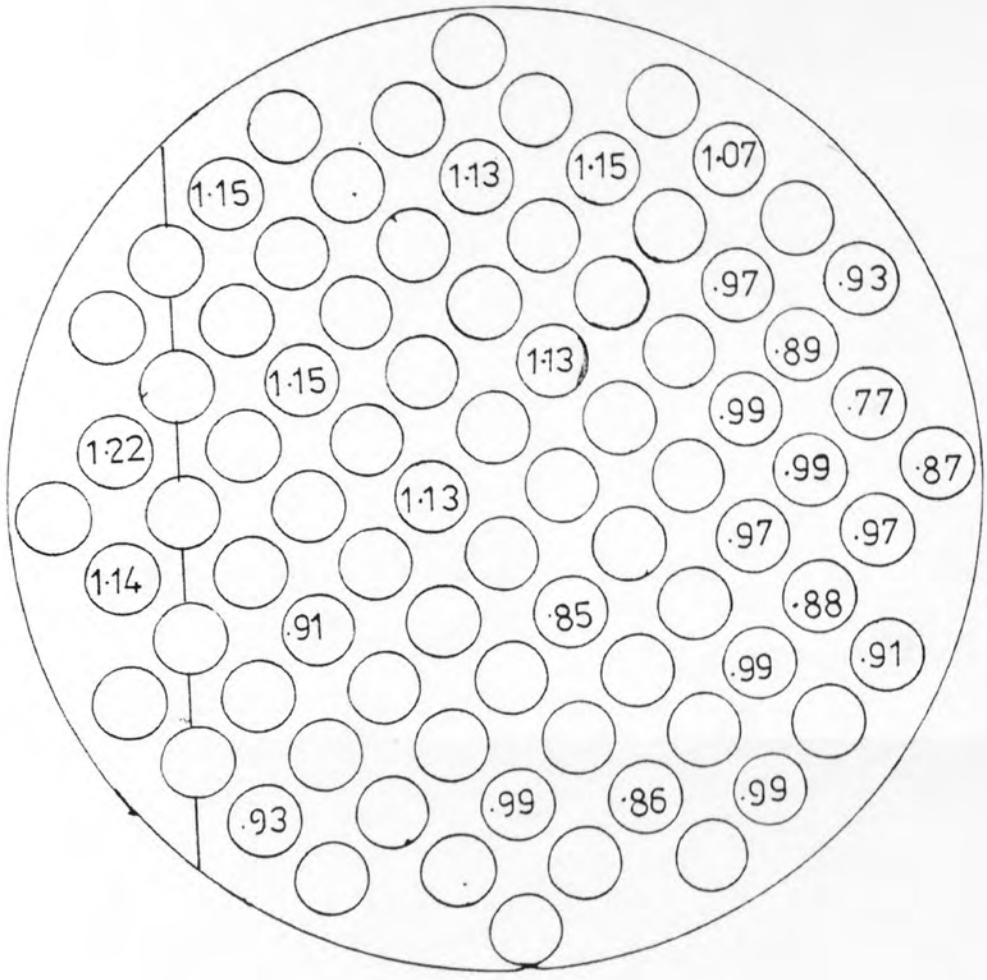

FIG 45 OUTLET j DISTRIBUTION
VERTICAL BAFFLE CUT
Bergelin ports, Re = 127
(normalised j - factors)

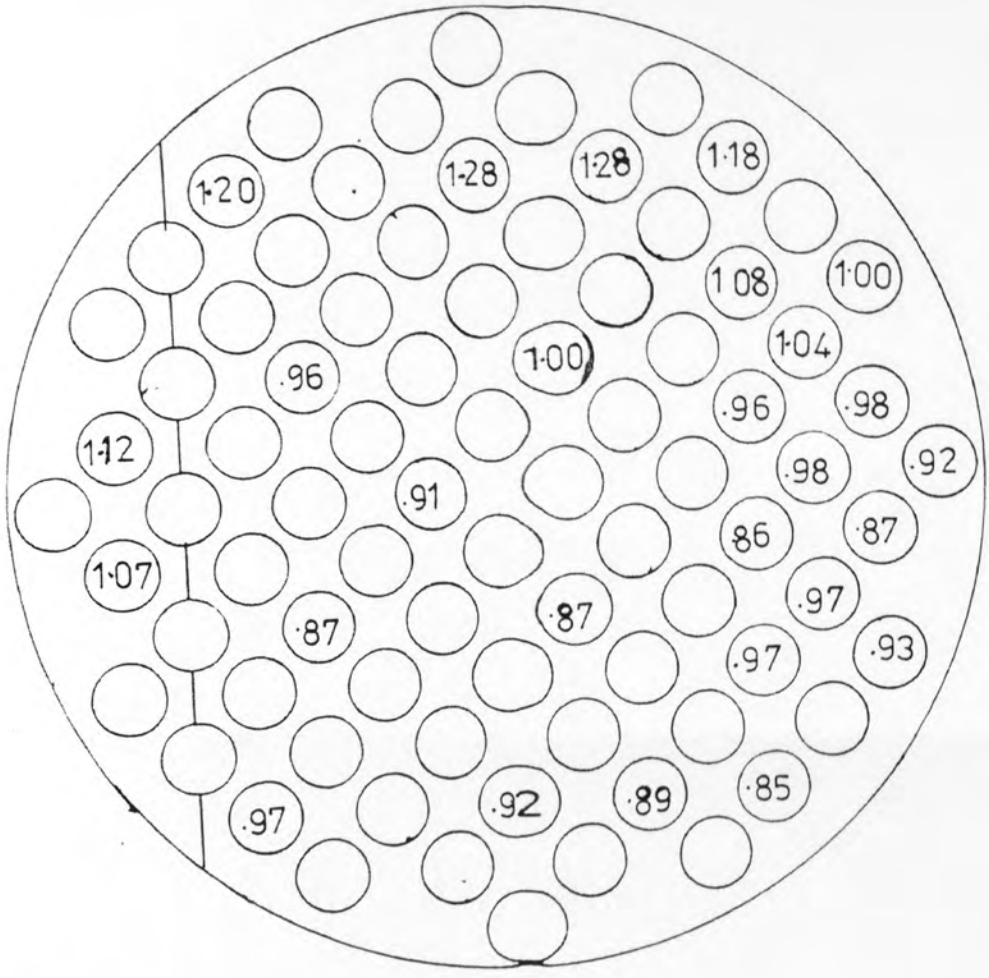

FIG 46 INLET j-DISTRIBUTION
VERTICAL BAFFLE CUT
commercial ports, Re=122
(normalised j-factors)

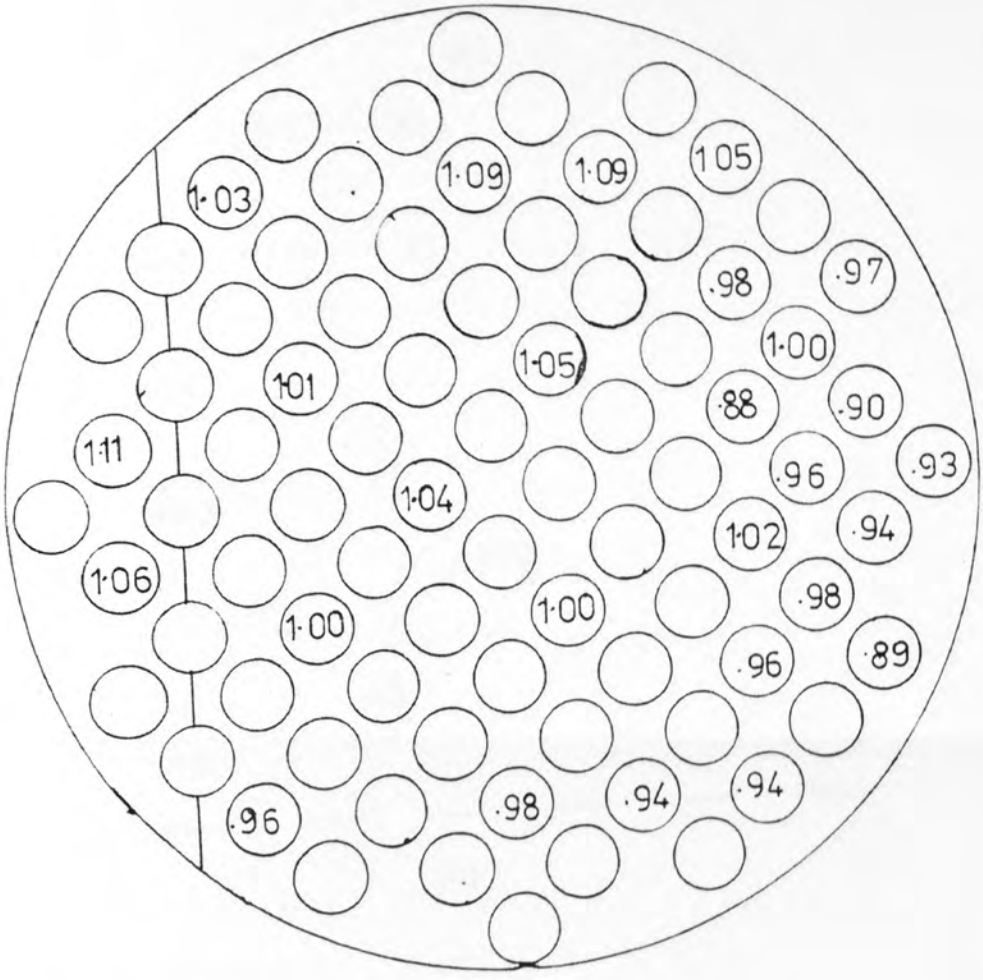

FIG 47 OUTLET j DISTRIBUTION

VERTICAL BAFFLE CUT

commercial ports, Re = 116

(normalised j - factors)

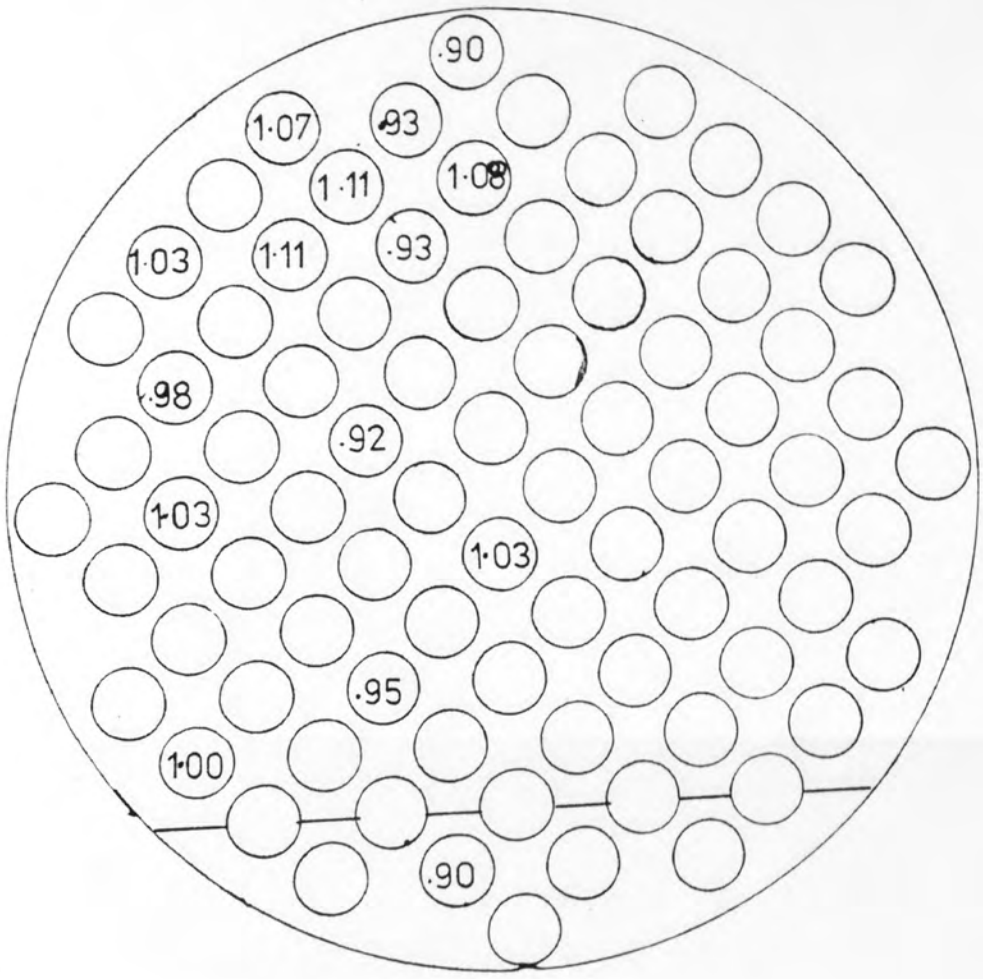

FIG 48 INLET j-DISTRIBUTION

HORIZONTAL BAFFLE CUT

Bergelin ports, Re = 10200

(normalised j - factors)

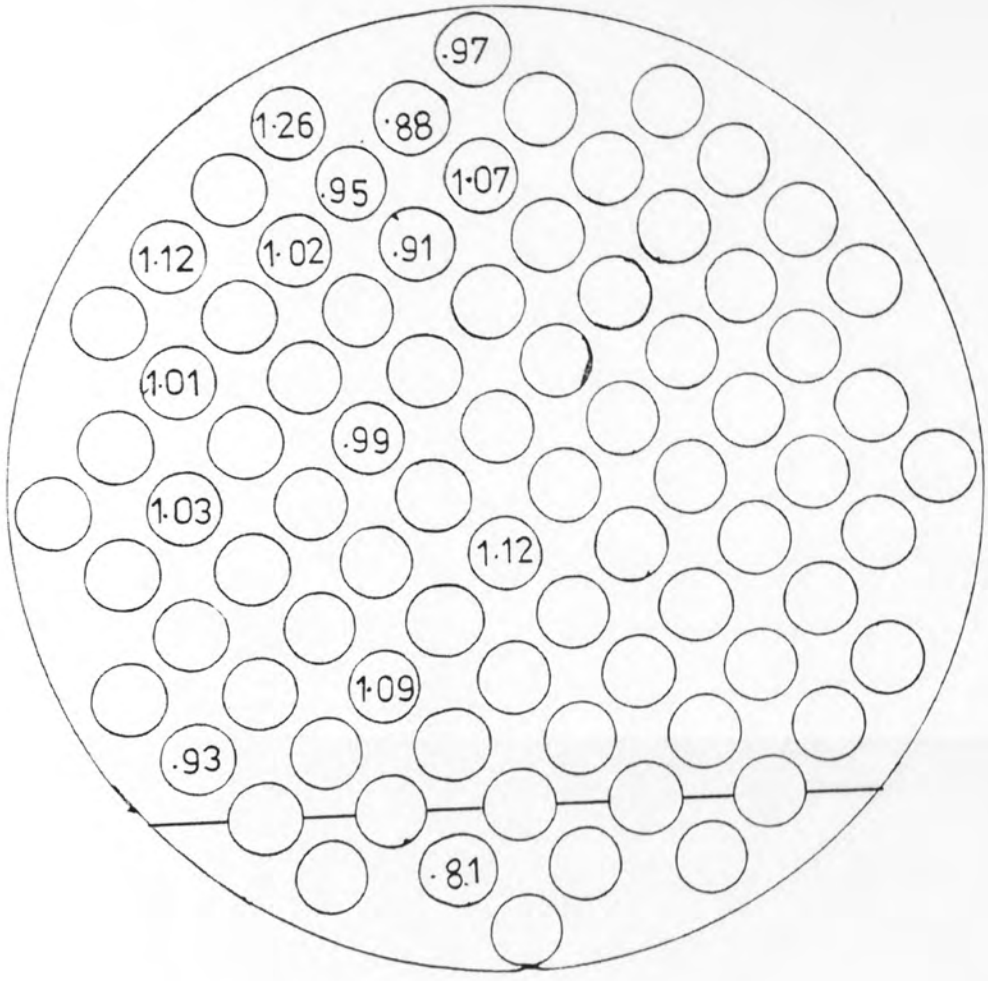

FIG 49 OUTLET j - DISTRIBUTION

HORIZONTAL BAFFLE CUT

Bergelin ports, Re = 9610

(normalised j-factors)

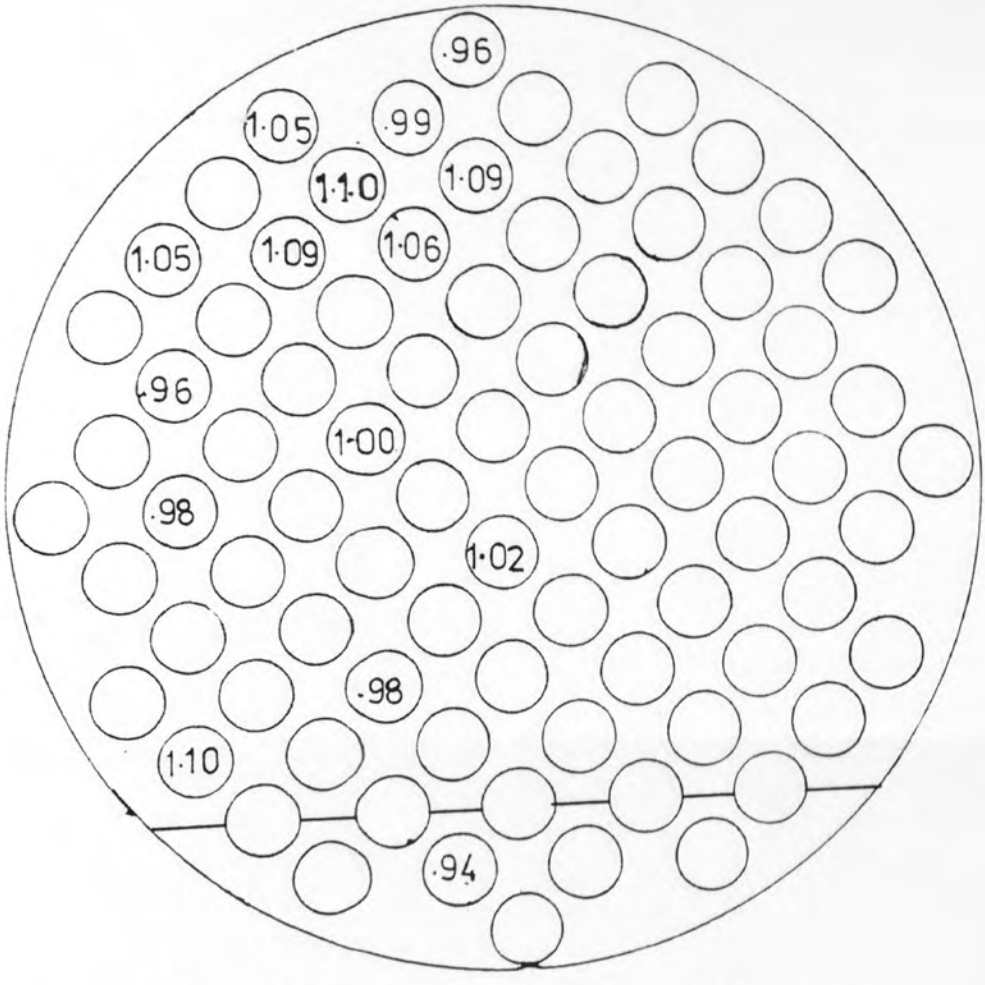

FIG 50 INLET j DISTRIBUTION

HORIZONTAL BAFFLE CUT

commercial ports, Re = 9850

(normalised j - factors)

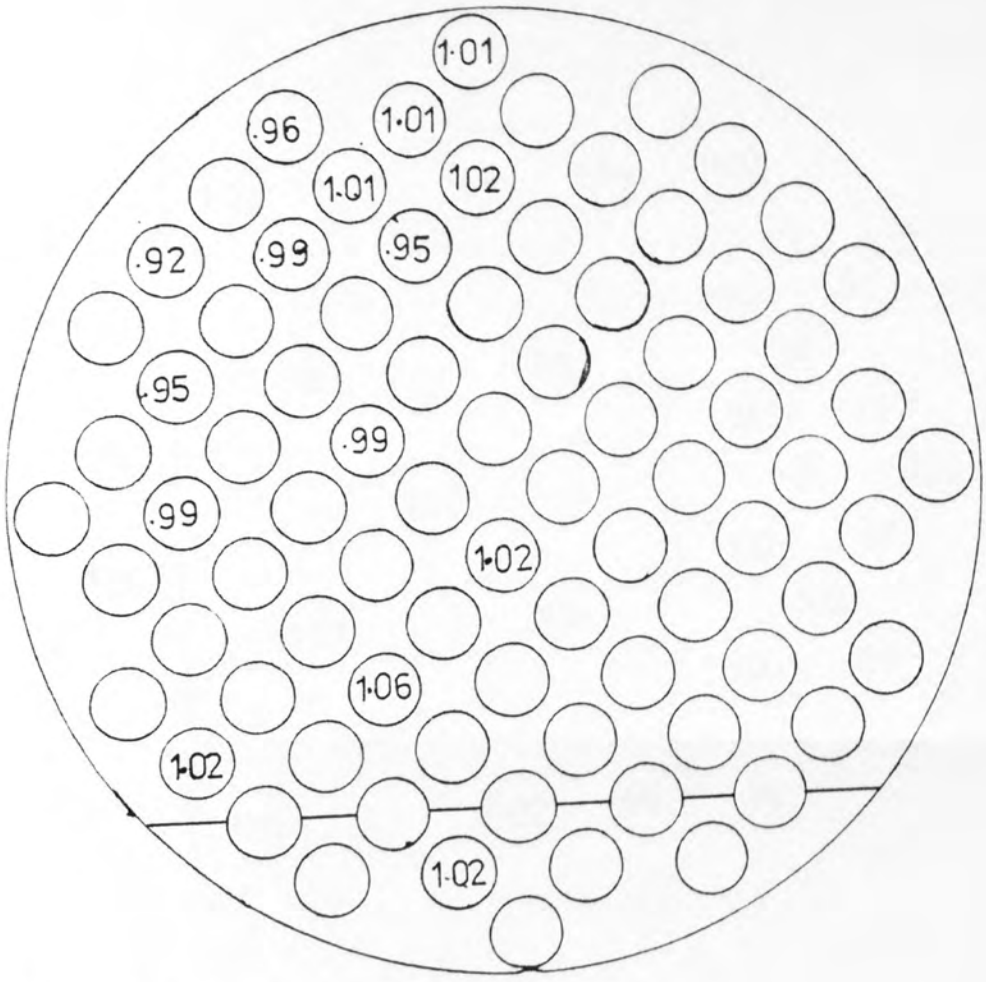

FIG 51 OUTLET j DISTRIBUTION

HORIZONTAL BAFFLE CUT

commercial ports, Re = 9540

(normalised j-factors)

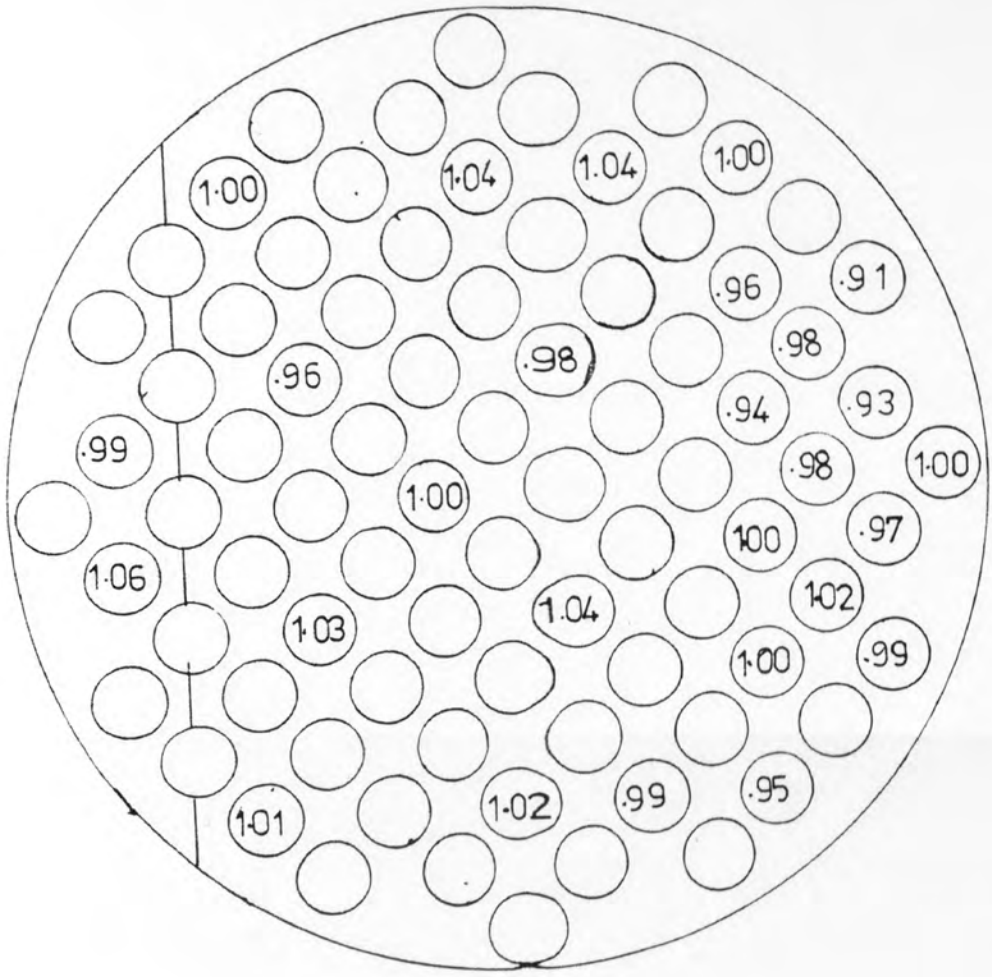

FIG 52 INLET j DISTRIBUTION
VERTICAL BAFFLE CUT

Bergelin ports, Re = 10 900
(normalised j-factors)

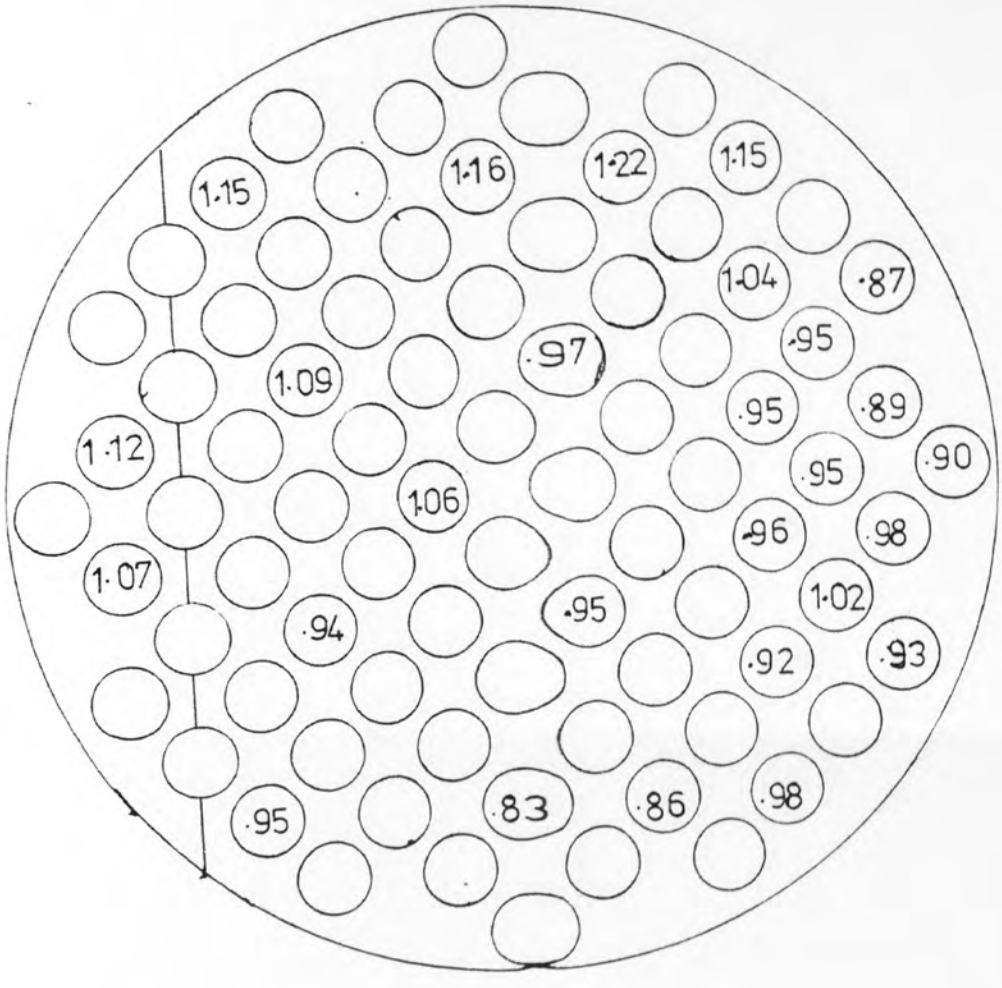

FIG 53 OUTLET j DISTRIBUTION

VERTICAL BAFFLE CUT

Bergelin ports, Re = 10700

(normalised j-factors)

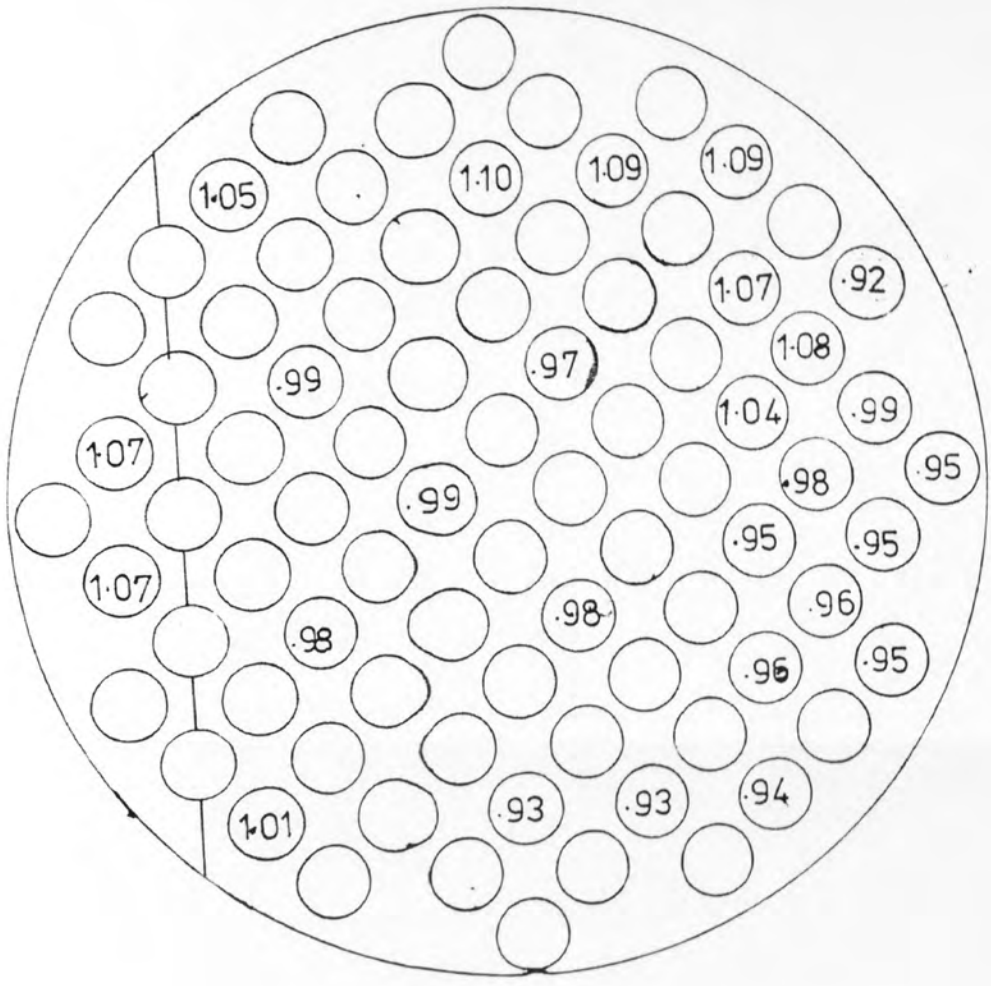

FIG 54 INLET j DISTRIBUTION

VERTICAL BAFFLE CUT

commercial ports, Re = 9640

(normalised j-factors)

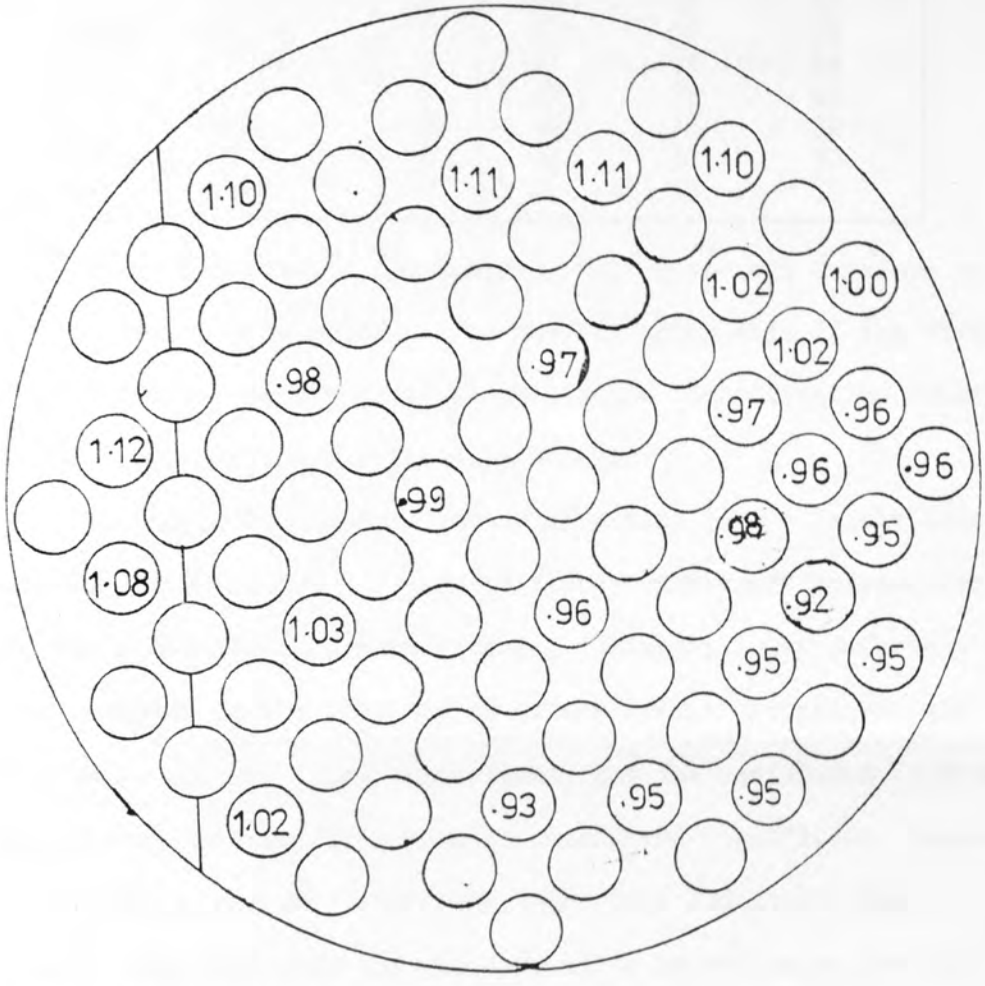

FIG 55 OUTLET j DISTRIBUTION

VERTICAL BAFFLE CUT

commercial ports, Re = 8970

(normalised j factors)

is included to show what each distribution diagram represents:

ORIENTATION	COMPARTMENT	PORT	Reynolds Number Ranges		
			Re = 120,	1200 ,	10000
horizontal	outlet	B	41	28	49
vertical	outlet	B	45	32	53
horizontal	outlet	C	43	30	51
vertical	outlet	C	47	34	54
horizontal	inlet	B	40	29	48
vertical	inlet	B	44	33	52
horizontal	inlet	C	42	31	50
vertical	inlet	C	46	35	55

Where B refers to the Bergelin type ports and C refers to the commercial type ports. The numbers under each of the three Reynolds number values refer to the figure identification number of the corresponding distribution diagram.

The horizontal baffle cut orientations gave a fairly even j-factor distribution for each port/end compartment combination for the whole Reynolds number range. Slightly lower j-factors were observed in the port region of the outlet compartment and the window area of inlet compartment, but the deviations from the average were not sufficient to be considered significant. However, the electrode directly under the inlet port had lower than average j-factors over the whole Reynolds number range for both ports. It can be argued that this tube has lower j-factors simply because it is in the direct path of the flow from the port, where the disturbance to the flow is a minimum. However, the horizontal baffle cut orientation gives very even j-factor distributions in the end compartments, regardless of the type of port or the flow rate.

The vertical baffle cut orientation, however, gave considerably uneven distributions in each case over the whole Reynolds number range, where the j-factors were considerably higher than average in the port and window zones. The j-factors

were extremely low in the region of the compartment furthest from both the port and window areas. This maldistribution of j-factors was less pronounced at the higher Reynolds numbers in the inlet compartment for the Bergelin type port. This is attributed to the unusually large size of the Bergelin port, allowing the electrolyte to reach the remote areas of the inlet compartment at the higher Reynolds numbers. Higher than average j-factors still existed in the port and window areas.

The maldistributions described for the vertical baffle cut orientation can be explained, as stated in (8.4), by the electrolyte taking the shortest path through the end compartments inducing recirculation and stagnant zones away from the port and window areas. The high j-factors in the port and window areas seem to compensate for the low j-factors elsewhere. This again can be explained by the 'shortest path' hypothesis, as the flow velocities would be higher in this region leading to higher transfer characteristics. Hence, the overall compartment average j-factors were similar to those found for the horizontal baffle cut.

However, it can be concluded here, that although baffle orientation does not affect the overall compartment average j-factor, it has a great effect on the distribution characteristics, with the j-factor distribution for the vertical baffle cut being extremely uneven.

8.6 COMPARISON OF PORT TYPES

The overall compartment average j-factors of the Bergelin and commercial type ports were compared in Figs.(56 to 59) for both baffle cut orientations in each end compartment.

The comparisons show that, on average, the data for the

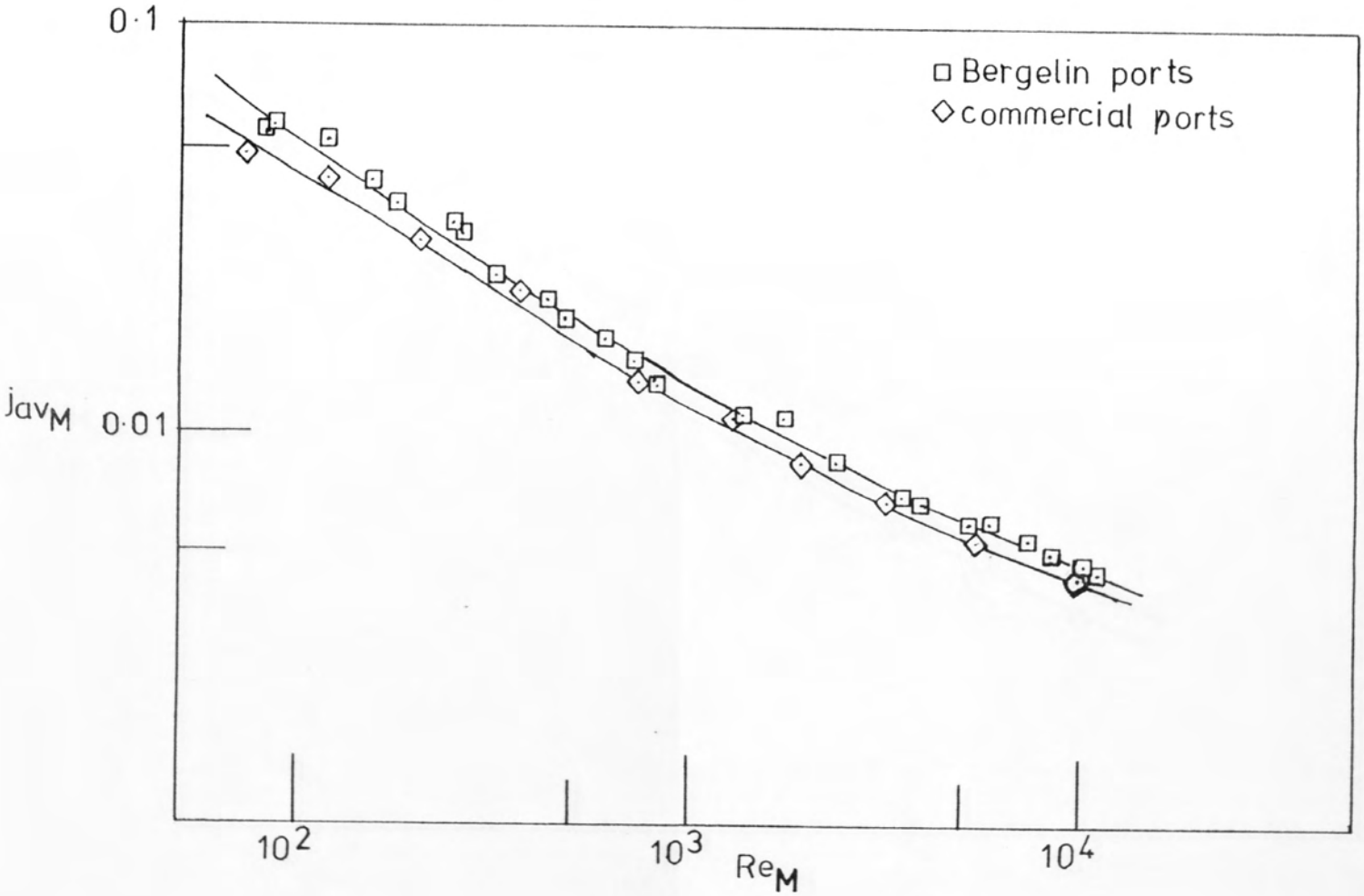

FIG 56 COMPARISON OF PORT TYPE
(inlet compartment, horizontal baffle cut)

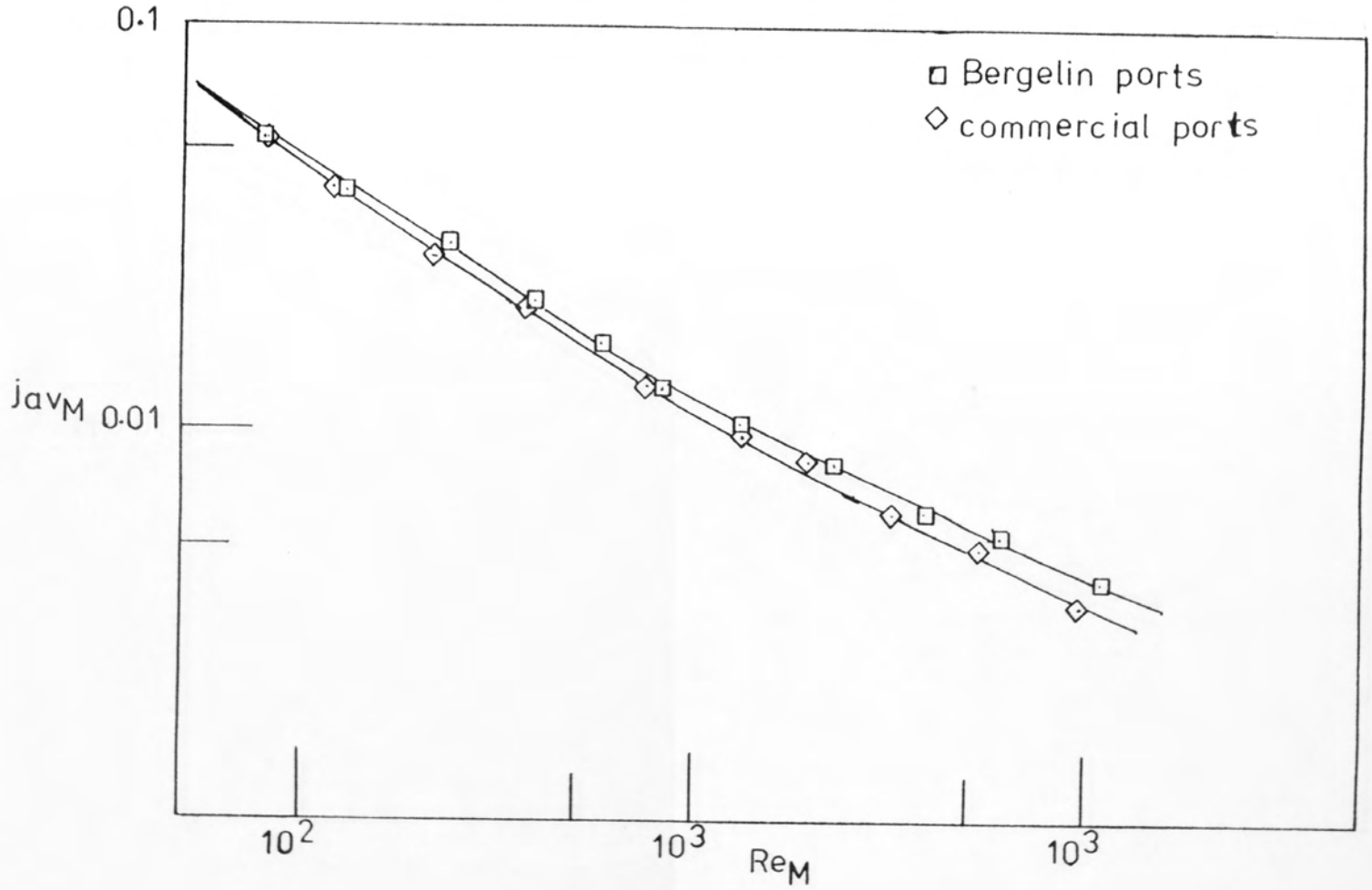

FIG 57 COMPARISON OF PORT TYPE
(inlet compartment, vertical baffle cut)

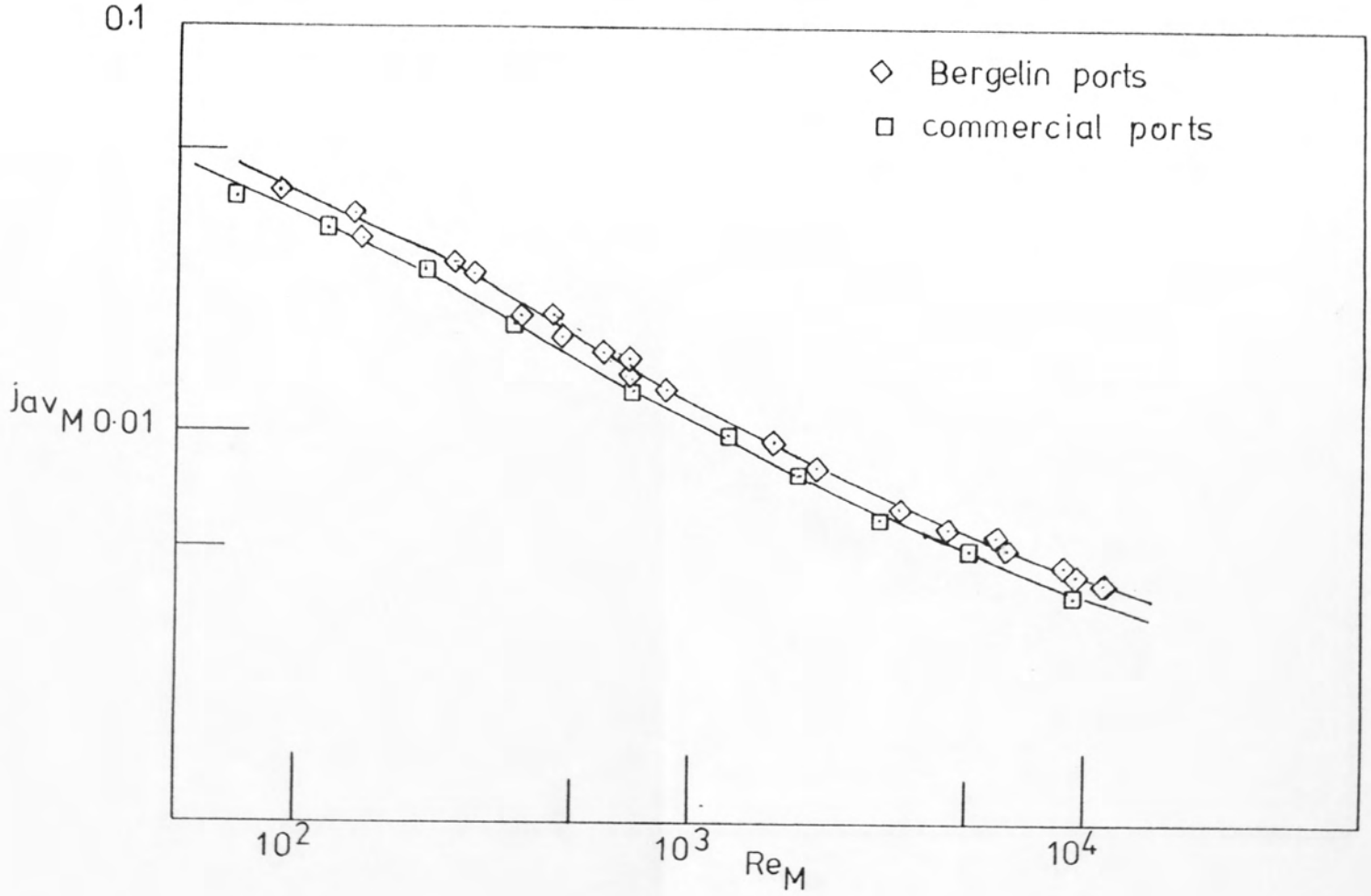

FIG 58 COMPARISON OF PORT TYPE
(outlet compartment, horizontal baffle cut)

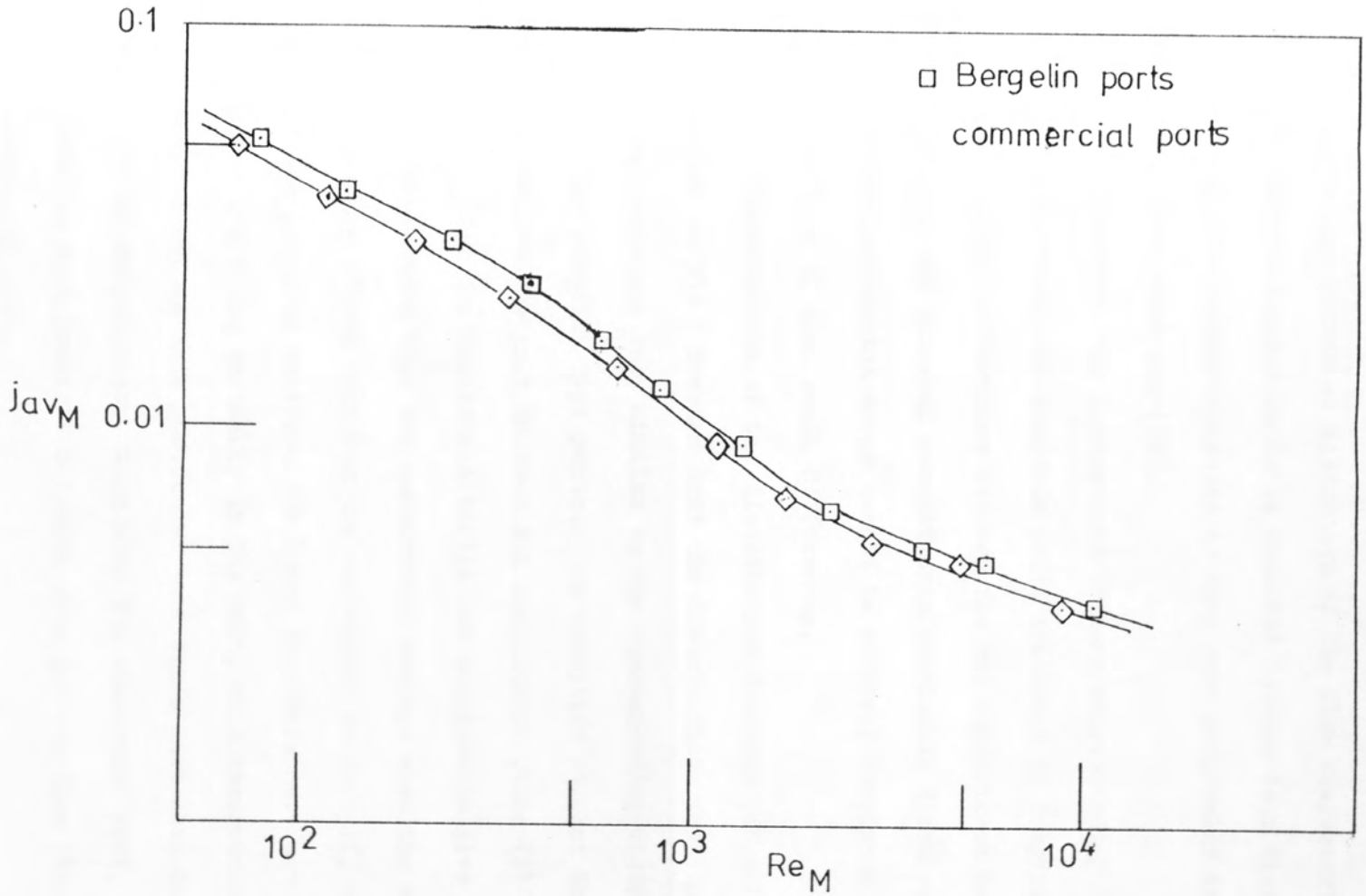

FIG 59 COMPARISON OF PORT TYPE
(outlet compartment, vertical baffle cut)

commercial ports fall about 10% below the corresponding Bergelin port data. An explanation may be that the decrease in heat transfer performance with the commercial type ports is due to the increased distortion of the flow characteristics. The Bergelin ports would be expected to show less distortion of the flow characteristics as they were originally designed to achieve that aim (29).

However, the differences between corresponding data for the commercial and Bergelin ports are small in comparison to the general differences between the end compartment data and that for the internal compartments previously discussed, and hence experimental error cannot be entirely dismissed from being the cause of such small differences.

Examination of the distribution diagrams (Figs.(28 to 35, and 40 to 55)) reveals that the distributions for the commercial type ports are very similar to the corresponding distributions for the Bergelin type ports. An exception is that the tube closest to the port in each end compartment (tube (1) from Fig. (12)) for the horizontal baffle cut orientation give a much lower j-factor than the compartment average when the Bergelin ports are fitted than for the commercial ports. If, as argued in the previous section, the lower j-factors here are due to the electrode being virtually in the port, this observation would make sense, as this particular tube would have less of the flow with the Bergelin port than with the commercial port, as the Bergelin port presents a larger area for the flow than the commercial port.

It can be concluded, however, that the commercial and Bergelin ports produce almost identical distributions of j-factors, and the overall compartment average j-factors are only slightly

lower with the commercial ports fitted than for the Bergelin ports.

8.7 EFFECT OF AN IMPINGEMENT BAFFLE IN THE INLET COMPARTMENT

In industry, impingement baffles are sometimes used in the inlet compartments of shell and tube heat exchangers to overcome erosion problems with the tubes nearest the inlet ports. As no data exists on the effect of impingement baffles on heat exchanger performance, investigations have been included in the scope of the present work (see Section 7 for details of the impingement baffle). Figs (60,61) show the compartment average j-factor comparisons with the commercial type ports without the impingement baffle for the horizontal and vertical baffle cut orientations. Also included for comparison are the Bergelin port data. Fig (62) shows the effect of baffle orientation on the compartment average j-factors with the impingement baffle fitted.

The normalised j-factor distributions for the end compartments are given in Figs. (63 to 68) for low, medium and high flow rates, to enable comparisons to be made with the non-impingement baffle cases.

Examination of Figs. (60,61) revealed that for the horizontal baffle cut orientation the impingement baffle data fell up to 10% higher than the corresponding non-impingement baffle, commercial port data for $500 < Re < 5000$. Outside this range the two sets of data tended to converge. The corresponding data for the non-impingement baffle Bergelin port tended to straddle the data for the impingement baffle case. For the vertical baffle cut orientation, the difference between the two sets of data for the commercial port varied from 0 at $Re = 100$

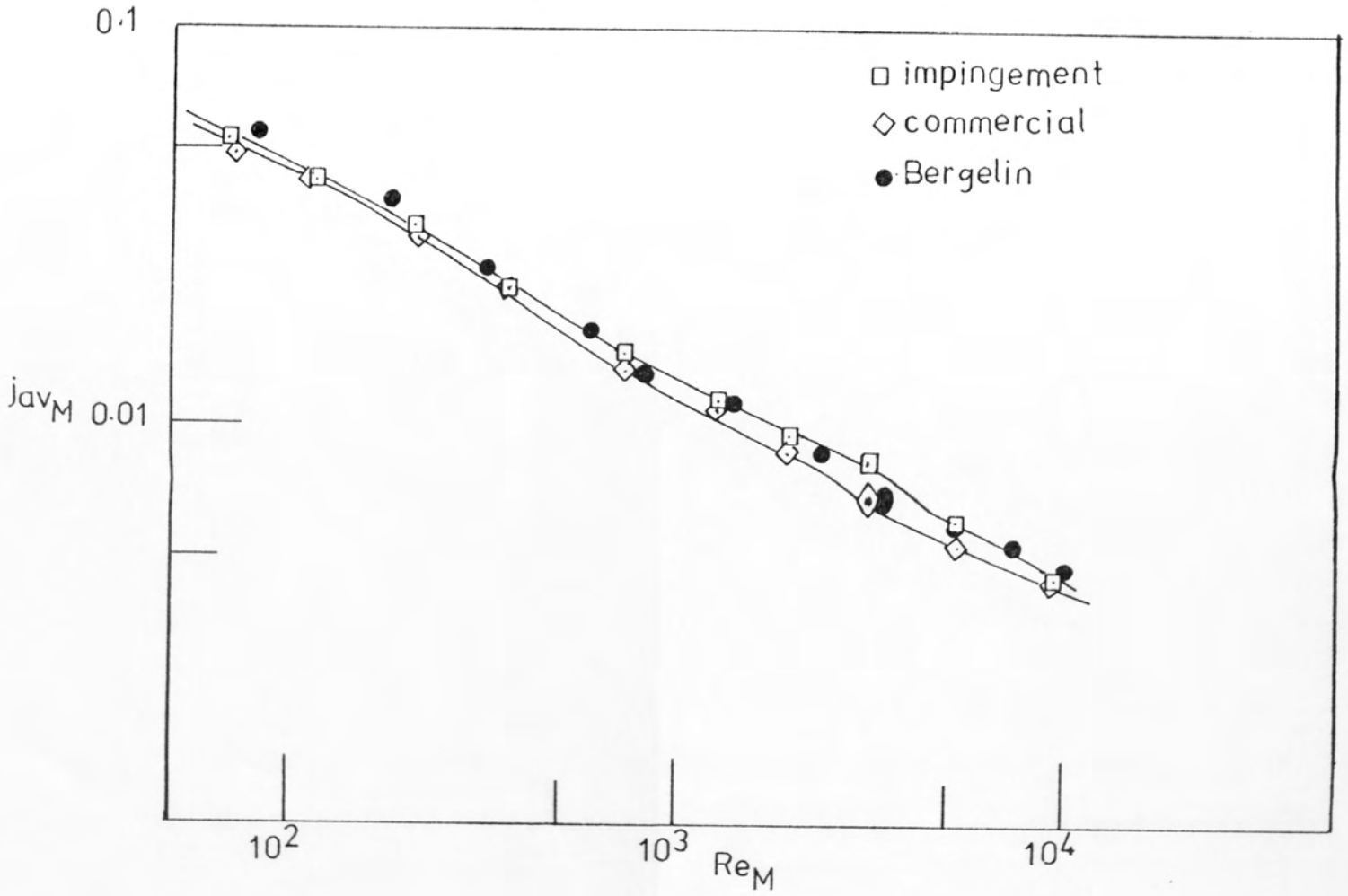

FIG 60 EFFECT OF IMPINGEMENT BAFFLE
(horizontal baffle cut)

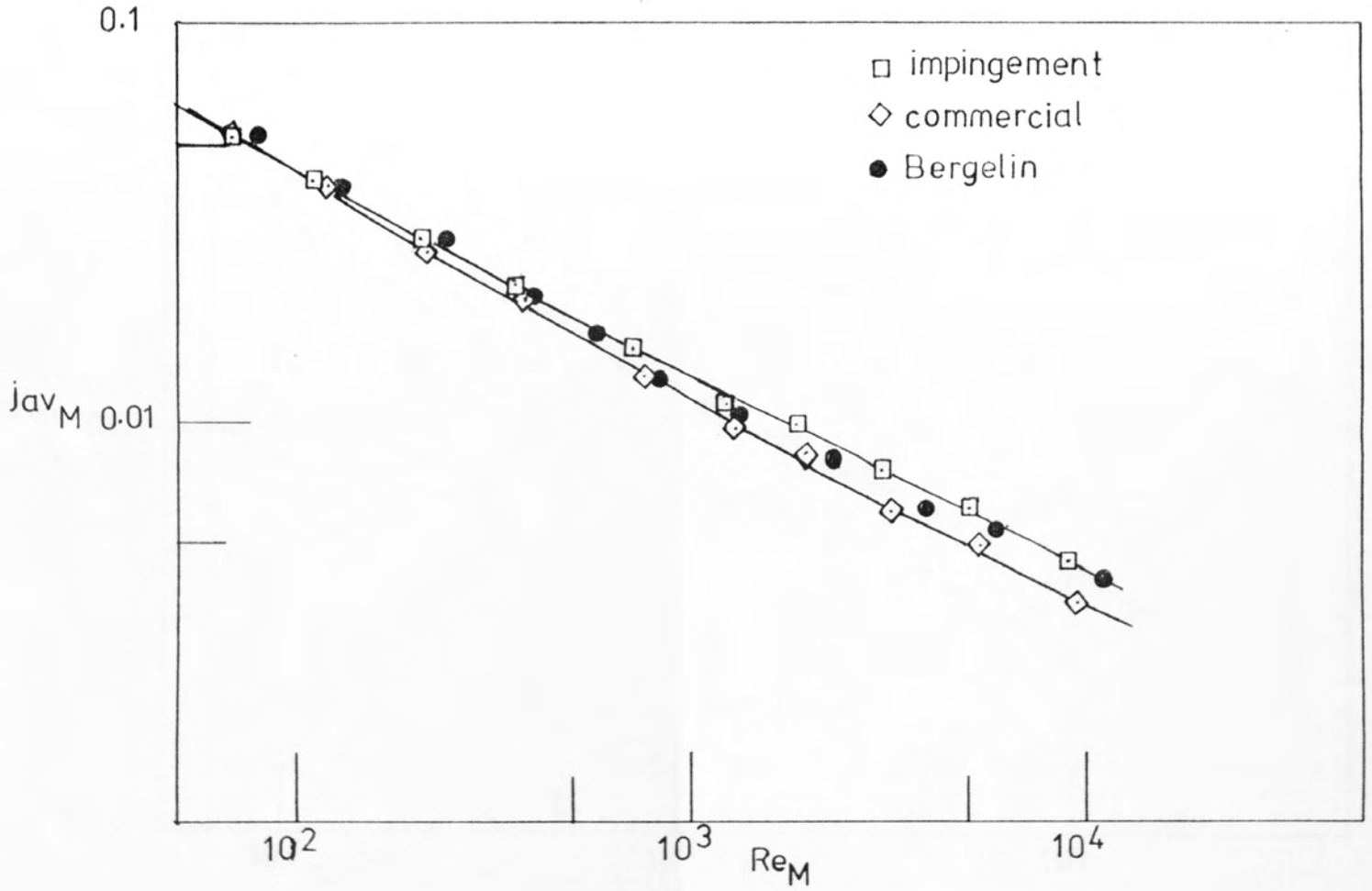

FIG 61 EFFECT OF IMPINGEMENT BAFFLE
(vertical baffle cut)

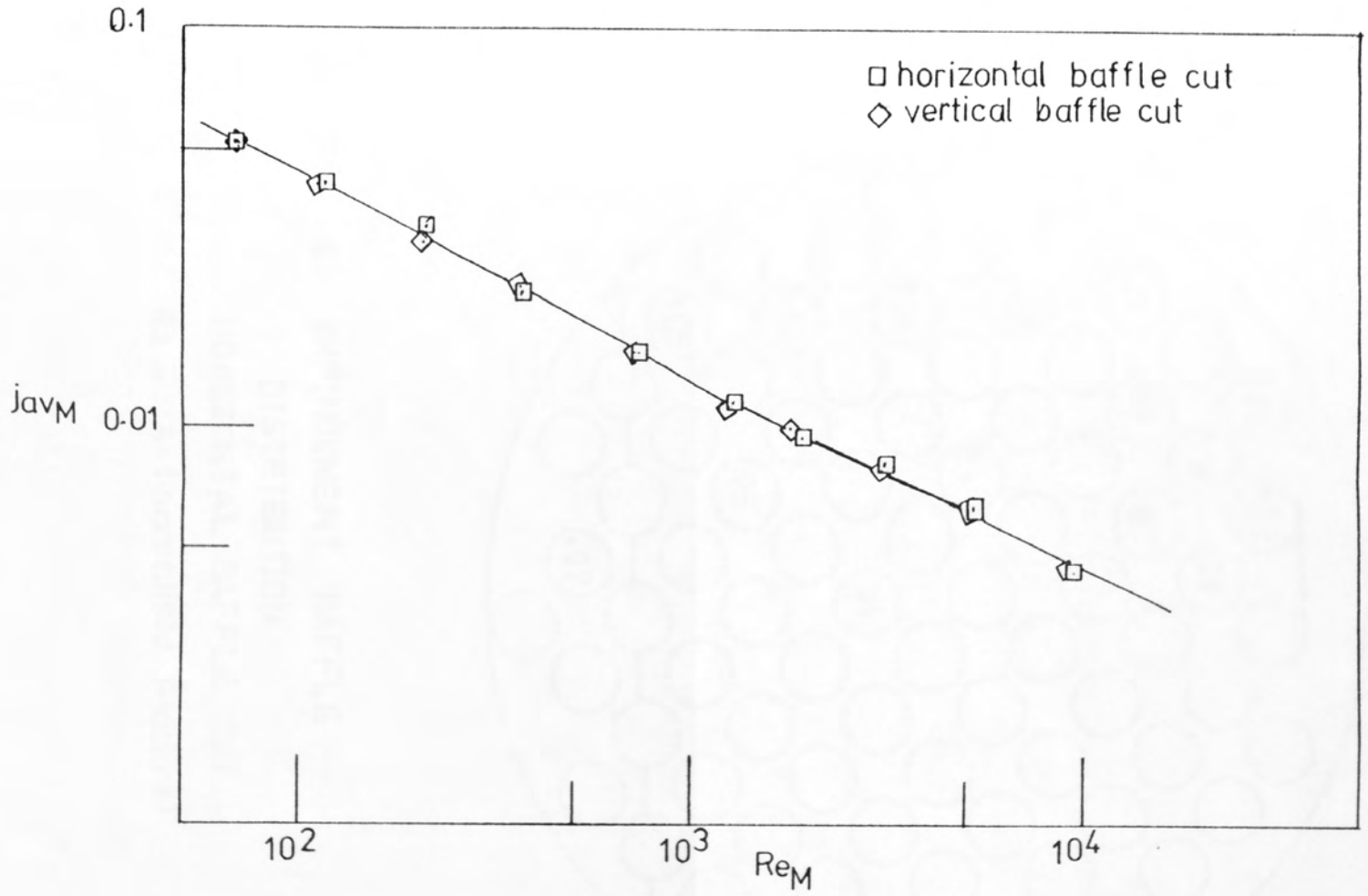

FIG 62 IMPINGEMENT BAFFLE - EFFECT OF BAFFLE ORIENTATION

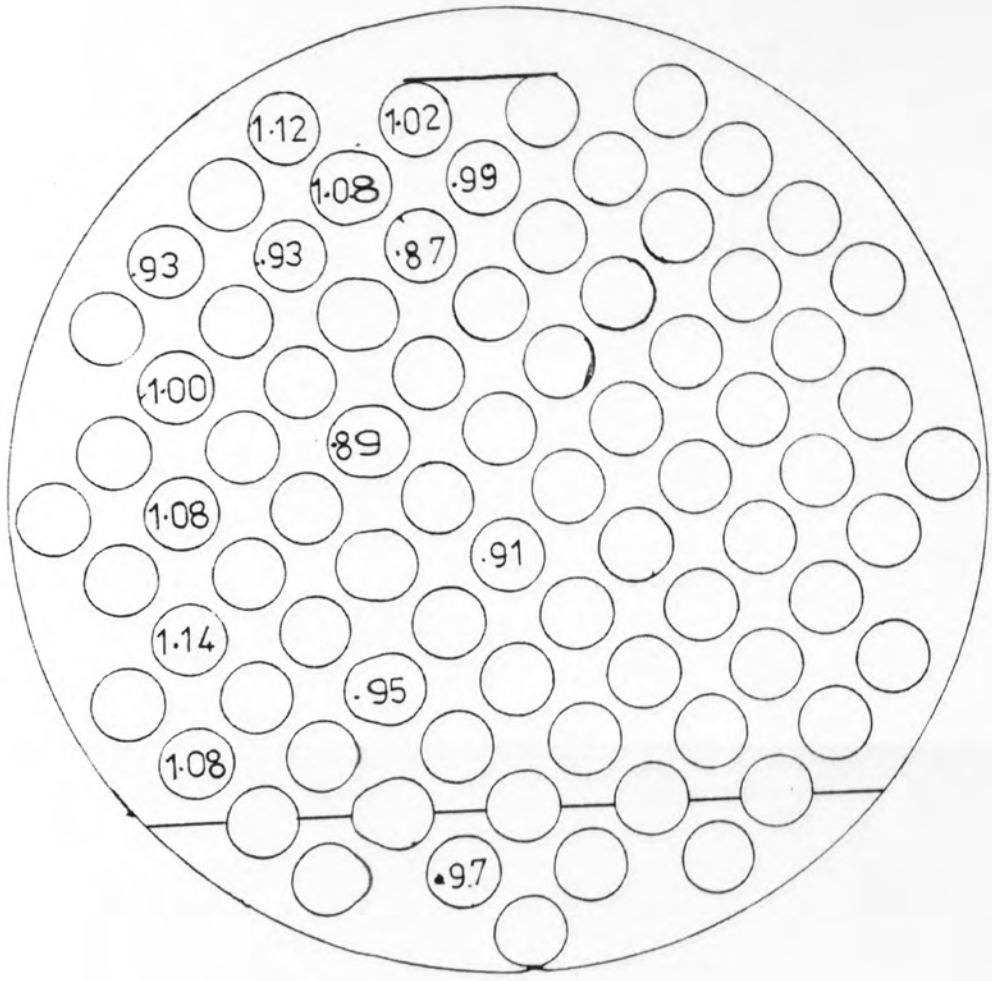

FIG 63 IMPINGEMENT BAFFLE
j DISTRIBUTION
HORIZONTAL BAFFLE CUT
Re = 116 (normalised j-factors)

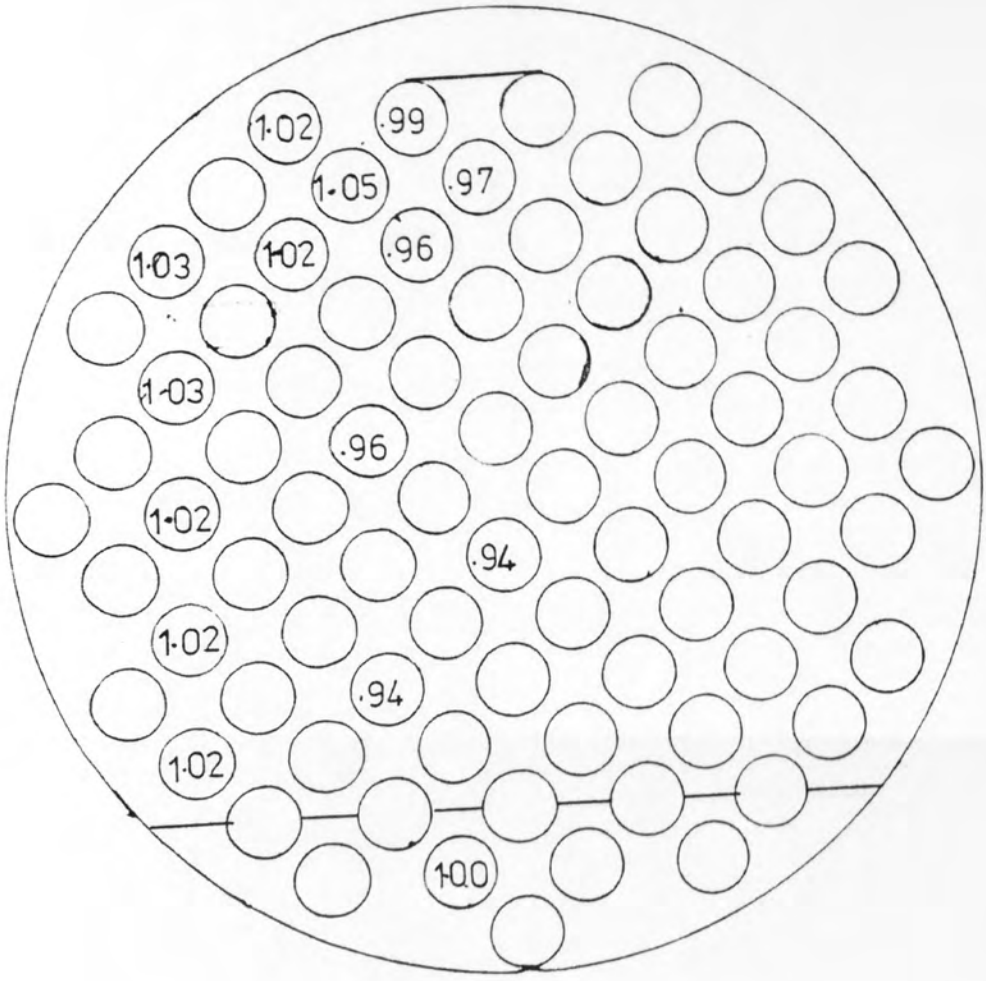

FIG 64 IMPINGEMENT BAFFLE
j DISTRIBUTION
HORIZONTAL BAFFLE CUT
Re = 1280 (normalised j-factors)

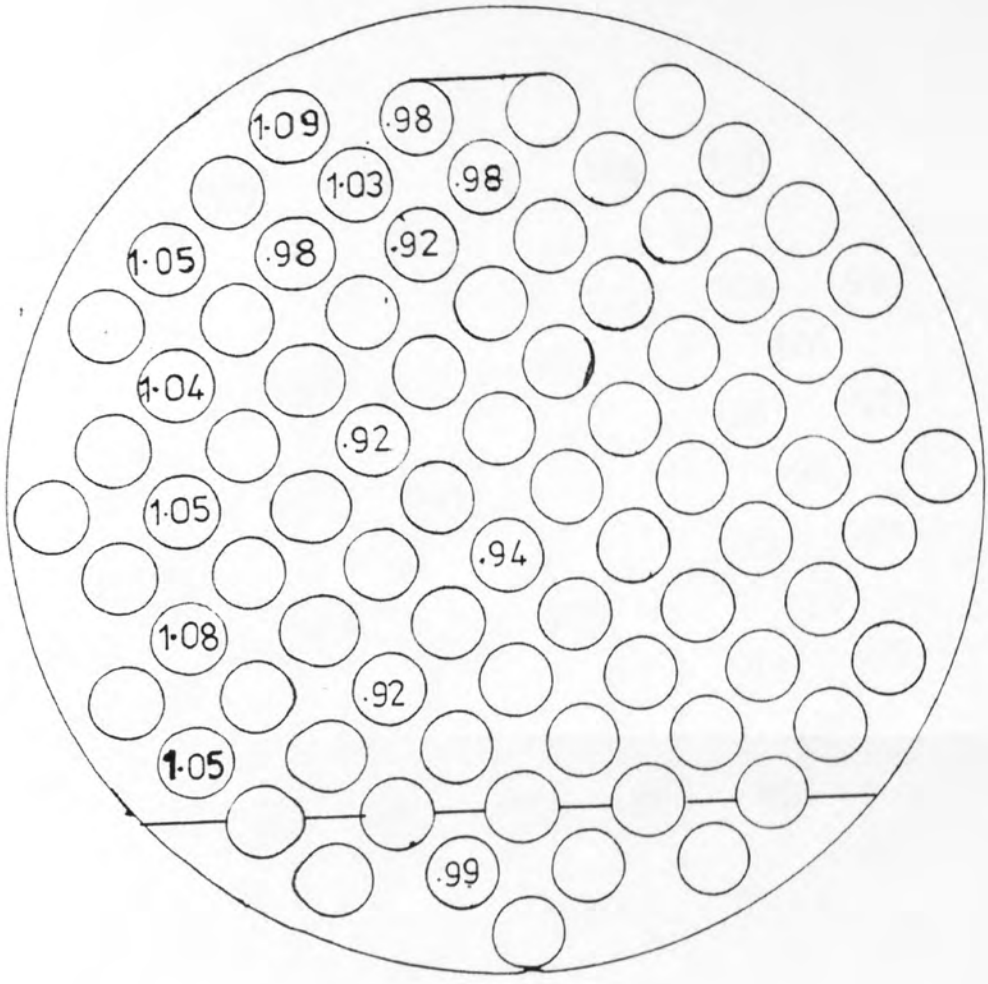

FIG 65 IMPINGEMENT BAFFLE
j DISTRIBUTION
HORIZONTAL BAFFLE CUT
Re = 9530 (normalised j-factors)

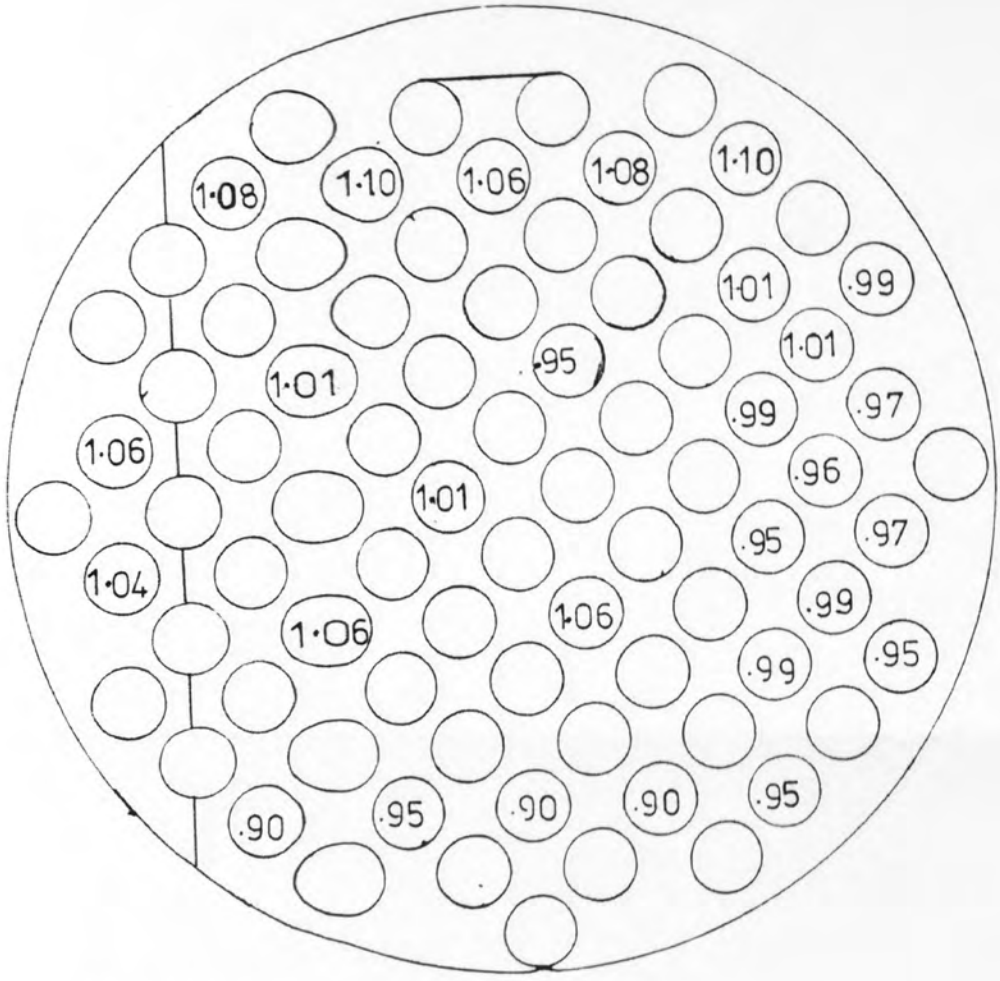

FIG 66 IMPINGEMENT BAFFLE

j DISTRIBUTION

VERTICAL BAFFLE CUT

Re = 110 (normalised j-factors)

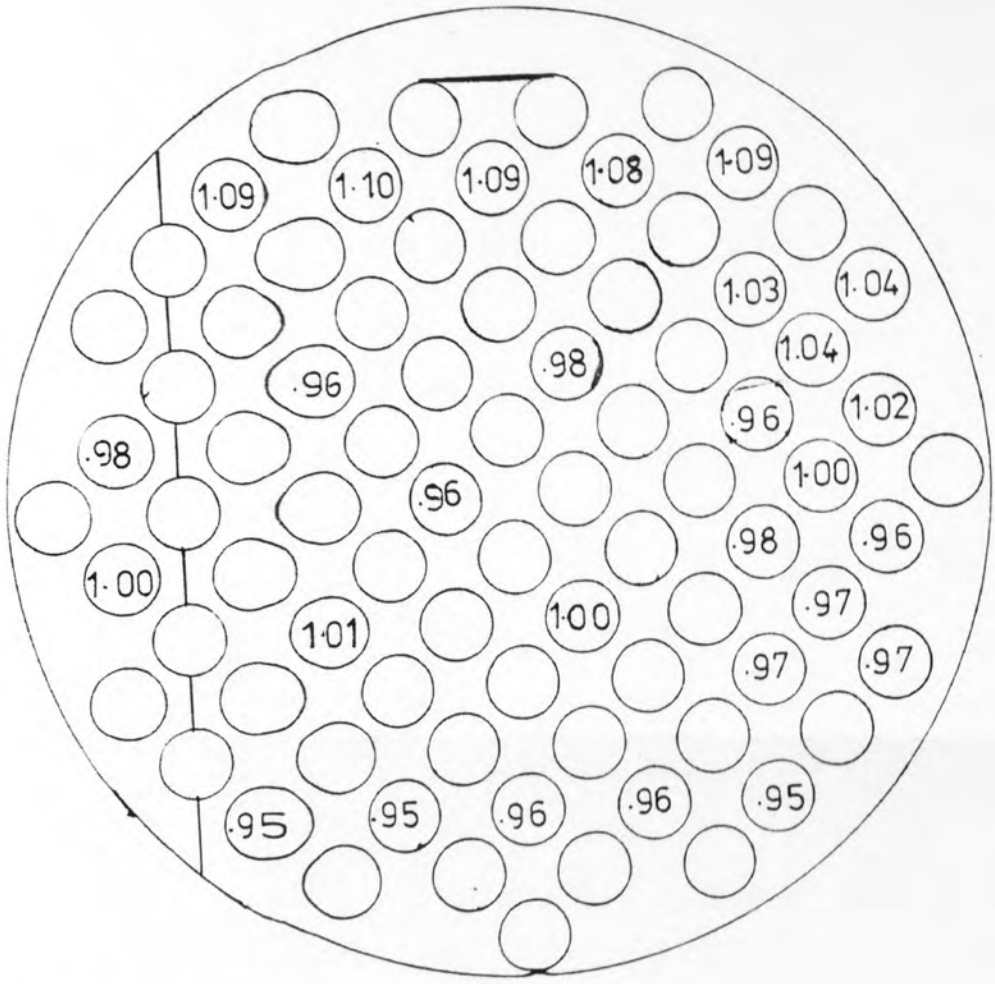

FIG 67 IMPINGEMENT BAFFLE

j DISTRIBUTION

VERTICAL BAFFLE CUT

Re =1240 (normalised j-factors)

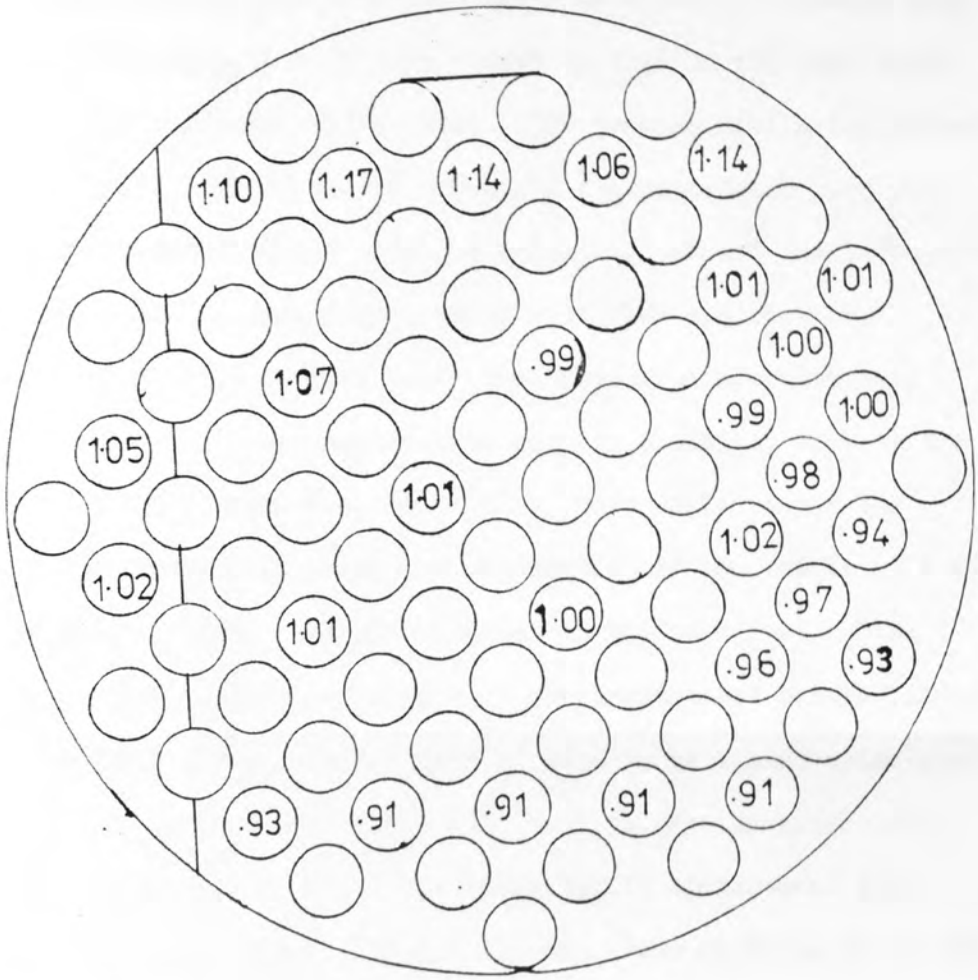

FIG 68 IMPINGEMENT BAFFLE
j DISTRIBUTION
VERTICAL BAFFLE CUT
Re = 9270 (normalised j factors)

to 25% at Re = 10,000, with the impingement baffle data having the higher compartment average j-factors. The corresponding Bergelin port (no impingement baffle) data fell between the two commercial port data sets for $500 < Re < 5000$. Outside this range the Bergelin port data tended to fall on the same curve as the impingement baffle data. The general similarity between the Bergelin port data and those for the commercial port with the impingement baffle might be expected, because the impingement baffle could be viewed as a shell side flow distributor, increasing the effective inlet port area from approximately 1000 mm^2 for the commercial type port to a similar area to the Bergelin type port, i.e. 3500 mm^2 . This would reduce the possibility of by-passing the extremities of the bundle by the shell side fluid. Baffle orientation had no effect on the compartment average j-factor with the impingement baffle fitted, as Fig.(62) showed the two sets of data to be almost coincident.

The impingement baffle was found to greatly affect the j-factor distributions of the inlet baffle compartment for both baffle cut orientations. It was shown in Figs.(63 to 65) that the presence of the impingement baffle adversely affected the inlet compartment j-factor distribution for the horizontal baffle cut orientation. The j-factors of the tubes in the central region of the inlet compartment were up to 20% lower than those for the tubes around the inlet compartment's perimeter. This effect could perhaps be predicted as the impingement baffle would direct the flow to the perimeter of the inlet compartment. The corresponding non-impingement baffle cases gave, by comparison, fairly even j-factor distributions (section 8.5). The vertical baffle cut orientation, however, produced

considerably more even j-factor distributions than with the non-impingement cases (section 8.5). The improvement with the impingement baffle would be predictable, as the flow could be directed to the region of the inlet compartment which was partially by-passed in previous cases.

Unfortunately, no pressure drop measurements were included in the scope of the present work, but Macbeth (86) in an extended study of the effect of shell side inlet nozzles on pressure drop in shell and tube heat exchangers found that the presence of impingement baffles greatly increased the pressure drop of shell and tube heat exchangers.

It may therefore be concluded that the inclusion of an impingement baffle in the inlet compartment of the model shell and tube heat exchanger of the present work does not significantly improve the compartment average j-factor in comparison with pressure drop for the horizontal baffle cut orientation, and furthermore, the impingement baffle has an adverse effect on the distribution of j-factors in the inlet compartment. Hence, it is thought that an impingement baffle should only be used when erosion is of prime concern.

However, for the vertical baffle cut orientation, there is a noticeable improvement in both the average and the distribution of j-factor when the impingement baffle is used, although the pressure drop would appear to be increased by an even greater proportion (86). However, in cases where the heat transfer performance and distribution is of major concern, then the inclusion of an impingement baffle may be justified, even when the erosion problem is not serious.

It must be stressed, however, that the present work included a study of only one impingement baffle design, and other designs should be investigated before any firm conclusions are drawn.

9. CONCLUSIONS

The following general conclusions can be drawn from the investigations into the end compartments of the model shell and tube heat exchanger.

(i) The end compartments of the model heat exchanger produced considerably lower compartment average j-factors than those obtained by Mackley (1) for the fifth compartment. A limited investigation into the second compartment of the heat exchanger gave data which fell between the fifth compartment data and those of the end compartments.

(ii) The outlet compartment average j-factors were generally slightly lower than those for the inlet compartment. Corresponding j-factor distributions for the inlet and outlet compartments were similar.

(iii) Baffle orientation had little effect on the compartment average j-factor. It had, however, a considerable effect on the j-factor distributions. Very even distributions were obtained for the horizontal baffle cut orientations with uneven distributions showing for the vertical baffle cut orientations. In the latter cases very low j-factors were obtained in the region of the end compartments away from the port and window zones. The port and window zones, however, produced high j-factors in comparison.

(iv) The commercial type ports produced average j-factors up to 10% lower than for the corresponding Bergelin type port cases in the end compartments. Both ports, however, produced similar j-factor distributions in the end compartments for

corresponding baffle cut orientations.

(v) The presence of an impingement baffle beneath the inlet port gave no significant improvement in the compartment average j-factor for the horizontal baffle cut, also the distribution of j-factor in the inlet compartment was adversely affected. Although other designs may lead to different results, it may be concluded that this particular impingement baffle design would only be useful where erosion was the prime concern. For the vertical baffle cut, however, the compartment average j-factors were improved by up to 25% at Re = 1000, with the distribution of j-factor being considerably improved. Hence, for the vertical baffle cut orientation, there may be occasions where the use of impingement baffles would prove beneficial regardless of the erosion factor, although the assumed increase in pressure drop (86) would have to be investigated.

(vi) It was shown earlier that the end compartment data for the present work was considerably lower than the internal compartment data of Mackley (1). Fig.(69) compares all the end compartment data from the present work to the corresponding Mackley data. The end compartment data fall within $\pm$ 20% of a mean, which in turn is approximately 125% lower than the Mackley data. It might therefore be concluded that the variations in the heat transfer performance of the end compartments with port type and baffle orientation could be considered insignificant in comparison to the overall differences with the results for the internal compartment. It must again be stressed that the results shown are only a preliminary investigation into the end compartment heat transfer characteristics and the main conclusion must be that further investigations into the end compartments must be carried out.

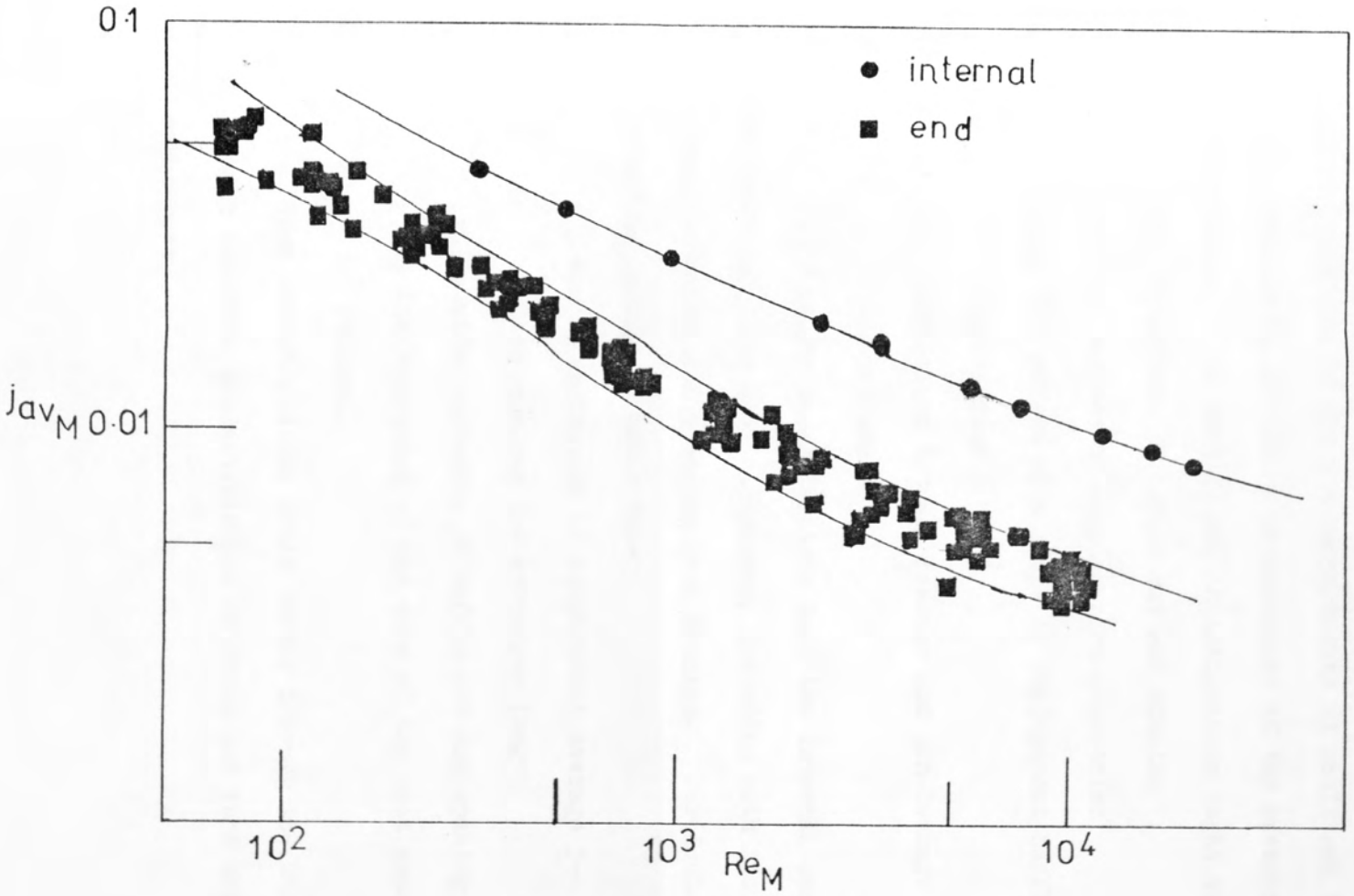

FIG 69 COMPARISON OF COMPARTMENT AVERAGES

10. RECOMMENDATIONS FOR FUTURE WORK

The following recommendations are made for future work:-

(1) More detailed investigations of the heat transfer characteristics of the end compartments of shell and tube heat exchangers, including measurements of the pressure drop are required. In particular, investigations ought to cover:-

(i) the effect of baffle cut and spacing

(ii) the effect of varying port geometries

(iii) the effect of a range of impingement baffle geometries

(iv) comparison between leakage and non-leakage situations

(2) Further investigations into the internal compartments of shell and tube heat exchangers, including both transfer characteristics and pressure drop studies. Particular reference should be taken to:-

(i) the distribution of compartment average j-factor along the exchanger length

(ii) a wide variation of baffle cut and spacing

(iii) the variation of the size of the heat exchanger bundle.

Such investigations would vastly improve the knowledge of heat transfer characteristics in shell and tube heat exchangers.

NOMENCLATURE

A	Shell side flow area	m^2
A_M	Minimum crossflow area at centre row of tubes	m^2
A_{SB}	Shell-to-baffle leakage area	m^2
A_{TB}	Tube-to-baffle leakage area	m^2
b	Coefficient in Weisman correlation	
b'	Coefficient dependent on tube arrangement	
C	Concentration	$k\,mole/m^3$
C_b	Bulk ferricyanide ion concentration	$kmole/m^3$
C_p	Specific heat evaluated at bulk temperature	$kJ/Kg°C$
C_s	Ferricyanide ion concentration at cathode surface	$k\,mole/m^3$
D_v	Diffusion coefficient	m^2/s
D_h	Shell hydraulic mean diameter	m
D_S	Shell inside diameter	m
d_t	Tube outside diameter	m
F	Faradays constant	C
F_E	End space factor	
G	Shell side fluid mass velocity	kg/m^2s
G_c	Crossflow mass velocity through widest section of shell	kg/m^2s
G_k	Mass velocity defined by Kern	kg/m^2s
G_{max}	Mass velocity based on Am	kg/m^2s
G_W	Window area mass velocity	kg/m^2s
G_{av}	Mass velocity defined by (63)	kg/m^2s
h	Heat transfer coefficient	$kW/m^2°C$
I	Electric current	A
I_L	Limiting (or diffusion) current	A
j	j-factor	

j_{c_M}	Crossflow zone average mass transfer j-factor	
j_{av_M}	Compartment average mass transfer j-factor	
K_c	Mass transfer coefficient	m/s
k	Thermal conductivity based on bulk temperature	W/m°C
L_S	Baffle spacing	m
m	Exponent	
N	Mass transfer flux	kg mole/m^2s
n	Exponent	
n_e	Valency of ion	
Nu	Nusselt Number, $\frac{h d_t}{k}$	
P	Tube Pitch	m
Pr	Prandtl Number, $\frac{C_p \mu}{k}$	
Q	Shell side fluid volumetric flow rate	m^3/s
$Re_{(M)}$	Shell side Reynolds number (based on A_m) $\frac{\rho u_M d_t}{\mu}$	
s	Cathode surface area	m^2
Sc	Schmidt number $\frac{\mu}{\rho D_v}$	
St	Stanton number $\frac{Nu}{Re\,Pr}$	
T	Temperature	°C
u	Fluid velocity	m/s
u_M	Fluid velocity based on A_m	m/s
Z	Orifice shape factor	
α_i	Effectiveness factors (i=1,5)	
γ	Tube row correction factor	
ε	Bundle voidage fraction	
ζ	Bundle by-pass stream correction factor	
ν	Kinematic viscosity	m^2/s
λ	Baffle leakage correction factor	

μ	Fluid viscosity evaluated at bulk temperature	Ns/m^2
ν	Ratio of velocity at edge of laminar sublayer to the stream velocity	
ρ	Fluid density evaluated at bulk temperature	kg/m^3
τ	Shear stress	N/m^2
ϕ'	Baffle window correction factor	
ϕ	Correction in Weissman correlation	

Subscripts

av	Based on compartment average
f	Evaluated at film temperature
h	Heat transfer
I	Ideal tube bank
w	Evaluated at wall temperature

BIBLIOGRAPHY

1. MACKLEY, N.V.
Ph.D. Thesis Univ. of Aston (1973)

2. WILLIAMS, T.A.
Ph.D. Thesis Univ. of Manchester (1962)

3. CHILTON, T.H. and COLBURN, A.P.
Ind. Eng. Chem. 26 1183 (1934)

4. REYNOLDS, O.
Proc. Manchester Lit. Phil. Soc. 14 7 (1874)

5. TAYLOR, G.I.
G.B. Advisory Comm. Aeronaut Rep. Memo.2272 (1916)

6. PRANDTL, L.
Physik Z, 29 487 (1928)

7. SHERWOOD, T.K.
Trans A.I.Ch.E. 36 817 (1940)

8. COLBURN, A.P.
Trans A.I.Ch.E. 29 174 (1933)

9. LUCAS, D.M. and DAVIES, R.M.
"Mass Transfer Modelling Techniques in the Prediction of Convective Heat Transfer Coefficients in Industrial Heating Processes."
Paper pres. 4th Int Heat Transfer Conf., Versailles (1970)

10. LEVICH, V.G.
Disc. Faraday Soc. 1 37 (1947)

11. AGAR, J.W.
Disc. Faraday Soc. 1 26 (1947)

12. MIZUSHINA, T.
Advances in Heat Transfer 7 87 (1971)

13. SHAW, P.V.; REISS and HANRATTY
A.I.Ch.E.Jnl. 9 362 (1963)

14. GRASSMAN, P.; IBL and TRUB
Chem. Ing. Teck. 33 529 (1961)

15. HUBBARD, D.W. and LIGHTFOOT, E.N.
Ind. Eng. Chem. Fundls. 5 (3) 370 (1966)

16. COSTELLO, J.
Ph.D. Thesis, Univ. of Aston (1969)

17. BAZAN, J.C. and ARVIA, A.J.
Electrochim. Acta. 9 667 (1964)

18. LIN, C.S.; DENTON; GASKILL and PUTNAM
Ind. Eng. Chem. 43 2136 (1951)

19. ROSS, T.K. and WRAGG, A.A.
Electrochim Acta 10 1093 (1965)

20. DOBRY, R. and FINN, R.K.
Ind. Eng . Chem. 48 1540 (1956)

21. MIZUSHINA, T.; VEDA and UMEMIYAN
Int J. Heat Mass Transfer 15 769 (1972)

22. VOGTLANDER, P.H. and BAKKER, C.
Chem. Eng. Sci. 18 583 (1963)

23. HICKS, R.E. and MANDERSLOOT, W.G.B.
Chem. Eng. Sci. 23 1201 (1968)

24. JOLLS, K.R. and HANRATTY, T.J.
A.I.Ch.E.J. 15 (2) 199 (1969)

25. KING, D.H. and SMITH, J.W.
CAn J. Chem. Eng. 45 329 (1967)

26. SUTEY, A.M. and KNUDSEN, G.
Ind. Eng. Chem. Fundls. 6 (1) 132 (1967)

27. WILKE, C.R.; EISENBURG and TOBIAS
J. Electrochemical Soc. 100 513 (1953)

28. EISENBURG, M.; TOBIAS and WILKE
J. Electrochemical Soc. 101 306 (1954)

29. BERGELIN, O.P.; BROWN and COLBURN
Trans A.S.M.E. 76 841 (1954)

30. BERGELIN, O.P.; BELL and LEIGHTON
Trans S.D.M.E. 80 53 (1958)

31. SUTTON, F.
"A Systematic handbook of Volumetric Analysis"
J.A. CHURCHILL LTD. Rev. (1935)

32. EISENBURG, M.; TOBIAS and WILKE
J. Electrochemical Soc. 103 413 (1956)

33. DAWSON, D.A. and TKASS
Int. J. Heat Mass Transfer 15 1317 (1972)

34. STANDARDS OF THE TUBULAR EXCHANGER MANUFACTURERS ASSOC.
Fourth Ed. (1959)

35. GRIMISON, E.D.
Trans. A.S.M.E. 59 (7) 583 (1937)

36. HUGE, E.C.
Trans. A.S.M.E. 59 (7) 573 (1937)

37. PIERSON, O.L.
Trans. A.S.M.E. 59 (7) 563 (1937)

38. McADAMS, W.H.
"Heat Transmission"
3rd Ed. McGraw Hill (1954)

39. SHEEHAN, T.V.; SCHOMER and DWYER
paper No. 54-F-19 ASME meeting New York (1954)

40. WRAGG, A.A.
The Chem. Engineer. Jan. 39-44 (1977)

41. BERGELIN, O.P.; DAVIES and HULL
Trans. A.S.M.E. 71 369 (1949)

42. BERGELIN, O.P.; BROWN; HULL and SULLIVAN
Trans. A.S.M.E. 72 881 (1950)

43. BERGELIN, O.P.; BROWN and DOBERSTEIN
Trans. A.S.M.E. 74 953 (1952)

44. BELL, K.J.
"Final Report of the Co-operative Research Programme on Shell and Tube Heat Exchangers".
Univ. of Delaware Eng. Ex. Station, Bulletin No. 5 (1963)

45. ZUKAUSKAS, A.
Advances in Heat Transfer 8 93 (1972)

46. WEISMAN, J.
A.I.Ch.E.J. 1 342 (1955)

47. KAYS, W.M.; LONDON and LO
Trans. A.S.M.E. 76 387 (1954)

48. WHITAKER
A.I.Ch.E.J. 18 (2) 361-371 (1972)

49. BERGELIN, O.P.; COLBURN and HULL
Univ. of Delaware Eng. Ex. Station,
Bulletin No.2 (1950)

50. BERGELIN, O.P.; LEIGHTON; LAFFERTY and PIGFORD
Univ. of Delaware Eng. Ex. Station,
Bulletin No.4 (1958)

51. FAIRCHILD, H.N. and WELSH
Paper No. 61 - WA - 250 ASME Meeting (1961)

52. EDWARDS, A. and FURBER
Proc. Inst. Mech. Eng. (LONDON) 170 941 (1956)

53. ZUKAUSKAS, A.; MAKAREVICIUS, V.J. and SLANCIAUSKAS
"Heat Transfer in Banks of Tubes in Crossflow of Fluid"
Mintis, Vilnius (1968) (in Russian)

54. JENKINS, J.D.; MACKLEY, N.V. and GAY, B.
Letters in Heat and Mass Transfer 3 105-110 (1976)

55. LUCAS, D.M.
Ph.D. Thesis Univ. of Aston (1971)

56. DONAHUE, D.
Ind. Eng. Chem. 41 2499 (1949)

57. KERN, D.Q.
"Process Heat Transfer"
Ist. Ed. McGraw H; 11 (1950)

58. SHORT, B.E.
Univ. of Texas publication no. 4324 (1943)

59. HEINRICH, E. and STUCKLER
Ingenierw., Heft 271 (1925) (in German)

60. GARDNER, H.S. and SILLER
Trans. ASME 69 (6) 687 (1947)

61. BOWMAN, R.A.
Unpublished A.S.M.E. paper no. 28, N.Y. (1936)

62. TINKER, T.
Paper No 47-A-130 A.S.M.E. Meeting N.Y. (1947)

63. BRITISH SHIPBUILDING RESEARCH ASSOC.
Rep. No. 148 (1955)

64. BELL, K.J.
Petrol Engr. 32 (11) C 26 to $C40_c$ (1960)

65. BROWN, G.A.
Ph.D. Thesis Univ. of Delaware (1956)

66. BERGELIN, O.P.; BELL and LEIGHTON
C.E.P. Symp. Series 55 (29) 45 (1959)

67. SULLIVAN, F.W. and BERGELIN
C.E.P. Symp. Series 52 (18) 85 (1956)

68. PALEN, J.W. and TABOREK
C.E.P. Symp. Series 65 (92) 53 (1968)

69. PARKER, R.O. and MOK
Brit. Chem. Eng. 13 124 (1968)

70. DEVORE, A.
Petrol Refin. 40 (5) 221 (1961)

71. EMERSON, W.H.
N.E.L. Rep. No. 45 East Kilbride, Glasgow.

72. PATANKAR, S.V. and SPALDING
"A Calculation Procedure for the Transient and Steady-state Behaviour of shell and tube Heat Exchangers".
Paper.Pres. TROGIR,YUGOSLAVIA.
Int. Sem. by Int. Centre for Heat & Mass Transfer (1972)

73. GRANT, I.D.R.
"Flow and Pressure Drop with Single Two Phase Flow on the Shell-side of Segmentally Baffled Shell and Tube Heat Exchangers"
N.E.L. Symp- "Advances in Thermal and Mechanical Design of Shell and Tube Heat Exchangers"
Paper No. 1 28th Nov. (1973)

74. GUNTER, A.Y.; SENNSTROM and KOPP
Paper No. 47-A-103, A.S.M.E. Meeting, Atlantic City N.J. (1947)

75. GUPTA, R.K. and KATZ, D.L.
Ind. Eng. Chem. 998 (1957)

76. AMBROSE, T.W. and KNUDSEN, J.G.
A.I.Ch.E.J. 4 332 (1958)

77. GURUSHANKARIAH, M.S. and KNUDSEN, J.G.
C.E.P. Symp. Series 55 (29) 29 (1959)

78. STACHIEWICZ, J.W. and SHORT
Int. Devlps. in Heat Transfer, Colorado, 959-966 (1961)

79. LEE, K.S. and KNUDSEN
A.I.Ch.E.J. 6 (4) 669-675 (1960)

80. GAY, B. and WILLIAMS
Trans. Instn. Chem. Engrs. 46 95 (1968)

81. ROBERTS, P.C.O.
"Individual tube transfer Coefficients in a Segmentally Baffled Shell and Tube Heat Exchanger"
Ph.D. Thesis Univ. of Aston (1969)

82. GAY, B. and ROBERTS
Trans. Intsn. Chem. Engrs. 48 3 (1970)

83. GAY, B.; MACKLEY and JENKINS
Int. J. Heat Mass Transfer 19 995-1002 (1976)

84. JENKINS, J.D.
Private Communication

85. JENKINS, J.D.; PROWSE and GAY
"The effect of baffle spacing on the shell side heat transfer coefficient for Segmentally Baffled Shell-and-Tube Heat Exchangers "
U.K.A.E.A. HARWELL Rep. No. RS.146 (1976)

86. MACBETH, R.V.
"The effect of shell-side inlet nozzles on single-phase pressure drop in shell-and-tube heat exchangers"
U.K.A.E.A. Commercial report (unpublished)

APPENDIX 1, FERRICYANIDE ION DETERMINATION

The concentration of the ferricyanide ion is determined by iodometric titration with a thiosulphate. Lucas (9), however, made use of colorimetric analysis with commercial absorptiometers, but Mackley (1) has found that this method is unreliable.

The ferricyanide ion determination is based on the method described by Sutton (31). A small amount of zinc sulphate (approx. 0.5 gm) is dissolved in about 15 ml of 4N hydrochloric acid. Precisely 10 ml of a sample of the electrolyte is pipetted into the above solution, to which approximately 10 mls of 0.025N potassium iodide is then added. At this stage, all the ferricyanide is converted into zinc ferrocyanide, releasing an equivalent of free iodine into solution. All the ferrocyanide is precipitated out as the zinc salt. Unsatisfactory results are obtained if the zinc sulphate is omitted as the basic reaction (given below) is reversible.

$$2K_3Fe(CN)_6 + 2KI \rightleftharpoons 2K_4Fe(CN)_6 + I_2$$

The reaction is driven to the right by the precipitation of zinc ferrocyanide. Direct titration with a thiosulphate can produce difficulties with the end point (starch indicator, blue → colourless), hence a known quantity to excess (20ml) of thiosulphate is pipetted into the solution, which is then back titrated with 0.01N Iodine, using a starch indicator, to an end point colourless- to-blue.

The accuracy of the method is estimated to be within ± 0.4% (see appendix 4).

APPENDIX 2, PRETREATMENT OF ELECTRODES

Previous users have found that chemical polarisation is an occasional problem when operating with the ferri-ferrocyanide system if the electrode surfaces are not pre-treated before operation. A series of pretreatment processes; proposed by Eisenburg et al.(32), have since been adopted. The nickel surface is polished with a fine emery cloth, and then washed in a degreasing solution. An activation process is then performed where hydrogen is evolved at the electrode surface. However, some workers,e.g. (15), claim to have found the activation process unnecessary.

For the case of mass transfer at rough surfaces, Dawson and Trass (33) have found that for such conditions the limiting current is dependent on electrode pretreatment. However, Mackley (1) has found that satisfactory results are obtained by polishing the electrodes with a fine emery paper and cathode treatment with a current density of 0.1 mA/mm^2 for 5 mins. No degreasing is necessary, as sodium hydroxide is a degreasant. Although most previous users have restricted the activation to the cathode, Mackley has extended it to the anode, as in his work the anode-to-cathode area ratio has been reduced by the use of multiple cathodes. In the present work only one cathode is in use at any one time, therefore, anode pretreatment is considered unnecessary in this case.

APPENDIX 3, ROTAMETER CALIBRATION

As stated previously, the electrolyte flow rate is measured by variable area flowmeters, as supplied by the "Rotameter Manufacturing Company", using stainless steel floats. Both rotameters are calibrated in situ, though a manufacturer's calibration chart is available for the metric size 18 (low flow) rotameter.

For the purpose of the calibration, the capacities of both the electrolyte tank and the activation tank have been measured. The activation tank has graduation marks at 2 L intervals with the electrolyte tank having graduation marks at 50 L intervals. The time taken to pump a known quantity of liquid from one tank to the other is measured at constant flow rates, hence the rotameters are calibrated in this way by accurately calculating the flow rates for a range of rotameter settings. Time is measured correct to .01s, using an electronic timing device.

Calibration runs are carried out for the complete range of the low flow rotameter, and details of the calibration are given in table (A 3.1), and the calibration plot is given in fig.(70), together with a comparison with the manufacturer's calibration. It is shown that the two sets of data are virtually identical. The process is repeated for the high flow rotameter, but the maximum flow rate with a sufficiently steady rotameter reading for the required accuracy occured at a reading of 120 mm. Above this flow rate the head variation in the electrolyte tank becomes critical, leading to a significant drop in the flow rate during the course of the calibration run. This imposes an upper limit on the high flow rotameter calibrations. The details of the calibration runs

for the high flow rotameter are given in table (A 312), with the calibration plot being shown in Fig. (71). A manufacturer's calibration chart is not available for this rotameter.

As stated previously, time is measured accurate to .01 s , and as the shortest time interval measured is approximately 30s, the error in time measurement is considered negligible. The graduation marks on the storage tanks are estimated to be correct to within 50 ml in every 2000 ml, leading to a maximum error in the calibrations of ± 2.5%.

Rotameter Reading MM	Quantity Timed L	Time Taken S	Flow Rate L/M
0	2	120.96	.992
46	2	51.68	2.32
98	2	30.42	3.95
158	4	39.41	6.09
253	12	73.13	9.85
213	16	119.01	8.07
181	12	105.23	6.84
123	8	100.13	4.79
63	4	82.50	2.91
21	2	74.51	1.61

TABLE A 3.1

LOW FLOW ROTAMETER CALIBRATION

Rotameter Reading MM	Quantity Timed L	Time Taken S	Flow Rate L/S
0	20	74.85	16.0
19	20	39.85	29.1
37	20	27.53	43.6
58	30	30.81	58.4
69	50	44.24	67.8
85	50	37.91	79.1
103	50	31.71	94.6
110	50	29.18	102.8
120	50	27.21	110.2

TABLE A 3.2

HIGH FLOW ROTAMETER CALIBRATION

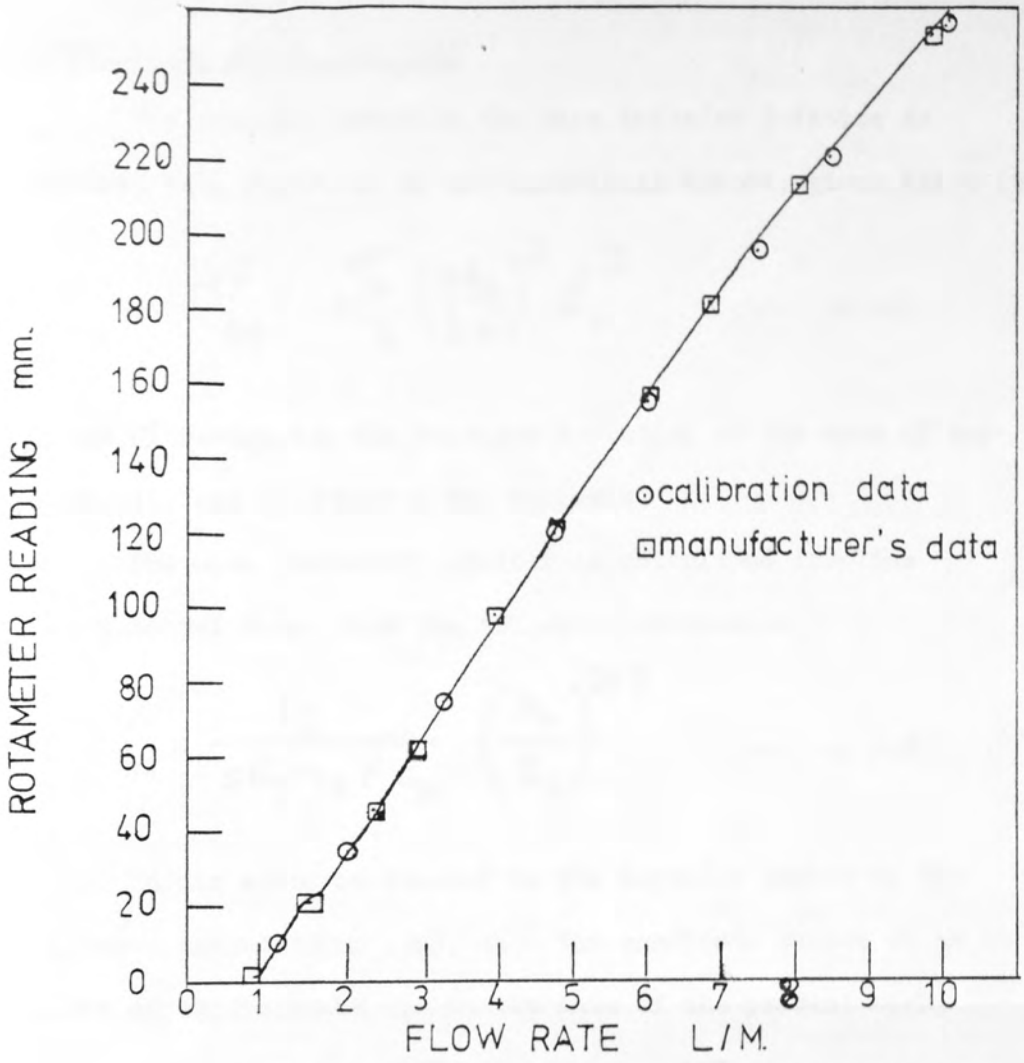

FIG 70 LOW FLOW CALIBRATION

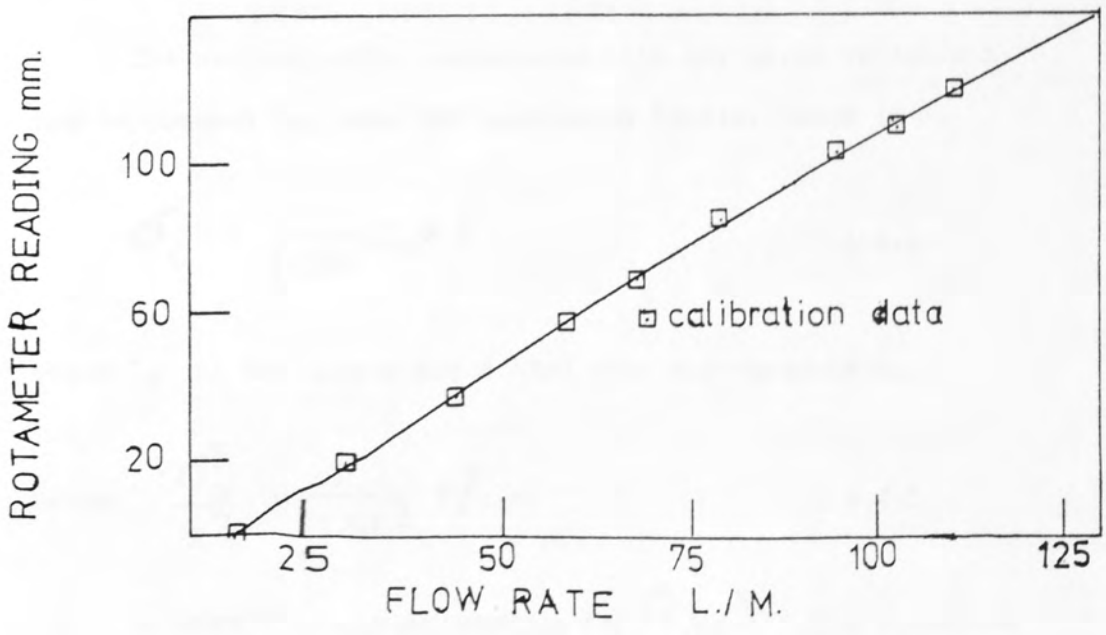

FIG 71 HIGH FLOW CALIBRATION

APPENDIX 4, ERROR ANALYSIS

The overall error in the mass transfer j-factor is related to a function of the individual errors, given below (84).

$$\sigma_{j_M}^2 = \sum_x \left(\frac{\partial j_M}{\partial x}\right)^2 \sigma_x^2 \qquad \ldots\ldots \text{A } 4.1$$

where σ refers to the standard deviation of the mean of any variable, and x denotes the variable.

The mass transfer j-factor is calculated from the experimental data from the following expression

$$j_M = \frac{I_L}{s C_b n_e F u_M} \left(\frac{n}{D_v}\right)^{2/3} \qquad \ldots\ldots \text{A } 4.2$$

It can also be related to the Reynolds number by the Whitaker correlation (48), with the constants chosen so as to give an approximate fit to the data of the present work.

$$j_M = 0.2\left(\frac{u\, d_t}{n}\right)^{-1/2} + 0.06\left(\frac{u\, d_t}{n}\right)^{-1/3} \qquad \ldots\ldots \text{A } 4.3$$

The maximum error associated with any given variable x can be assumed to have 95% confidence limits, hence :-

$$\sigma_x = \frac{1}{1.96}(r_x x) \qquad \ldots\ldots \text{A } 4.4$$

where r_x is the error associated with the variable x.

hence $$\frac{\sigma_x^2}{x^2} = \frac{1}{1.96^2} r_x^2 \qquad \ldots\ldots \text{A } 4.5$$

By substituting expressions for $\left(\frac{\partial j_M}{\partial x}\right)$ from equations

A 4.2 and A 4.3 into A 4.1, and simplifying the resulting equation by using the relationship in A 4.5, we obtain:-

$$\frac{1.96^2 \sigma_{j_M}^2}{j_M^2} = r_{I_L}^2 + r_{C_b}^2 + r_s^2 + 4/9\, r_{D_v}^2 + \left(0.1 \frac{Re^{-1/2}}{j_M} + 0.02 \frac{Re^{-1/3}}{j_M}\right)^2 r_{d_t}^2 + \left(1 + \frac{.1 Re^{-1/2}}{j_M} + .02 \frac{Re^{-1/3}}{j_M}\right)^2 r_u^2 + \left(2/3 + \frac{.1 Re^{-1/2}}{j_M} + .02 \frac{Re^{-1/3}}{j_M}\right)^2 r_\nu^2 \quad \ldots\ldots \text{A 4.6}$$

The estimated relative errors of the individual parameters are as follows:-

(I)	Diffusivity D_v	.03	(Mackley (1))
(2)	Kinimatic viscosity ν	.025	(Mackley (1))
(3)	Velocity u (error in A_M negligible by comparison)	.025	(Appendix 3)
(4)	Tube diameter d_t	.001	(limit of micrometer)
(5)	Surface area s	.003	(limit of micrometer + vernier)
(6)	Concentration C_b	.004	(accuracy of readings for titration + standardisation)
(7)	Limiting Current I_L	.02 .002	jm = 100 jm = 10000

(limit of accuracy of scale reading. Manufacturer's estimated instrument error assumed negligible by comparison).

The overall error is now calculated at Re = 100 ($j_M \simeq 0.05$) and Re = 10000 ($j_M \simeq 0.0045$).

By substituting these values into A 4.6, we obtain:-

$$1.96^2 \frac{\sigma_{j_M}^2}{j_M^2} = 0.00243 \quad (Re = 100)$$

and $0.00186 \quad (Re = 10000)$

As $$\sigma_{j_M} = \frac{1}{1.96} [r_{j_M} \cdot j_M]$$

hence $$1.96^2 \frac{\sigma_{j_M}^2}{j_M} = r_{j_M}^2$$

hence $$1.96 \frac{\sigma_{j_M}}{j_M} = r_{j_M}$$ for 95% confidence limits

$= 0.0493 \quad$ at $\quad Re = 100$

and $\quad 0.0431 \quad$ at $\quad Re = 10000$

hence the overall error in the experimental values of j_M varies from $\pm$ 4.9% at Re = 100 to $\pm$ 4.3% at Re = 10000, both errors being for 95% confidence limits.

APENDIX 5 - TABULATED EXPERIMENTAL DATA

A.51 COMPARTMENT AVERAGE j FACTORS

A.511 BERGELIN TYPE PORT, HORIZONTAL BAFFLE CUT

(a) Inlet Compartment

Re_M	j_{av_M}
82.3	.0550
5340	.00606
5970	.00599
177	.0371
7440	.00544
8420	.00503
321	.0247
10200	.00472
11000	.00437
606	.0174
118	.0531
86.5	.0579
834	.0135
248	.0336
153	.0425
1380	.0114
436	.0218
263	.0315
2390	.00849
1750	.0111
477	.0195
3440	.00706
3930	.00679
728	.0154

(b) Outlet Compartment

Re_M	j_{av_M}
372	.0197
141	.0350
90.5	.00396
598	.0160
248	.0267
148	.0301
880	.0130
449	.0198
277	.0248
1640	.00953
702	.0155
472	.0174
3420	.00653
2110	.00820
814	.0138
6030	.00543
4560	.00570
8980	.00453
6420	.00506
11400	.00411
9610	.00431

A.512 BERGELIN TYPE PORT, VERTICAL BAFFLE CUT

(a) Inlet Compartment

Re_M	j_{av_M}
79.0	.0531
578	.0169
3890	.00619
129	.0395
831	.0129
6090	.00544
238	.0294
1330	.0106
10900	.00415
394	.0214
2300	.00823

(a) Outlet Compartment

Re_M	j_{av_M}
77.1	.0528
577	.0169
3940	.00522
127	.0391
835	.0127
5700	.00484
241	.0299
1410	.00936
10700	.00374
386	.0238
2280	.00648

A.513 COMMERCIAL TYPE PORT, HORIZONTAL BAFFLE CUT

(a) Inlet Compartment

Re_M	j_{av_M}
73.4	.0489
117	.0431
215	.0301
371	.0231
740	.0138
1290	.0112
1950	.00857
3220	.00696
5450	.00541
9850	.00433

(b) Outlet Compartment

Re_M	j_{av_M}
69.0	.0386
121	.0326
211	.0255
361	.0189
726	.0130
1250	.00990
1880	.00787
3050	.00605
5160	.00507
9540	.00382

A.514 COMMERCIAL TYPE PORT, VERTICAL BAFFLE CUT

(a) Inlet Compartment

Re_M	j_{av_M}
71.4	.0533
122	.0403
217	.0272
380	.0212
764	.0133
1320	.00985
1980	.00847
3220	.00613
5390	.00499
9640	.00357

(b) Outlet Compartment

Re_M	j_{av_M}
68.2	.0504
116	.0386
196	.0291
340	.0217
675	.0146
1170	.00940
1760	.00713
2910	.00546
4910	.00489
8970	.00371

A.515 COMMERCIAL TYPE PORT, INLET COMPARTMENT WITH IMPINGEMENT BAFFLE

(a) Horizontal Baffle Cut

Re_M	j_{av_M}
68.8	.0523
116	.0416
211	.0323
367	.0224
737	.0156
1280	.0117
1930	.00957
3140	.00811
5290	.00634
9530	.00441

(b) Vertical Baffle Cut

Re_M	j_{av_M}
69.7	.0525
110	.0410
207	.0292
363	.0232
720	.0155
1240	.0114
1870	.0100
3050	.00775
5150	.00626
9270	.00454

A.516 COMMERCIAL TYPE PORT, HORIZONTAL BAFFLE CUT SECOND COMPARTMENT, CROSSFLOW DATA

Re_M	j_1	j_2	j_3	j_{c_M}
122	.0627	.0661	.0694	.0664
350	.0346	.0358	.0378	.0361
1290	.0171	.0187	.0181	.0181
4930	.0100	.0102	.0101	.0101
9290	.00774	.00803	.00820	.00799

A.52 INDIVIDUAL TUBE J FACTORS

A.521 BERGELIN PORT, HORIZONTAL BAFFLE CUT

(a) Inlet

Tube No.	j_M					
Re_M =	82.3	177	321	606	834	1330
1	.0432	.0350	.0229	.0157	.0123	.0093
2	.0667	.0463	.0297	.0200	.0152	.0123
3	.0494	.0361	.0254	.0177	.0128	.0114
4	.0580	.0412	.0276	.0189	.0140	.0116
5	.0568	.0406	.0266	.0200	.0147	.0122
6	.0519	.0350	.0223	.0170	.0123	.0118
7	.0568	.0368	.0256	.0193	.0140	.0128
8	.0617	.0385	.0288	.0216	.0157	.0138
9	.0568	.0378	.0248	.0174	.0145	,0119
10	.0568	.0385	.0222	.0167	.0145	.0120
11	.0617	.0385	.0248	.0170	.0130	.0109
12	.0543	.0385	.0254	.0170	.0136	.0117
13	.0543	.0282	.0229	.0160	.0128	.0110
14	.0568	.0385	.0254	.0170	.0135	.0119
15	.0494	.0327	.0229	.0164	.0121	.0108

Tube No.	j_M					
Re_M =	2390	3490	5340	7440	10200	118
1	.00707	.00649	.00525	.00477	.00425	.0458
2	.00979	.00790	.00659	.00530	.00506	.0633
3	.00798	.00688	.00578	.00454	.00440	.0528
4	.00882	.00739	.00618	.00545	.00526	.0581
5.	.00962	.00796	.00671	.00538	.00509	.0545
6	.00872	.00688	.00601	.00475	.00484	.0458
7	.00935	.00762	.00643	.00538	.00524	.0502
8	.01000	.00835	.00685	.00522	.00438	.0545
9	.00851	.00699	.00601	.00553	.00461	.0528
10	.00859	.00711	.00612	.00567	.00434	.0545
11	.00790	.00654	.00560	.00524	.00484	.0545
12	.00880	.00733	.00634	.00593	.00487	.0519
13	.00822	.00677	.00582	.00584	.00447	.0545
14	.00880	.00728	.00623	.00577	.00472	.0563
15	.00814	.00649	.00623	.00519	.00423	.0492

Tube No.	j_M					
Re_M	248	436	1750	3930	5960	8460
1	.0313	.0198	.00910	.00586	.00494	.00435
2	.0391	.0250	.0126	.00808	.00656	.00540
3	.0339	.0224	.0102	.00678	.00564	.00447
4	.0365	.0237	.0114	.00743	.00602	.00512
5	.0348	.0236	.0117	.00829	.00698	.00566
6	.0330	.0196	.0117	.00732	.00611	.00507
7	.0358	.0223	.0121	.00776	.00701	.00567
8	.0386	.0250	.0125	.00821	.00583	.00556
9	.0330	.0224	.0119	.00580	.00609	.00498
10	.0339	.0219	.0119	.00680	.00609	.00500
11	.0339	.0210	.0108	.00636	.00539	.00469
12	.0344	.0219	.0118	.00717	.00656	.00545
13	.0313	.0205	.0106	.00657	.00588	.00493
14	.0339	.0224	.0113	.00693	.00616	.00514
15	.0296	.0201	.0101	.00620	.00527	.00464

Tube No.	j_M					
Re_M	11000	86.5	153	263	477	728
1	.00370	.0463	.0393	.0321	.0181	.0145
2	.00472	.0593	.0432	.0302	.0192	.0148
3	.00388	.0613	.0473	.0362	.0205	.0171
4	.00461	.0628	.0498	.0352	.0227	.0171
5	.00497	.0588	.0469	.0322	.0220	.0168
6	.00452	.0502	.0446	.0291	.0187	.0141
7	.00499	.0551	.0430	.0312	.0201	.0169
8	.00519	.0580	.0402	.0303	.0191	.0153
9	.00437	.0584	.0429	.0316	.0192	.0148
10	.00434	.0605	.0453	.0327	.0201	.0161
11	.00397	.0635	.0421	.0311	.0190	.0147
12	.00479	.0602	.0420	.0331	.0199	.0163
13	.00416	.0622	.0412	.0308	.0190	.0157
14	.00452	.0573	.0435	.0310	.0200	.0150
15	.00382	.0533	.0352	.0273	.0182	.0142

(b) Outlet

Tube No.	j_M					
Re_M	372	598	880	1640	3420	6030
1	.0162	.0133	.0106	.00807	.00575	.00493
2	.0219	.0178	.0146	.01090	.00766	.00654
3	.0190	.0157	.0126	.00910	.00618	.00549
4	.0208	.0164	.0131	.00955	.00615	.00516
5	.0205	.0168	.0135	.00999	.00666	.00555
6	.0167	.0139	.0116	.00858	.00632	.00546
7	.0190	.0163	.0133	.00954	.00660	.00528
8	.0208	.0169	.0138	.00999	.00683	.00545
9	.0184	.0150	.0121	.00897	.00612	.00521
10	.0208	.0166	.0135	.00999	.00669	.00545
11	.0191	.0146	.0120	.00884	.00626	.00490
12	.0208	.0168	.0140	.0105	.00734	.00635
13	.0216	.0173	.0143	.0108	.00726	.00602
14	.0200	.0157	.0128	.00961	.00652	.00527
15	.0202	.0161	.0128	.00916	.00594	.00488

Tube No.	j_M				
Re_M	8960	11400	141	248	449
1	.00426	.00430	.0249	.0226	.0171
2	.00564	.00511	.0299	.0306	.0230
3	.00406	.00370	.0299	.0259	.0181
4	.00388	.00344	.0333	.0273	.0194
5	.00454	.00400	.0333	.0269	.0202
6	.00483	.00436	.0349	.0259	.0184
7	.00454	.00435	.0366	.0269	.0202
8	.00460	.00423	.0366	.0274	.0207
9	.00408	.00385	.0375	.0264	.0197
10	.00476	.00412	.0391	.0278	.0212
11	.00461	.00387	.0341	.0264	.0192
12	.00565	.00471	.0383	.0278	.0207
13	.00482	.00423	.0358	.0273	.0212
14	.00407	.00419	.0382	.0269	.0197
15	.00388	.00350	.0382	.0264	.0194

Tube No.	j_M				
Re_M =	702	2110	4560	6420	9610
1	.0132	.00722	.00511	.00463	.00419
2	.0178	.00953	.00674	.00602	.00542
3	.0145	.00772	.00524	.00454	.00379
4	.0149	.00761	.00499	.00449	.00408
5	.0154	.00838	.00579	.00495	.00462
6	.0148	.00854	.00617	.00540	.00482
7	.0154	.00837	.00579	.00511	.00441
8	.0158	.00832	.00567	.00493	.00394
9	.0153	.00788	.00551	.00479	.00436
10	.0167	.00876	.00599	.00534	.00427
11	.0148	.00767	.00536	.00483	.00445
12	.0166	.00926	.00674	.00600	.00482
13	.0165	.00871	.00617	.00543	.00469
14	.0151	.00810	.00556	.00508	.00401
15	.0151	.00756	.00499	.00442	.00347

Tube No.	j_M				
Re_M =	90.5	148	277	472	814
1	.0382	.0288	.0241	.0171	.0136
2	.0416	.0334	.0252	.0177	.0129
3	.0390	.0293	.0252	.0180	.0136
4	.0433	.0303	.0255	.0172	.0136
5	.0399	.0288	.0252	.0174	.0139
6	.0365	.0298	.0250	.0171	.0136
7	.0408	.0319	.0250	.0177	.0147
8	.0357	.0298	.0260	.0174	.0137
9	.0399	.0308	.0244	.0175	.0134
10	.0408	.0313	.0239	.0175	.0133
11	.0399	.0288	.0250	.0166	.0133
12	.0390	.0288	.0247	.0169	.0143
13	.0399	.0293	.0250	.0180	.0137
14	.0390	.0324	.0255	.0183	.0131
15	.0390	.0293	.0244	.0172	.0131

A.522 BERGELIN PORT, VERTICAL BAFFLE CUT

(a) Inlet

Tube No.	j_M					
Re_M	79.1	129	239	389	578	827
1	.0461	.0309	.0229	.0164	.0149	.0117
2	.0388	.0353	.0225	.0175	.0139	.0116
3	.0364	.0287	.0233	.0173	.0142	.0115
4	.0461	.0338	.0210	.0164	.0128	.0114
5	.0473	.0338	.0249	.0205	.0149	.0127
6	.0606	.0536	.0387	.0281	.0208	.0146
7	.0485	.0441	.0289	.0215	.0154	.0113
8	.0400	.0360	.0289	.0224	.0171	.0141
9	.0680	.0580	.0368	.0266	.0188	.0135
10	.0510	.0382	.0269	.0212	.0161	.0121
11	.0704	.0603	.0384	.0266	.0192	.0153
12	.0509	.0360	.0261	.0207	.0159	.0115
13	.0582	.0412	.0289	.0217	.0171	.0126
14	.0643	.0559	.0356	.0278	.0204	.0150
15	.0594	.0441	.0340	.0227	.0177	.0130

Tube No.	j_M					
Re_M	79.0	129	236	398	578	835
16	.0476	.0315	.0239	.0171	.0169	.0122
17	.0448	.0308	.0235	.0169	.0166	.0121
18	.0435	.0369	.0239	.0174	.0137	.0120
19	.0480	.0362	.0243	.0172	.0139	.0127
20	.0528	.0377	.0272	.0201	.0159	.0132
21	.0407	.0308	.0226	.0174	.0139	.0114
22	.0476	.0339	.0235	.0174	.0144	.0113
23	.0515	.0362	.0298	.0226	.0178	.0138
24	.0463	.0316	.0273	.0209	.0166	.0137
25	.0448	.0354	.0281	.0214	.0168	.0122
26	.0463	.0331	.0277	.0216	.0168	.0119
27	.0634	.0385	.0289	.0209	.0174	.0121
28	.0512	.0385	.0298	.0219	.0183	.0130
29	.0515	.0370	.0289	.0256	.0208	.0151
30	.0686	.0446	.0339	.0234	.0173	.0136

Tube No.	j_M				
Re_M =	1330	2300	3890	6030	10900
1	.00976	.00726	.00577	.00526	.00400
2	.00913	.00763	.00615	.00546	.00376
3	.00976	.00767	.00613	.00532	.00387
4	.00969	.00767	.00572	.00517	.00405
5	.00912	.00763	.00622	.00484	.00394
6	.01050	.00840	.00643	.00555	.00415
7	.01040	.00803	.00625	.00481	.00400
8	.01050	.00810	.00601	.00487	.00391
9	.01140	.00925	.00665	.00578	.00432
10	.00984	.00763	.00591	.00547	,00408
11	.01200	.00917	.00627	.00594	.00432
12	.01080	.00803	.00629	.00561	.00399
13	.01070	.00787	.00601	.00567	.00398
14	.01220	.00957	.00632	.00572	.00416
15	.01000	.00848	.00625	.00556	.00409

Tube No.	j_M				
Re_M =	1330	2300	3880	6150	10800
16	.01020	.00747	.00595	.00542	.00431
17	.00887	.00688	.00568	.00510	.00412
18	.01010	.00811	.00625	.00525	.00402
19	.01010	.00844	.00601	.00464	.00423
20	.00940	.00789	.00655	.00510	.00421
21	.00911	.00713	.00596	.00481	.00395
22	.01090	.00751	.00618	.00512	.00413
23	.01040	.00835	.00626	.00493	.00415
24	.01040	.00848	.00641	.00493	.00413
25	.01040	.00806	.00600	.00553	.00430
26	.01040	.00787	.00571	.00536	.00423
27	.01120	.00823	.00670	.00572	.00430
28	.01090	.00970	.00636	.00569	.00429
29	.0127⁰	.00814	.00655	.00562	.00418
30	.0122⁰	.00887	.00638	.00573	.00440

(b) Outlet

Tube No.	j_M					
Re_M =	77.1	128	246	383	589	834
1	.0429	.0355	.0254	.0208	.0156	.0122
2	.0456	.0363	.0258	.0219	.0154	.0118
3	.0389	.0300	.0247	.0198	.0147	.0115
4	.0509	.0349	.0262	.0213	.0150	.0116
5	.0496	.0371	.0274	.0229	.0159	.0111
6	.0536	.0418	.0314	.0240	.0186	.0139
7	.0536	.0379	.0290	.0237	.0167	.0132
8	.0509	.0387	.0303	.0219	.0164	.0126
9	.0643	.0450	.0359	.0280	.0191	.0143
10	.0563	.0411	.0319	.0269	.0184	.0134
11	.0643	.0442	.0359	.0277	.0189	.0142
12	.0657	.0442	.0351	.0261	.0177	.0133
13	.0643	.0410	.0335	.0256	.0174	.0140
14	.0643	.0450	.0290	.0269	.0184	.0137
15	.0643	.0478	.0367	.0282	.0194	.0141

Tube No.	j_M					
Re_M =	77.1	126	235	389	564	835
16	.0393	.0329	.0262	.0210	.0158	.0119
17	.0461	.0354	.0283	.0226	.0167	.0127
18	.0420	.0387	.0271	.0218	.0158	.0118
19	.0488	.0346	.0292	.0208	.0156	.0118
20	.0474	.0404	.0283	.0216	.0158	.0118
21	.0478	.0387	.0266	.0208	.0154	.0116
22	.0515	.0387	.0283	.0221	.0158	.0115
23	.0478	.0379	.0283	.0206	.0153	.0116
24	.0474	.0338	.0275	.0208	.0154	.0112
25	.0434	.0329	.0267	.0242	.0174	.0127
26	.0460	.0387	.0271	.0205	.0142	.0110
27	.0542	.0420	.0262	.0254	.0183	.0132
28	.0542	.0354	.0314	.0239	.0172	.0126
29	.0474	.0362	.0271	.0205	.0151	.0117
30	.0583	.0445	.0367	.0260	.0194	.0137

Tube No	j_M				
Re_M =	1400	2290	3890	5690	10600
1	.00897	.00618	.00471	.00433	.00334
2	.00883	.00623	.00476	.00435	.00327
3	.00904	.00632	.00496	.00433	.00333
4	.00883	.00605	.00482	.00434	.00354
5	.00869	.00614	.00509	.00488	.00353
6	.00945	.00636	.00600	.00567	.00429
7	.00952	.00677	.00532	.00504	.00389
8	.00897	.00636	.00507	.00451	.00357
9	.01040	.00739	.00608	.00486	.00452
10	.00987	.00686	.00530	.00468	.00362
11	.01060	.00762	.00630	.00589	.00435
12	.00987	.00672	.00527	.00497	.00394
13	.01040	.00695	.00557	.00532	.00408
14	.01060	.00748	.00625	.00591	.00429
15	.01090	.00739	.00625	.00572	.00421

Tube No.	j_M				
Re_M =	1420	2270	3990	5710	10800
16	.00919	.00616	.00475	.00423	.00338
17	.00864	.00595	.00443	.00423	.00347
18	.00898	.00612	.00490	.00464	.00368
19	.00878	.00603	.00488	.00449	.00380
20	.00892	.00600	.00518	.00476	.00358
21	.00802	.00568	.00443	.00427	.00368
22	.00823	.00582	.00468	.00427	.00345
23	.00878	.00594	.00488	.00461	.00359
24	.00823	.00568	.00433	.00411	.00322
25	.00878	.00607	.00490	.00457	.00355
26	.00809	.00572	.00443	.00408	.00311
27	.00988	.00669	.00525	.00481	.00401
28	.00871	.00616	.00562	.00491	.00350
29	.00823	.00576	.00461	.00442	.00355
30	.01090	.00713	.00572	.00523	.00402

A.523 COMMERCIAL PORT, HORIZONTAL BAFFLE CUT

(a) Inlet

Tube No.	j_M				
Re_M =	73.4	117	215	371	740
1	.0536	.0400	.0315	.0239	.0127
2	.0471	.0448	.0337	.0258	.0155
3	.0536	.0472	.0332	.0241	.0132
4	.0523	.0464	.0302	.0239	.0138
5	.0562	.0456	.0315	.0243	.0150
6	.0432	.0384	.0281	.0211	.0130
7	.0471	.0456	.0320	.0245	.0143
8	.0523	.0448	.0320	.0251	.0159
9	.0471	.0400	.0311	.0234	.0152
10	.0510	.0464	.0315	.0221	.0147
11	.0458	.0400	.0293	.0221	.0133
12	.0484	.0472	.0297	.0228	.0139
13	.0471	.0440	.0302	.0221	.0133
14	.0471	.0424	.0294	.0234	.0136
15	.0458	.0392	.0294	.0216	.0124

Tube No.	j_M				
Re_M =	1290	1950	3220	5450	9840
1	.0103	.00830	.00633	.00483	.00415
2	.0119	.00906	.00702	.00562	.00453
3	.0103	.00818	.00696	.00530	.00428
4	.0104	.00874	.00666	.00598	.00478
5	.0120	.00911	.00691	.00586	.00470
6	.0104	.00828	.00693	.00524	.00453
7	.0118	.00841	.00710	.00580	.00473
8	.0133	.00911	.00748	.00596	.00459
9	.0116	.00878	.00707	.00540	.00415
10	.0119	.00888	.00685	.00528	.00433
11	.0110	.00901	.00767	.00498	.00425
12	.0109	.00846	.00710	.00556	.00443
13	.0113	.00828	.00680	.00538	.00423
14	.0115	.00828	.00711	.00575	.00478
15	.0107	.00810	.00671	.00532	.00409

(b) Outlet

Tube No.	j_M				
Re_M =	69.0	121	211	361	726
1	.0383	.0338	.0266	.0198	.0134
2	.0344	.0300	.0241	.0181	.0132
3	.0409	.0338	.0261	.0186	.0134
4	.0396	.0323	.0257	.0188	.0130
5	.0409	.0338	.0266	.0191	.0132
6	.0357	.0308	.0257	.0181	.0127
7	.0396	.0323	.0253	.0186	.0130
8	.0396	.0300	.0266	.0193	.0132
9	.0370	.0315	.0245	.0183	.0126
10	.0383	.0323	.0261	.0195	.0131
11	.0370	.0331	.0237	.0183	.0127
12	.0383	.0346	.0261	.0191	.0132
13	.0409	.0315	.0253	.0185	.0131
14	.0409	.0346	.0257	.0195	.0130
15	.0383	.0315	.0257	.0185	.0130

Tube No.	j_M				
Re_M =	1250	1880	3050	5160	9540
1	.01010	.00816	.00633	.00520	.00387
2	.00959	.00803	.00533	.00483	.00368
3	.00980	.00807	.00598	.00499	.00387
4	.00986	.00798	.00590	.00489	.00385
5	.00993	.00816	.00603	.00514	.00390
6	.00912	.00740	.00576	.00496	.00351
7	.00959	.00762	.00592	.00506	.00377
8	.00101	.00816	.00623	.00528	.00361
9	.00919	.00744	.00546	.00485	.00363
10	.00101	.00758	.00636	.00528	.00380
11	.00100	.00740	.00606	.00488	.00377
12	.00993	.00816	.00620	.00513	.00391
13	.01000	.00798	.00631	.00423	.00396
14	.01010	.00807	.00612	.00507	.00390
15	.01010	.00798	.00603	.00507	.00388

A.524 COMMERCIAL PORT, VERTICAL BAFFLE CUT

(a) Inlet

Tube No.	j_M				
Re_M =	71.4	121	215	374	758
1	.0440	.0363	.0266	.0198	.0123
2	.0479	.0404	.0274	.0205	.0129
3	.0453	.0396	.0260	.0219	.0126
4	.0504	.0420	.0291	.0219	.0131
5	.0466	.0388	.0245	.0193	.0125
6	.0608	.0476	.0291	.0233	.0148
7	.0543	.0436	.0286	.0219	.0126
8	.0530	.0388	.0282	.0195	.0131
9	.0647	.0517	.0316	.0243	.0157
10	.0543	.0404	.0258	.0210	.0130
11	.0659	.0517	.0324	.0284	.0152
12	.0569	.0371	.0250	.0210	.0132
13	.0595	.0388	.0266	.0205	.0131
14	.0635	.0485	.0291	.0241	.0151
15	.0659	.0452	.0295	.0238	.0130

Tube No.	j_M				
Re_M =	71.4	123	219	387	769
16	.0428	.0375	.0267	.0196	.0122
17	.0416	.0375	.0275	.0200	.0122
18	.0403	.0351	.0246	.0203	.0127
19	.0442	.0392	.0250	.0204	.0128
20	.0480	.0400	.0283	.0196	.0130
21	.0442	.0343	.0259	.0194	.0128
22	.0428	.0367	.0267	.0194	.0130
23	.0428	.0346	.0246	.0204	.0132
24	.0468	.0359	.0250	.0192	.0128
25	.0519	.0351	.0250	.0196	.0127
26	.0494	.0392	.0271	.0198	.0128
27	.0580	.0359	.0250	.0213	.0140
28	.0480	.0351	.0259	.0176	.0127
29	.0546	.0392	.0267	.0198	.0139
30	.0623	.0432	.0283	.0235	.0142

Tube No.	j_M				
Re_M =	1310	1970	3190	5330	9530
1.	.00945	.00811	.00604	.00497	.00336
2	.00959	.00824	.00612	.00481	.00327
3	.00932	.00824	.00606	.00479	.00354
4	.00952	.00848	.00614	.00481	.00385
5	.00986	.00834	.00601	.00489	.00343
6	.01110	.00867	.00620	.00539	.00390
7	.01000	.00852	.00601	.00484	.00381
8	.00959	.00848	.00595	.00473	.00372
9	.01180	.00918	.00639	.00548	.00388
10	.00945	.00880	.00614	.00503	.00348
11	.01170	.00918	.00683	.00556	.00392
12	.00945	.00880	.00620	.00498	.00347
13	.00925	.00876	.00617	.00469	.00354
14	.0114	.00908	.00628	.00545	.00374
15	.0105	.00890	.00630	.00556	.00383

Tube No.	j_M				
Re_M =	1330	1980	3240	5450	9740
16	.00928	.00810	.00600	.00509	.00343
17	.00874	.00824	.00581	.00481	.00339
18	.00894	.00824	.00592	.00479	.00340
19	.00914	.00810	.00597	.00476	.00343
20	.00960	.00834	.00600	.00497	.00359
21	.00900	.00791	.00584	.00462	.00334
22	.00887	.00796	.00595	.00466	.00342
23	.00910	.00810	.00608	.00481	.00349
24	.00928	.00801	.00597	.00470	.00332
25	.00955	.00815	.00587	.00495	.00349
26	.00961	.00810	.00606	.00487	.00332
27	.00941	.00820	.00617	.00501	.00361
28	.00934	.00833	.00600	.00489	.00351
29	.00934	.00838	.00597	.00495	.00361
30	.01000	.00857	.00672	.00514	.00382

OUTLET

Tube No.	j_M				
Re_M =	68.6	116	197	341	679
1	.0476	.0356	.0258	.0199	.0139
2	.0489	.0375	.0262	.0211	.0146
3	.0476	.0348	.0262	.0188	.0148
4	.0476	.0388	.0293	.0226	.0153
5	.0450	.0364	.0289	.0193	.0135
6	.0553	.0404	.0315	.0235	.0155
7	.0514	.0380	.0293	.0226	.0143
8	.0489	.0339	.0275	.0199	.0136
9	.0617	.0420	.0329	.0260	.0176
10	.0553	.0404	.0289	.0204	.0154
11	.0617	.0420	.0338	.0273	.0160
12	.0514	.0396	.0298	.0229	.0147
13	.0514	.0388	.0329	.0204	.0152
14	.0579	.0396	.0329	.0240	.0163
15	.0592	.0428	.0338	.0269	.0170

Tube No.	j_M				
Re_M =	67.7	116	195	339	671
16	.0477	.0361	.0268	.0204	.0139
17	.0410	.0344	.0263	.0199	.0134
18	.0463	.0361	.0241	.0181	.0125
19	.0477	.0377	.0268	.0199	.0136
20	.0463	.0377	.0286	.0194	.0139
21	.0424	.0361	.0268	.0183	.0129
22	.0463	.0369	.0272	.0204	.0130
23	.0477	.0393	.0250	.0204	.0127
24	.0424	.0361	.0263	.0207	.0126
25	.0450	.0385	.0263	.0210	.0136
26	.0450	.0377	.0277	.0215	.0140
27	.0503	.0410	.0282	.0215	.0137
28	.0499	.0385	.0300	.0220	.0139
29	.0477	.0361	.0304	.0231	.0141
30	.0503	.0410	.0318	.0246	.0157

Tube No.	j_M				
Re_M =	1170	1760	2890	4910	8970
1	.00868	.00683	.00525	.00485	.00352
2	.00943	.00688	.00535	.00492	.00372
3	.00913	.00672	.00547	.00490	.00355
4	.00936	.00724	.00544	.00476	.00380
5	.00838	.00631	.00556	.00494	.00359
6	.00973	.00776	.00588	.00526	.00408
7	.00934	.00709	.00574	.00511	.00382
8	.00853	.00672	.00553	.00522	.00361
9	.01130	.00807	.00594	.00544	.00413
10	.01030	.00724	.00535	.00490	.00360
11	.01090	.00791	.00615	.00541	.00414
12	.00973	.00771	.00537	.00483	.00363
13	.00965	.00672	.00535	.00476	.00362
14	.01020	.00776	.00594	.00543	.00407
15	.01090	.00820	.00597	.00527	.00416

Tube No.	j_M				
Re_M =	1160	1750	2930	4900	8970
16	.00870	.00665	.00532	.00485	.00357
17	.00832	.00623	.00510	.00452	.00351
18	.00798	.00644	.00532	.00461	.00354
19	.00824	.00670	.00502	.00458	.00343
20	.00862	.00649	.00555	.00496	.00353
21	.00817	.00628	.00526	.00447	.00353
22	.00832	.00665	.00526	.00454	.00354
23	.00809	.00644	.00534	.00487	.00364
24	.00794	.00628	.00499	.00443	.00352
25	.00839	.00681	.00528	.00480	.00358
26	.00870	.00670	.00502	.00445	.00345
27	.00946	.00760	.00549	.00489	.00371
28	.00870	.00728	.00559	.00509	.00381
29	.00908	.00718	.00570	.00480	.00379
30	.00985	.00713	.00585	.00537	.00400

A.525 COMMERCIAL PORT, INLET COMPARTMENT FITTED WITH IMPINGEMENT BAFFLE

(a) HORIZONTAL BAFFLE CUT

Tube No.	j_M				
Re_M =	68.8	116	211	367	737
1	.0608	.0474	.0350	.0248	.0166
2	.0584	.0466	.0342	.0236	.0166
3	.0505	.0426	.0315	.0232	.0159
4	.0584	.0450	.0333	.0232	.0164
5	.0518	.0410	.0315	.0215	.0149
6	.0518	.0386	.0324	.0223	.0164
7	.0465	.0386	.0315	.0215	.0151
8	.0452	.0362	.0298	.0210	.0148
9	.0483	.0418	.0333	.0232	.0156
10	.0478	.0370	.0298	.0208	.0146
11	.0584	.0450	.0350	.0236	.0163
12	.0452	.0378	.0302	.0210	.0154
13	.0505	.0394	.0298	.0208	.0147
14	.0584	.0450	.0332	.0227	.0161
15	.0478	.0402	.0332	.0225	.0156

Tube No.	j_M				
Re_M =	1280	1930	3140	5290	9530
1	.0123	.0101	.00843	.00658	.00475
2	.0120	.00948	.00832	.00644	.00479
3	.0116	.00915	.00807	.00613	.00430
4	.0124	.00952	.00838	.00661	.00456
5	.0114	.00906	.00810	.00590	.00430
6	.0123	.00989	.00846	.00661	.00462
7	.0119	.00961	.00821	.00624	.00431
8	.0112	.00948	.00790	.00598	.00407
9	.0122	.01000	.00816	.00649	.00460
10	.0112	.00902	.00793	.00617	.00407
11	.0122	.01000	.00838	.00661	.00461
12	.0110	.00817	.00782	.00603	.00416
13	.0110	.00911	.00714	.00604	.00406
14	.0122	.00994	.00818	.00654	.00462
15	.0117	.00966	.00804	.00634	.00438

(b) VERTICAL BAFFLE CUT

Tube No.	j_M				
Re_M =	69.6	110	208	365	723
1	.0594	.0450	.0316	.0248	.0178
2	.0539	.0407	.0270	.0228	.0153
3	.0483	.0398	.0261	.0225	.0152
4	.0539	.0416	.0302	.0233	.0160
5	.0511	.0390	.0280	.0228	.0151
6	.0580	.0450	.0320	.0251	.0173
7	.0525	.0416	.0302	.0233	.0165
8	.0525	.0407	.0293	.0228	.0155
9	.0580	.0442	.0320	.0245	.0174
10	.0511	.0390	.0289	.0225	.0152
11	.0580	.0433	.0316	.0245	.0175
12	.0525	.0416	.0302	.0223	.0151
13	.0553	.0416	.0311	.0225	.0151
14	.0567	.0442	.0316	.0253	.0173
15	.0553	.0433	.0307	.0235	.0157

Tube No.	j_M				
Re_M =	69.6	109	206	361	717
16	.0452	.0388	.0277	.0217	.0138
17	.0480	.0388	.0282	.0222	.0141
18	.0508	.0397	.0272	.0235	.0144
19	.0522	.0406	.0267	.0225	.0142
20	.0522	.0397	.0287	.0228	.0153
21	.0480	.0388	.0263	.0222	.0137
22	.0494	.0397	.0277	.0230	.0145
23	.0508	.0388	.0291	.0241	.0157
24	.0480	.0370	.0267	.0217	.0140
25	.0536	.0434	.0291	.0236	.0159
26	.0452	.0370	.0267	.0220	.0141
27	.0522	.0406	.0296	.0228	.0152
28	.0538	.0416	.0282	.0241	.0157
29	.0466	.0370	.0277	.0225	.0138
30	.0538	.0425	.0296	.0238	.0157

Tube No.	j_M				
Re_M =	1250	1890	3070	5190	9310
1	.0125	.0108	.00846	.00706	.00530
2	.0119	.0101	.00790	.00639	.00460
3	.0116	.0100	.00775	.00634	.00456
4	.0119	.0103	.00769	.00637	.00456
5	.0112	.0100	.00739	.00602	.00441
6	.0124	.0107	.00843	.00701	.00519
7	.0117	.0106	.00813	.00662	.00458
8	.0110	.00988	.00766	.00632	.00449
9	.0123	.0107	.00828	.00685	.00479
10	.0112	.00968	.00796	.00653	.00448
11	.0124	.01060	.00837	.00701	.00517
12	.0110	.00988	.00796	.00636	.00459
13	.0110	.0100	.00742	.00630	.00457
14	.0124	.0106	.00837	.00687	.00499
15	.0112	.0102	.00804	.00669	.00478

Tube No.	j_M				
Re_M =	1230	1850	3030	5110	9230
16	.0108	.00932	.00728	.00558	.00412
17	.0111	.00948	.00732	.00555	.00424
18	.0110	.00953	.00750	.00564	.00428
19	.0111	.00963	.00744	.00573	.00440
20	.0115	.01010	.00750	.00609	.00451
21	.0108	.00947	.00732	.00560	.00411
22	.0111	.00979	.00747	.00583	.00435
23	.0112	.00999	.00760	.00614	.00461
24	.0109	.00963	.00738	.00562	.00413
25	.0114	.00953	.00757	.00620	.00455
26	.0109	.0100	.00728	.00553	.00414
27	.0112	.00984	.00769	.00632	.00455
28	.0115	.01010	.00757	.00611	.00460
29	.0108	.00927	.00725	.00559	.00420
30	.0114	.01010	.00801	.00659	.00463

A.53 PHYSICAL DIMENSIONS

A.531 ELECTRODE DIMENSIONS

DIAMETER	0.0098 m
LENGTH	0.0481 m
SURFACE AREA	0.00148 m^2

A.532 BAFFLE DIMENSIONS

SPACING	0.0476 m
CUT	18.4 %
THICKNESS	0.00318 m
DIA.	.132 m (TO FIT SHELL)

A.533 SHELL DIMENSIONS

O.D.	.1524 m
I.D.	.1321 m
LENGTH	.6096 m

A.534 FLOW AREA DATA

TUBE PITCH	0.01225 m
MIN. FLOW PATH	0.03778 m
MIN. FLOW AREA (at centre row of tubes)	0.01798 m^2

APPENDIX 6 CALCULATION PROCEDURE

The mass transfer j-factor can be represented by the expression:-

$$j_M = \frac{I_L}{C_b s n_e F u_M} Sc^{2/3} \quad \ldots\ldots (A\ 6.1)$$

Also, the Reynolds number can be represented by:-

$$Re_M = \frac{1}{\nu} d_t u_M \quad \ldots\ldots (A\ 6.2)$$

where $$u_M = \frac{Q}{A_M} \quad \ldots\ldots (A\ 6.3)$$

Hence, j_M and Re_M can be calculated from a knowledge of the physical properties of the electrolyte and measurements of the limiting current and the volumetric flow rate, together with a knowledge of the geometry of the test section. Mackley (1) simplified the calculation procedure by correlating Sc and ν for variations with temperature. The correlations were applicable in the range $15 < T < 35$ for an electrolyte concentration of 0.01N potassium ferricyanide, 0.01N potassium ferrocyanide, 1 N sodium hydroxide. Small variations in the ferri-ferrocyanide ion concentrations were insignificant. The correlations are:-

$$Sc = 5950 - 319\,T + 7.90\,T^2 - 0.0983\,T^3 + 0.000496\,T^4 \quad \ldots\ldots (A\ 6.3)$$

$$\nu = 0.205 \times 10^{-5} - 0.598 \times 10^{-7} T + 0.943 \times 10^{-9} T^2 - 0.608 \times 10^{-11} T^3 \ m^2/s \quad \ldots\ldots (A\ 6.4)$$

The calculation procedure can be further eased by considering the group $Sc^{2/3} / s \cdot n_e \cdot F$ as varying with temperature, as shown in Fig. (72). Fig. (73) gives the corresponding variation of η with temperature.

Worked Example:

Inlet compartment, 35.8 mm. diameter port, with impingement baffle.

TUBE 1

$I_L = 4.5$ mA

$d_t = 9.8$ mm

$A_M = .00180\ m^2$

$Q = .0000167\ m^3/s$

$T = 16.6\ ^\circ C$

$C_b = .01205$ k mole/m^3

η at $16.6\ ^\circ C = .132 \times 10^{-5}\ m^2/s$ (fig 73)

$$u_M = \frac{.0000167}{.00180} = .00927 \text{ m/s}$$

hence
$$Re_M = \frac{.00927 \times 9.8 \times 10^{-3}}{.132 \times 10^{-5}}$$

$$= \underline{\underline{68.8}}$$

now
$$j_M = \frac{I_L}{u_M \cdot C_b} \cdot \frac{Sc^{2/3}}{s \cdot F \cdot n_e}$$

with $\frac{Sc^{2/3}}{s F n_e}$ at $16.6\ ^\circ C = 1.285 \times 10^{-3}$ (fig 72)

hence
$$j_M = \frac{4.5 \times 10^{-3}}{.00927 \times .01205} \times 1.285 \times 10^{-3}$$

$$= \underline{\underline{.0608}}$$

Hence the mass transfer j-factor for tube 1 of the inlet compartment with the commercial type port and impingement baffle fitted is 0.0608 at a Reynolds number of 68.8.

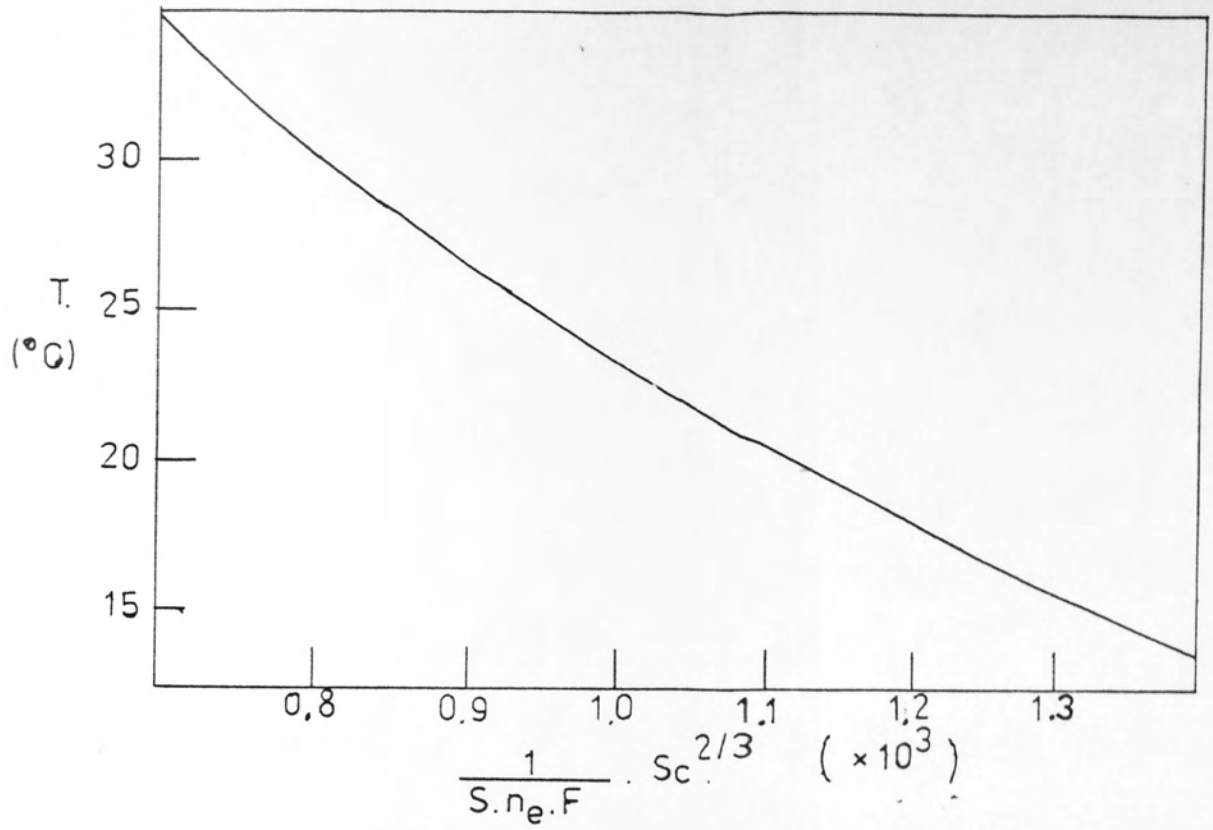
T.
(°C)
30
25
20
15
0,8
0.9
1.0
1.1
1,2
1.3
$\frac{1}{S.n_e.F} . Sc^{2/3}$ ($\times 10^3$)

FIG. 72

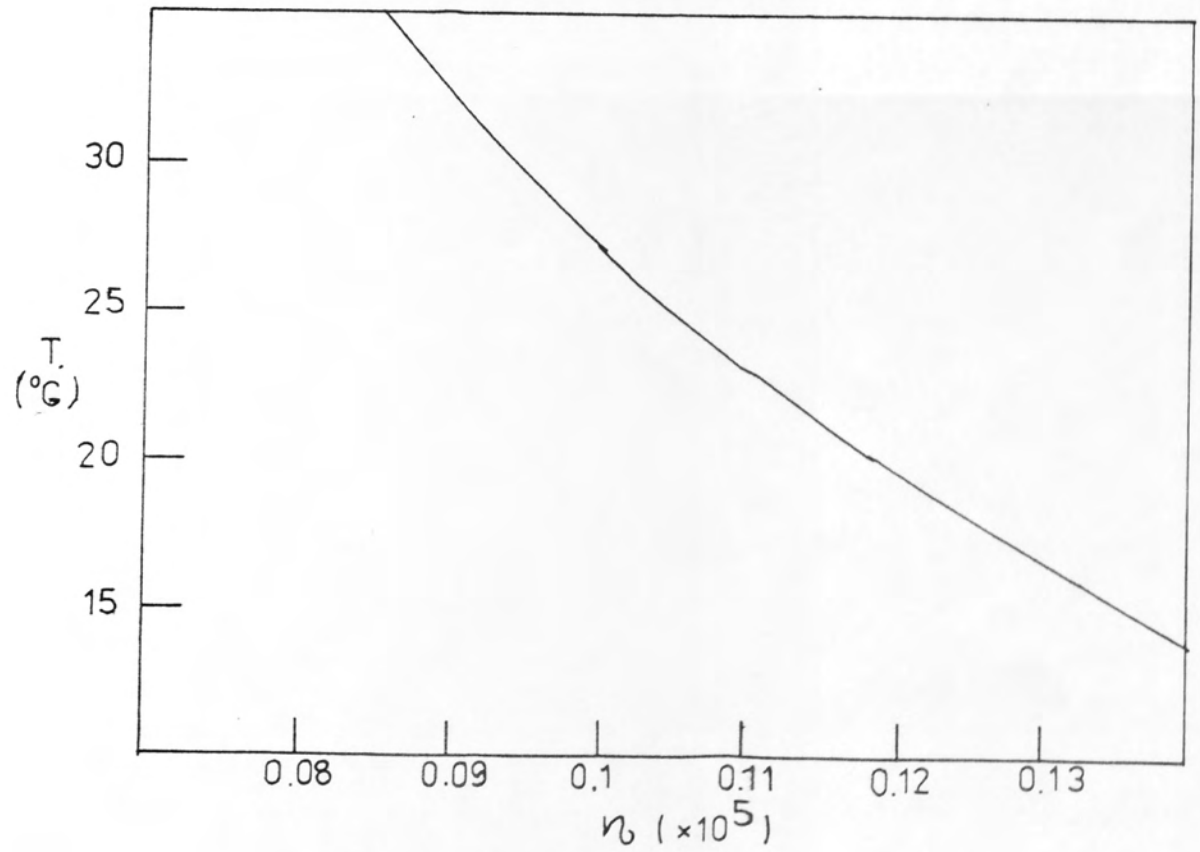
T.
(°C)
30
25
20
15
0.08
0.09
0.1
0.11
0.12
0.13
n_0 ($\times 10^5$)

FIG. 73